RECORD 2020/4

THE DEFLECTOR AU–CU DEPOSIT: DEFINING AN ANOMALOUS YILGARN CRATON MINERALISATION STYLE USING TRACE ELEMENT GEOCHEMISTRY

by
JFB Egan

Government of **Western Australia**
Department of **Mines, Industry Regulation and Safety**

THE UNIVERSITY OF SYDNEY

Geological Survey of Western Australia

Government of **Western Australia**
Department of **Mines, Industry Regulation and Safety**

RECORD 2020/4

THE DEFLECTOR AU–CU DEPOSIT: DEFINING AN ANOMALOUS YILGARN CRATON MINERALISATION STYLE USING TRACE ELEMENT GEOCHEMISTRY

by
JFB Egan

The University of Sydney

PERTH 2020

Geological Survey of Western Australia

MINISTER FOR MINES AND PETROLEUM
Hon Bill Johnston MLA

DIRECTOR GENERAL, DEPARTMENT OF MINES, INDUSTRY REGULATION AND SAFETY
David Smith

EXECUTIVE DIRECTOR, GEOLOGICAL SURVEY AND RESOURCE STRATEGY
Jeff Haworth

REFERENCE
The recommended reference for this publication is:
Egan, JFB 2020, The Deflector Au–Cu deposit: defining an anomalous Yilgarn Craton mineralisation style using trace element geochemistry: Geological Survey of Western Australia, Record 2020/4, 88p.

ISBN 978-1-74168-883-2
ISSN 2204-4345

Grid references in this publication refer to the Geocentric Datum of Australia 1994 (GDA94). Locations mentioned in the text are referenced using Map Grid Australia (MGA) coordinates, Zone 50. All locations are quoted to at least the nearest 100 m.

About this publication
This Record is an Honours thesis researched, written and compiled as part of an ongoing collaborative project between Geological Survey and Resource Strategy (GSRS) and the University of Sydney, New South Wales. The scientific content of the Record, and the drafting of figures, was the responsibility of the author. No editing has been undertaken by GSRS.

THE UNIVERSITY OF SYDNEY

Published 2020 by the Geological Survey of Western Australia
This Record is published in digital format (PDF) and is available online at <www.dmp.wa.gov.au/GSWApublications>.

Further details of geoscience products are available from:
Information Centre
Department of Mines, Industry Regulation and Safety
100 Plain Street
EAST PERTH WESTERN AUSTRALIA 6004
Telephone: +61 8 9222 3459 Facsimile: +61 8 9222 3444
www.dmirs.wa.gov.au/GSWApublications

Cover image: Packing up the campsite in a claypan about 5 km south of Minilya in the southern Pilbara (photo by Olga Blay)

The Deflector Au-Cu Deposit: Defining an Anomalous Yilgarn Craton Mineralisation Style using Trace Element Geochemistry

By: **James F. B. Egan**

Supervisor: Derek Wyman

A thesis submitted as a requirement for the attainment of the Bachelor of Science Geology and Geophysics Honours Degree

The University of Sydney

Faculty of Science

School of Geoscience

Submitted on: 21/10/2016

Word Count: 18,466

THE UNIVERSITY OF SYDNEY

DORAY MINERALS LIMITED

Acknowledgements

I would like to express my deepest thanks to my supervisor, Associate Professor Derek Wyman, for his on-going support, expert guidance and patience throughout the duration of my study and research. The complexity of this project challenged me on many different levels, whereby Derek's valuable insights guided my overall understanding significantly. Working with Derek allowed me to realise the enormous contribution he has made to the research community in his field of expertise, and I feel grateful as an Honours student to have been exposed on a daily basis to his depth of knowledge.

To Doray Minerals Ltd., thank you for providing the funding for this project and your continuing support throughout. I hope that the results of this project are beneficial, and in some way contributes to the success of your organisation.

Lastly, thanks to Bailey and all the other Honours students who were there from start to finish, who were a great bunch of people to complete the year with.

ABSTRACT

The mineral systems approach is confounded when a particular system of interest does not fall categorically into a distinct mineral deposit type. When mineral systems do not conform to any one particular model, it may suggest a complex evolutionary history that was the result of multiple events. The Deflector Au-Cu deposit has long been known as an unusual Yilgarn deposit due to its anomalous Au + base-metal inventory, as well as its atypical structural characteristics. This Honours study performed a petrographic and trace element geochemical analysis on 80 samples taken from the three lodes in the deposit in order to determine whether the system is a modified orogenic deposit, an orogenic overprint on an existing deposit, or a distinct Au-Cu deposit type. In addition, this project also endeavoured to determine the source of the mineralising fluids, and establish geochemical vectors to mineralisation in the surrounding Gullewa Greenstone Belt.

The evidence provided by the results of this Honours project indicate that Deflector is a superimposed Au-Cu system, whereby orogenic fluids have been superimposed on existing base-metal sulphides. The presence of two textural types of pyrite, as well as disequilibrium textures within the thin sections, provides evidence that there has been an interaction between two independent hydrothermal fluids. Structural evidence, as well as hydrothermal zoning that is present in the Deflector system, suggests base-metal rich fluids were remobilised by a granite intrusion at depth, and re-precipitated within structural traps at Deflector. A later major shearing event resulted in the tapping of orogenic Au-sourced fluids from base of the crust, resulting in these fluids flowing into the Deflector system, where the earlier base-metal sulphides provided a chemical trap for the orogenic fluids to be superimposed on. Geochemical modelling strongly supports these observations, given that high Au is always accompanied by high Cu, even though a simple mathematical correlation is not possible. In addition, Au and Zn are poorly correlated within the lodes. Geochemical vectors to mineralisation include W, As, Zn and Ba, although a more comprehensive geochemical dataset needs to be acquired in order to determine a more definitive geochemical signature for the Deflector system. A thorough geochemical understanding of superimposed systems is essential in mineral

exploration and targeting due to the complex trace element behaviours in these deposit types.

Table of Contents

List of Figures

List of Abbreviations

Ag – Silver

Al_2O_3 – Aluminum Oxide

ALS – Australian Laboratory Services

As - Arsenic

Au – Au

CaO – Calcium Oxide

Cd – Cadmium

Ce – Cerium

Cr – Chromium

Cr_2O_3 – Chromium (III) Oxide

Cs – Caesium

Cu – Copper

Co - Cobalt

Ba – Barium

BaO – Barium Oxide

Bi – Bismuth

BIF – Banded Iron Formation

Dy – Dysprosium

EGS – Eastern Goldfields Superterrane

Er – Erbium

Fe – Iron

Fe_2O_3 – Iron (III) Oxide

Ga – Gallium

Gd – Gadolinium

Ge – Germanium

GGB – Gullewa Greenstone Belt

g/t – Grams per Tonne

Hf – Hafnium

Hg – Mercury

Ho – Holmium

ICP – Inductively Coupled Plasma

ICP-AES – Inductively Coupled Plasma Atomic Emission Spectrometer

ICP-MS – Inductively Coupled Mass Spectrometer

In – Indium

IRGS – Intrusion-Related Au System

K_2O – Potassium Oxide

LOI – Loss on Ignition

Lu – Lutetium

Mg – Magnesium

MgO – Magnesium Oxide

MnO – Manganese Oxide

Mo – Molybdenum

Moz – Million Ounces

Mt – Million Tonnes

Na_2B_4O - Borax

Na_2CO_3 – Sodium Carbonate

Na_2O – Sodium Dioxide

Nb – Niobium

Nd – Neodymium

Ni – Nickel

oz – Ounces

P_2O_5 – Phosphorous Pentoxide

Pb – Lead

PbO_2 – Lead Oxide

PPM – Part Per Million

PPT – Part Per Trillion

Pr – Praseodymium

Rb - Rubidium

REE – Rare Earth Element

RIRGS – Reduced Intrusion-Related Au Systems

S – Sulphur

Sb – Antimony

Se – Selenium

SiO_2 – Silicon Dioxide

Sm – Samarium

Sn – Tin

Sr – Strontium

SrO – Strontium Oxide

Ta – Tantalum

Te – Tellurium

Yb – Ytterbium

Zn – Zinc

Zr – Zirconium

TGP – Tintina Au Province

Th – Thorium

Ti – Titanium

TiO_2 – Titanium Dioxide

Tm – Thulium

TTG - Tonalite-Trondjemite-Granodiorite

U – Uranium

V - Vanadium

W – Tungsten

VMS – Volcanogenic Massive Sulphide

Y – Yttrium

1. INTRODUCTION

The Deflector deposit is a high-grade, Au-Cu mineral system located in the southern Murchison Domain of the Yilgarn Craton, Western Australia. Situated in the Gullewa Greenstone Belt (GGB), 400 km north of Perth and 160 km east of Geraldton, Deflector has many characteristics of a Au-only orogenic style deposit, but also exhibits substantial but variable amounts of Cu-Ag-Zn within the Au lodes (Hayden and Steemson, 1998). In addition, Deflector lacks the well-developed shear zone commonly associated with late Archean orogenic Au deposits, with mineralisation instead occurring as quartz-sulphide veins that in many cases fill open spaces (Hayden and Steemson, 1998). These atypical characteristics do not allow Deflector to be categorised into a distinct deposit type, given that deposit-scale features raise the possibility that either mineralisation is not of the "normal" orogenic type, or two mineralisation events have been superimposed.

A mineral deposit is a naturally occurring accumulation or concentration of minerals or metals that have been created through various geologic processes in an environment that favours preservation (Soloman and Groves, 2000). Their distribution is controlled by both the local scale geologic processes that resulted in ore deposition and, in many cases, large-scale tectonic or geodynamic processes that mobilise metals from their sources. As a result, particular deposit types are clustered in geologic provinces that exhibit strong endowments in particular mineral commodities (Jaireth and Huston, 2010) and occur in specific intervals of the geologic record. The deposits form as part of the natural earth processes that have occurred both in the subsurface environment and on the seafloor from approximately 3500 Ma – present day (Soloman and Groves, 2000).

The Yilgarn Block in Western Australia is the largest Archean craton in Australia, and is well-known as one of the world's most economically productive regions in terms of mineral wealth (Witt and Hammond, 2000). The Yilgarn is predominantly made up of 3050 to 2650 Ma granitoid-greenstone successions that are well-known for their world-class endowments of Au and komatiite-hosted NiS deposits. In addition, appreciable high-grade Fe deposits have been located, as well as significant volcanogenic massive sulphide (VMS) deposits. However, the orogenic Au-deposits of the Yilgarn Craton are the

dominant mineral deposit type, and have produced 170 million oz of Au from this region since the 1890s (Phillips, 2004). The abundance of Au has been attributed to the complex structural evolution of the craton during the Archean, whereby a developing plate tectonic regime resulted in a variety of geologic processes related to orogeny (Bleeker, 2015). Czarnota et al. (2009) discuss the relevance of the Yilgarn Cratons regional-scale anastomosing fault networks and explain that these high-strain structures are essential for tapping Au and metal-rich fluids from deep in the mantle. Providing a pathway for these deep mantle-sourced fluids is therefore a key factor controlling the formation of an orogenic lode-Au system (Wyman et al., 2016). As such, the geodynamic evolution of a craton is a major influence on the formation of mineralising systems, and understanding the structural geology and tectonics in a region of interest is essential in mineral exploration and targeting (Czarnota et al., 2009).

Similarities that exist between global mineralising systems allow these systems to be classified into a distinct deposit type. Classification is assigned according to the various geologic parameters that the system exhibits, such as geologic setting, host rocks, metal inventory, or conceptual model of formation. However, there are a multitude of deposits, such as Deflector, that do not conform to any one mineral deposit type, indicating the deposit may have had a complex history of formation that has been the result of multiple mineralisation events. Deflector's unusual structural characteristics in light of a typical Yilgarn Au deposit, as well as the fact that it contains significant reserves of both Au and Cu, warranted further research on this mineral system. As such, this Honours study undertook a petrographic and geochemical analysis on the three lodes in the deposit in order to determine Deflector's style of mineralisation. With the above issues in mind, the study assessed whether Deflector is a modified orogenic deposit, an orogenic Au overprint on an earlier deposit, or a distinct Au-Cu type. In addition, this project also endeavoured to determine the source of the mineralising fluids, and establish geochemical vectors to mineralisation in the surrounding GGB. Doray Minerals' decision to develop the property further highlighted the need for additional study, and the company agreed to support this research project.

2. LITERATURE REVIEW

2.1 THE LATE ARCHEAN

The late Archean refers to a period of time spanning from 2800 to 2500 Ma, and is recognised as being a period of fundamental change in many aspects of the geologic record (Laurent et al., 2014). The importance of this geologic era can be attributed to a number of significant events that were continuing or beginning to take place during this time, and which subsequently resulted in the development and preservation of many complex and diverse geologic structures that may be host to a large number of economically significant mineral resources (Anhaeusser, 2014)

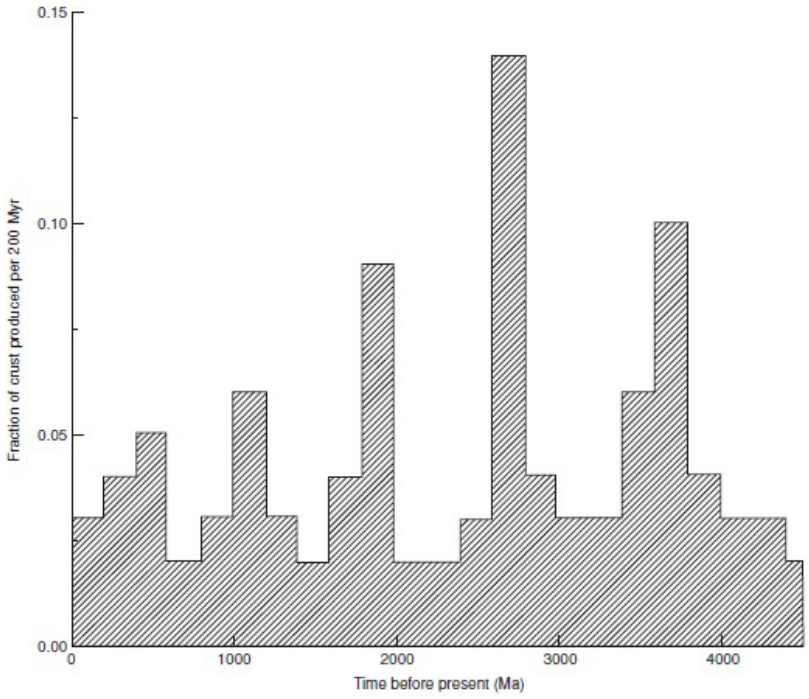

***Figure 1**: Histogram showing the estimates rates of continental growth averages over 2 million year intervals based on Sm-Nd model ages (Robb, 2008).*

2.1.1 Late Archean Crustal Growth

One of these fundamental changes includes the formation of the Earth's crust: the late Archean records the most important period of crustal growth in Earth history (Robb, 2008). Figure 1 illustrates that there are discrete episodes of enhanced crustal growth throughout Earth's development and approximately 50-60% of the Earth's present day crustal volume had been produced by the end of the Archean (Robb, 2008). The data

presented in figure 1 suggests that this occurred in two major episodes; the first at 3600 – 3500 Ma, and the second during the late Archean at 2800 – 2500 Ma (Robb, 2008). During the earlier Archean, heat production from the decay of long-lived isotopes such as U, Th, and K, was greater by a factor of two to three times than it is at present day but it had dropped significantly by the late Archean (McCulloch and Bennett, 1994).

2.1.2 Late Archean Geodynamics

Whilst the late Archean marks the time of an evolving geodynamic regime, it should be noted that geodynamic processes resembling plate tectonics are widely considered to have appeared by ~ 3000 Ma (Korenaga, 2006). Some researchers suggest that the structural evolution of late Archean greenstones was primarily controlled by gravitational influences (plume-driven tectonics), whilst others argue for a compressive style of deformation that resulted entirely from the "horizontal" forces of plate tectonics (Anhaeusser, 2014). In most cases, however, researchers accept the possibility of both plume and plate tectonics in the Late Archean (Davis, 1992; Czarnota et al., 2009; Bleeker, 2015). Davis (1992), for example, suggests plume-tectonics are not an alternative for plate tectonics, and explains that mantle plumes most commonly arise from a lower, hot thermal boundary layer, whereas plates arise in the upper, cold thermal boundary layer. Furthermore, Davies (1992) draws the conclusion that plates and plumes are thus complementary processes, rather than being mutually exclusive. In support of plate tectonics during the Archean, Kerrich and Polat (2006) suggest that a vigorously convecting mantle in the hotter Archean Earth is expected to have resulted in the operation of horizontal plate motion. Proponents of subduction tectonics provide geochemical evidence that shows some Archean rocks have an "arc" signature, where the core features of the arc signature are the decoupling of high-field strength elements and large-ion lithophile elements (Polat and Kerrich, 2006). These features indicate subduction related processes, as their development relies on the burial of hydrated crust down into the mantle. Thus, the importance of this period can be attributed to a number of developments, including a changing geodynamic regime, a dramatic increase in crustal growth and a transition from a carbon dioxide rich to oxygen rich atmosphere (Anhaeusser, 2014; Robb, 2008). These changes likely contributed to the first widespread occurrence of many ore deposit types at this time (Barley and Groves, 1992).

2.1.3 Late Archean Greenstones

A typical segment of late Archean cratonic crust consists of three contrasting lithologies, including: (i) "grey gneisses", comprising a meta-sedimentary and meta-igneous rock assemblage of major low-K granitoid gneisses; (ii) supracrustal, meta-sedimentary and meta-volcanic rocks forming the greenstone belts; and (iii) late high-K granitoid plutons and batholiths, which typically intrude the two former lithologies (Laurent et al., 2014). The greenstone belts in these assemblages are elongate to variably shaped Archean to Proterozoic aged rocks that comprise felsic volcanics, intrusive to extrusive mafic to ultramafic igneous rocks, and interflow or cover sedimentary rocks (Laurent et al., 2014). The late Archean greenstones are most commonly of low to intermediate metamorphic grade (however, they can exhibit higher grades), and their green colour is attributed to their mafic to ultramafic mineral constituents (Laurent et al., 2014). These greenstones are significant due to the fact that they have been intruded by successive igneous bodies, including a variety of ultramafic, mafic, and granitoid rocks that were emplaced as batholiths, stocks, plutons, igneous complexes, and accompanying dyke-like intrusions (Laurent et al., 2014). As a result, the late Archean greenstones record multiple phases of metamorphism, deformation, and metasomatic alteration, and collectively provide evidence of the fundamental geodynamic changes occurring at this time (Anhaeusser, 2014). Therefore, the late Archean marks the moment when the volume of the continental crust grew rapidly (Korenaga, 2006). In addition, the continental crust became stiff enough for deformation to be focused along sub-linear orogenic belts during this time. Rey and Coltice (2008) explain that during much of the Archean, the continental crust was too weak and hot to sustain high topographic anomalies. Therefore, the development of collisional orogens may only have become possible between 3000 and 2500 Ma (Laurent et al., 2014).

2.1.4 Recent Structural Frameworks and Lode Au Systems

Detailed structural studies around Au districts in Australia and Canada have provided similar details concerning crustal events during late Archean orogenies. Czarnota et al. (2009) developed a new integrated tectonic framework of the Eastern Goldfields Superterrane (EGS) in the Yilgarn Craton, Western Australia, by building upon the tectonic model put forward by Swager (1997). It was proposed that in order to

account for the EGS regional-scale fault systems and their associated anastomosing network of high-strain zones, a combination of long-lived extension and transtension/transpression events, greenstone deposition, late basin development, contraction events, folding and strike-slip shearing, and granite emplacement must have occurred to account for these structures. Bleeker (2015) sought to resolve the same issues as Czarnota et al. (2008) but conducted his research in Ontario, Canada. The tectonic framework arrived at by Bleeker (2015) is very similar to that of Czarnota et al. (2008), with Bleeker (2015) further emphasising the importance of thrust tectonics in favouring the preservation of Au deposits and synorogenic basin remnants.

The strong structural control of lode Au systems within or close proximity to major fault zones in Late Archean granite-greenstone terranes suggests a relationship to the complicated kinematic history of these structures. Czarnota et al., (2009) suggest shear zones developed during the Late Archean were imperative in order to tap deep fluids and metals from the mantle (Czarnota et al., 2009). In order for lode Au deposits to be able to form in these structures, plate tectonics must have been active well before the formation of the lode Au systems (Bleeker, 2015).

2.2 THE LATE ARCHEAN AU METALLOGENESIS AND MINERAL DEPOSIT TYPES

The late Archean is host to significant metallogenic provinces of Au, Ni, Fe, and Cu-Zn. Komatiite-hosted Ni deposits are, naturally, restricted to the Archean because of their association with the ultramafic flows (Kerrich and Polat, 2006). Base-metal massive sulphides, which require heat and the convection of seawater through ocean floor crust, are relatively easy to form in ocean floor environments and are recorded throughout most of Earth's preserved geological history. A number of Au deposit types, however, also become common in the late Archean for the first time. In fact, every common Au deposit of the Phanerozoic (Figure 2; Dube and Gosselin, 2007) has been claimed to exist in the late Archean, thus emphasising the importance of geodynamics in their formation.

2.2.1. Reduced Intrusion-Related Au Systems

Reduced intrusion-related Au systems (IRGS) are a relatively new class of economically significant Au deposits that are associated with the emplacement of granitic plutons behind a collisional or accretionary orogen (Hart, 2005).

Simplistically, reduced IRGS imply a genetic connection between granitic plutons and Au ores, and are best developed in intrusions that were emplaced into rocks of the deformed continental margin backstop (subduction-related magmatic arcs) (Hart, 2005). Observations of reduced IRGS suggest that these systems are preferentially hosted in strata that include reducing basinal miogeoclinal sedimentary or metasedimentary rocks (Groves et al., 2003). The ore is variably intrusion and country-rock hosted consisting of disseminations, skarns, replacements, stockworks, and veins (Hart, 2005). However, sheeted veins are the most distinctive style of Au mineralisation in reduced IRGS, and consist of sheeted arrays of parallel, single-stage, low-sulphide quartz veins that are preferentially located in the pluton's cupola, and found over 10s to 100s of metres (Groves et al., 2003). These veins are a distinguishing feature, as they are unlike the interconnected, multidirectional stockworks that are characteristic of porphyry systems, or antithetic tensional vein arrays that are typical of orogenic Au deposits (Bierlein et al., 2003). In terms of the pluton that is responsible for mineralisation, the thermal gradients in the intermediate areas surrounding the pluton are steep, with the results being metal zones that develop just beyond the thermal aureole. The pluton should exhibit physical features, as well as geochemical support, for fluid exsolution, high volatile contents, evidence of rapid fractionation, porphyry textures, zoned plutons, and/or unidirectional-solidification textures, preferentially in the pluton's apices (Hart, 2004). Hart (2004) suggest reduced IRGS are coeval (± 2 million years) with their associated, causative pluton.

Reduced IRGS have been commonly misclassified as orogenic Au deposits as a result of the wide ranging characteristics that both these deposit types share (Bierlein et al., 2003). Both deposit types form from fluids with similar compositions, as well as form in environments that host large volumes of felsic magma (Hart, 2005). Whilst the EGS in Western Australia contains many orogenic Au systems, the Carosue Dam Au camp represents an important example of a large Archean, intrusion-related hydrothermal system, with a number of contrasting styles of Au mineralisation (Witt and Hammond, 2008). Within the Carosue Dam district, large-scale hydrothermal and geochemical zoning is observed, which are hypothesised to be spatially related to monzonitic, syenitic,

and lamprophyric intrusions. As of June 2004, approximately 0.5 Moz of Au had been produced from the camp (Witt and Hammond, 2008).

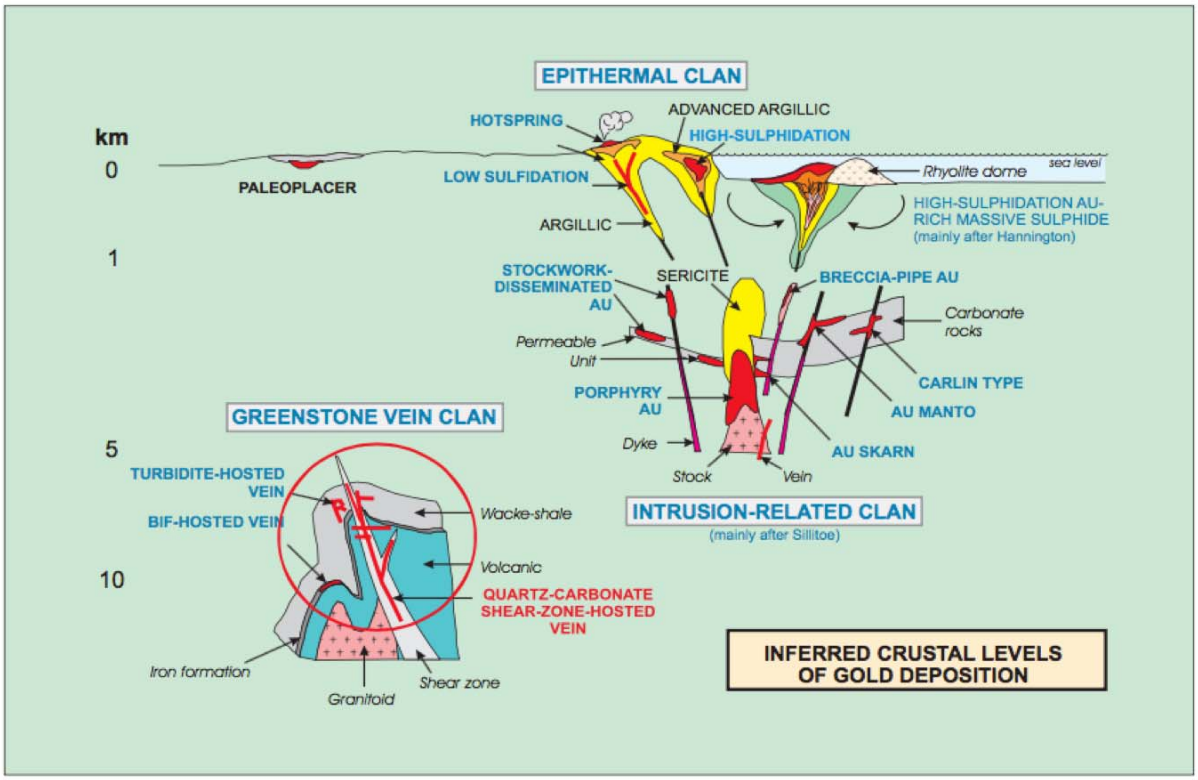

Figure 2: *Inferred crustal levels of various mineral deposit types (Dube and Gosselin, 2007).*

2.2.2 Porphyry Cu-Au

Porphyry deposits are hydrothermal mineral systems that are significant repositories of Cu, Au, Ag, and Mo (Cooke et al., 2005). The global distribution of porphyry systems suggest these deposits most commonly occur along convergent plate margins, where oceanic lithosphere is subducting back down into the Earth's mantle (Figure 3; Wilkinson, 2013). As a result, they are clearly linked to plate tectonic geodynamic regimes. The giant deposits are clustered within three provinces around the world: southwest Arizona to northern Mexico, central Chile, and northern Chile (Corbett, 2009).

Porphyry systems are most commonly found in variably eroded calc-alkaline magmatic island arcs, and may also be coupled with back arc rifts (Corbett, 2009). The ore systems result from the condensation of supercritical fluids that are derived either from a crystallising magma reservoir, or a number of linked reservoirs in the shallow crust at depths of 6 - 8 km (Wilkinson, 2003). As the oceanic plates are subducted down

into the mantle, they become dehydrated with increasing temperature, causing them to release fluids (Goldfarb et al., 2001). The introduction of fluids lowers the melting point of the overlying crust, causing it to melt and form magmas that ascend to generate volcanoes and associated porphyry Cu systems (Corbett, 2009). Ore mineralisation and associated alteration haloes occur between 1 - 4 km depth below surface, and are genetically related to the emplacement of magma reservoirs that are located in the shallow crust. Fluids resulting in the formation of porphyry deposits are high-temperature, between 300 - 700 °C (Richards, 2013). The size, grade, and type of mineralisation generated in porphyry Cu systems is thought to be strongly influenced by the rheology and composition of the host rocks (Sillitoe, 2010).

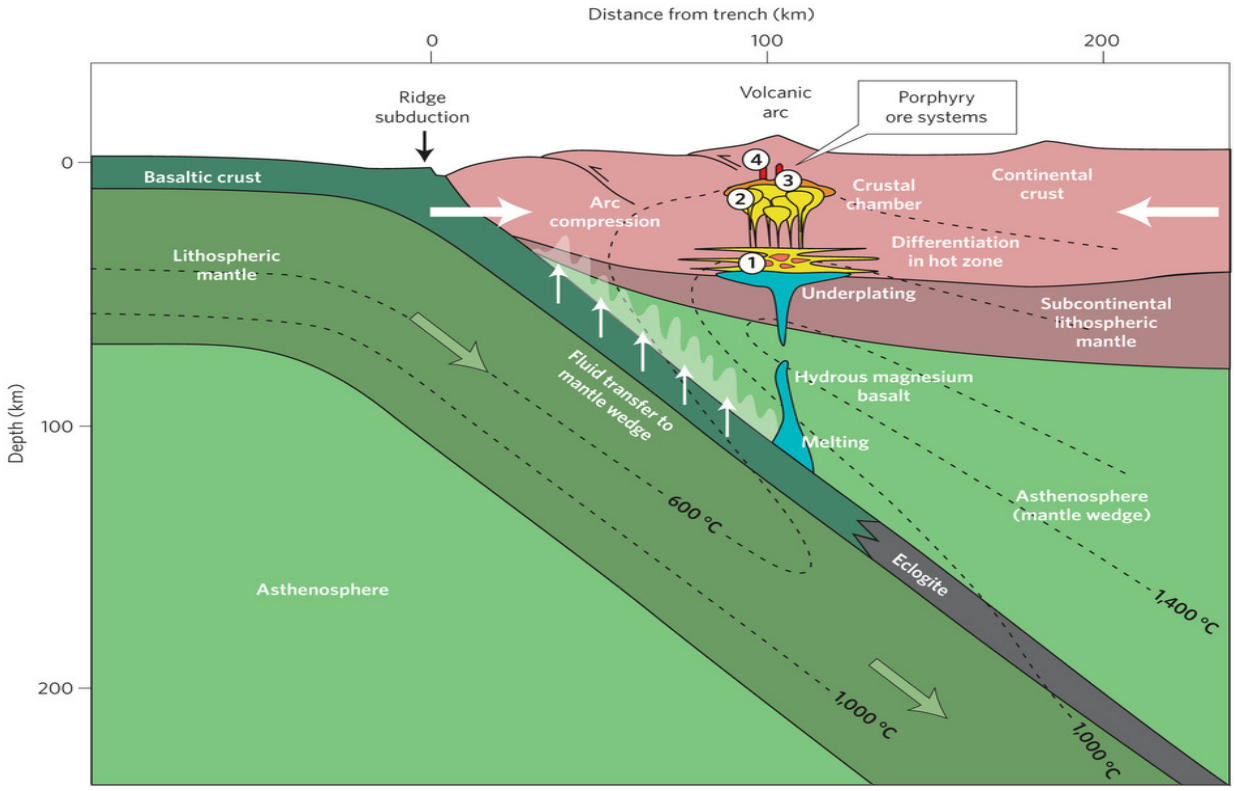

Figure 3: *Suprasubduction zone setting for the formation of porphyry ore deposits (Wilkinson, 2013).*

The Boddington Au-Cu resource located in the southwest Yilgarn craton in the Western Gneiss terrane of Western Australia is a distinct porphyry type (Roth et al., 1991). This late Archean porphyry example has experienced multiple mineralisation and deformation events as determined by Re–Os dating, and is hosted in the northernmost part of the Saddleback greenstone belt. The first is associated with an intermediate shallow level intrusion, which supports the interpretation of an Archean analogy to Phanerozoic porphyry-style mineralisation (Stein et al., 2001). The second

mineralisation event is interpreted to be associated with the development of a late orogenic Au event, which was also responsible for the development of a large number of other Au systems within the Yilgarn. At Boddington, the superposition of two Au-Cu bearing events widely spaced in time has resulted in the formation of a large and economically significant mineral system (Allibone et al., 1998).

2.2.3 Epithermal Au-Cu-Ag

In contrast to the porphyry Cu-Au systems, epithermal Au (± Cu-Ag) resources form at shallower crustal levels, and include precious and base-metal deposits that form at depths of <1.5 km and at temperatures <300 °C (Corbett, 2002). Corbett (2002) documents that the deposits occur within volcanic arcs in subaerial environments at convergent plate margin settings, as well as intra- and back-arc and post-collisional extensional settings. Once a deposit has been classified as epithermal, they can subsequently be classified into either high or low sulphidation deposits, based on variations observed in their hypogene sulphide assemblages (Sillitoe and Hedenquist, 2003). This classification is mainly derived from two varying fluid types and also different paths of fluid evolution (Corbett and Leach, 1998).

High sulphidation epithermal systems have a very wide occurrence in young, poorly eroded volcanic arcs worldwide, with deposits ranging from shallow host-rock or breccia-controlled examples to structurally controlled and deeper-seated examples (Robert et al., 2007). Many high sulphidation systems occur in volcanic rocks and are frequently associated with subvolcanic intrusions. In terms of fluid characteristics, high sulphidation systems are usually generated from fluids that are enriched in magmatic volatiles (Corbett, 2002). In addition, the fluids in high sulphidation systems have migrated to elevated epithermal crustal settings from intrusion source rocks at depth, experiencing minimal dilution by ground waters or interaction with host rocks (Robert et al., 2007). In comparison, low sulphidation epithermal deposits are established from reduced, dilute, near neautral pH fluids, whereby a progressive dilution of these fluids has occurred as they migrate to higher crustal levels further away from the intrusion heat source (White and Hedenquist, 1995). This is caused by the incorporation of increased

quantities of ground water as the fluids reach shallower levels of the crust (Corbett, 2002).

The Campbell Mine in northwestern Ontario, Canada, is a well-known Archean epithermal system. The mine has been developed within Archean volcanic rocks of the Red Lake greenstone belt, with geochronological evidence suggesting that deposit formation occurred after volcanism but prior to regional metamorphism and late felsic plutonism, between 2722 – 2710 Ma (Penczak and Mason, 1997). Structurally, the orebodies are hosted in epithermal-style veins and vein stockworks associated with strike-slip faults (Penczak and Mason, 1997). Production at Campbell Mine has occurred continuously since 1949, and has produced more than 11 Moz of Au since that time, with an average grade of 20.5 g/t (Goldcorp, 2013).

2.2.4 Volcanogenic Massive Sulphide

VMS deposits are accumulations of metal sulphides (mainly Zn, Cu, Pb, Ag, and Au) that precipitate from heated hydrothermal fluid associated with volcanically active under-sea environments (Ridley, 2010). Volcanism in this context is associated with rifting in the Earth's crust, which is caused by extensional forces that pull the crust apart (Mason et al., 2005). As a result, magma rises up from the mantle into the area experiencing extension, where it eventually cools and expels volatiles that carry valuable elements towards the surface. Gaboury and Pearson (2008) report that there are over 850 deposits worldwide that contain over 200,000 tonnes of resource, ranging from 3400 Ma deposits in the Pilbara Block in Australia, to actively forming deposits in modern seafloor spreading such as in the Manus Basin. Au-rich VMS deposits are known in some Archean greenstone belts, including the Horne deposit of the Abitibi belt (54 Mt at 6 g/t: Dube, et al., 2005).

2.2.5 Classic Orogenic Lode Au

Orogenic lode Au deposits (also greenstone Au; Archean lode Au; Shear zone hosted mesothermal Au; Quartz-carbonate lode Au) are a distinct class of mineral deposit that have been the source of a large proportion of world Au production (Goldfarb et al., 2001). As the name suggests, these deposits form in accretionary or collsional environments, dominantly in metamorphic rocks in the mid- to shallow crust at approximately 5 – 15

km depth, at or above the brittle ductile transition (Tomkins, 2013). The compressional setting of these deposits facilitates the transfer of hot Au-bearing fluids from deeper levels of the lower crust, whereby the deformation induced by the structural setting results in the development of large fault networks (Tomkins, 2013). These structures and their associated splay faults provide a transporting medium within which the mineralising fluids can migrate to shallower crustal levels. The rapid rise of these Au-rich fluids from deeper levels in the crust results in them being taken out of equilibrium with their surrounding environment, promoting the Au to precipitate out of solution (Groves and Foster, 1991). This results in the primary (hypogene) Au ores existing in quartz-rich veins surrounded by large alteration haloes in both metamorphosed supracrustal rocks, and granitoids in granitoid-greenstone belts (Eilu and Groves, 2001).

Orogenic deposits are thus epigenetic, structurally controlled deposits, in which Au is frequently the only economic material (Eilu and Groves, 2001). Whilst they are often referred to as mesothermal deposits, petrographic, textural, and structural relationships indicate that orogenic lode Au deposits can form under a range of metamorphic PT conditions, which extend from sub-greenschist to lower-granuite facies conditions (Knight et al., 2000). It is believed that these metamorphic rocks, as well as the fluid provided by the felsic to intermediate magmas that develop in this tectonic setting, are the source of Au (Tomkins, 2013).

Goldfarb et al. (2001) explain that the late Archean was an exceptionally favourable period for the formation of orogenic Au deposits, and attribute this to the changes that were occurring during this geologic time. Goldfarb et al. (2001) assert that collisional orogeny accompanying developing plate motions involved the widespread emplacement of felsic alkaline igneous rocks, and the reactivation of earlier formed faults and shear zones, including terrane and superterrane boundaries, and may have been a critical influencing factor for the large-scale migration of Au vein-forming fluids (Robert et al. 2007). Individual orogenic veins may vary from a few centimetres to approximately 5 metres thick, and from 10 to 1000 metres long (Eilu and Groves, 2001). The vertical extent of the orebody is frequently larger than 1 km and sometimes exceeds 2 km in a few cases (Tomkins, 2010). Kalgoorlie in Western Australia is host to a significant giant lode-Au system, which has a recognised resource of > 130 Moz Au (Goldfarb et al., 2001).

2.3 CHEMICAL EXPRESSION OF HYDROTHERMAL AU DEPOSITS

Ore deposits are expressed chemically as the crustal concentrations of valuable elements consisting of minerals formed by diverse geologic processes (Robert et al., 2007). Trace element abundances are very important in this context, and whilst they only constitute a very small fraction of a system of interest, their variations are much larger than that of major elements and thus provide much more crucial information that is not available with variations in the major element concentrations (Gifkins et al., 2005). In addition, trace elements have a much larger range in behaviour than major elements, and some are much more sensitive to processes to which major elements are insensitive (Rollinson, 1993).

Distinct Au deposit types have a unique geochemical signature expressed through their trace element abundances, allowing differentiation from other mineral deposit types. Knowledge of these trace element abundances is beneficial in exploration geoscience and mineral targeting, as it provides a means to 'vector-in' towards as yet undiscovered zones of mineralisation.

2.3.1 Reduced Intrusion-Related Au System

Reduced intrusion-related Au systems are most commonly expressed by a metal assemblage variably combining Au with As ± Bi ± Mo ± Sb ± Te ± W, with a low base-metal content (< 5%) (Hart, 2005). The ore mineral assemblage is reduced, and typically comprises arsenopyrite, pyrrhotite, and pyrite, whilst lacking any magnetite or hematite (Bierlein et al., 2013). Vertical mineral zoning is common in reduced intrusion-related Au systems, but tends to differ with the depth of each respective system (Sillitoe and Thompson, 1998).

2.3.2 Porphyry Cu-Au and Epithermal Au (± Cu-Ag)

Porphyry Cu-Au systems exhibit primary Cu mineralisation with Au ± Mo ± Ag being the most important by-products (Corbett, 2009). Trace element studies at the deposit scale have illustrated that Cu, Mo, Au, Ag, Ba, Pb, Zn, As, Sb, and Te make up suites relating to alteration zoning within porphyry systems (Corbett, 2009). In the hypogene areas of

porphyry Cu systems, chalcopyrite is the most predominant Cu-bearing mineral, with bornite, enargite, and chalcocite also making an important contribution (Corbett, 2009). Other associated minerals may include galena, sphalerite, tetrahedite, and Au-tellurides.

Epithermal Au-Cu-Ag can be subdivided into either high or low sulphidation systems, whereby high sulphidation epithermal veins have an Au-Ag-Te-As ± Cu-Pb-Zn geochemical signature, whilst low sulphidation epithermal veins have an Au-Ag-Te geochemical signature (Corbett, 2002). Corbett (2002) reports that higher Cu contents appear in deeper systems, with Au occurring more abundantly at higher crustal levels.

2.3.3 Volcanogenic Massive Sulphide

Trace element studies of VMS systems show a geochemical signature of Cu-Pb-Zn ± Co-Ni-Fe-Ga-Ge-As-Se-Mo-Ag-Cd-In-Sn-Sb-W-Au-Hg-Ti and Bi (Gibson et al., 2007). The relative proportions of these elements and their concentrations are a function of the overall rock associations and fluid chemistry (Ridley, 2010). All VMS deposits exhibit some degree of geochemical mineralogical zoning, which is a function of temperature, fluid-composition, fluid mixing, and porosity/permeability (Ridley, 2010). VMS deposits may exhibit low to very high sulphidation minerals (Gibson et al., 2007).

2.3.4 Classic Orogenic Lode Au

Orogenic lode Au deposits are characterised by quartz-dominant vein systems with ~5-15 % carbonate minerals and ~3-15 % sulphide minerals (Dube and Gosselin, 2007). These structurally-controlled Au-bearing vein systems exhibit variable enrichments in Ag ± As ± B ± Bi ± Hg ± Sb ± Te ± W, with Cu, Pb, and Zn concentrations being only slightly elevated above regional background levels (Goldfarb et al., 2001). Native Au with pyrite, pyrrhotite, and arsenopyrite are the most common ore minerals (Tomkins, 2010). Orogenic systems exhibit a strong lateral zonation of alteration phases from proximal to distal assemblages on the scale of metres (Figure 4, McQueen, 2004; Dube and Gosselin, 2006).

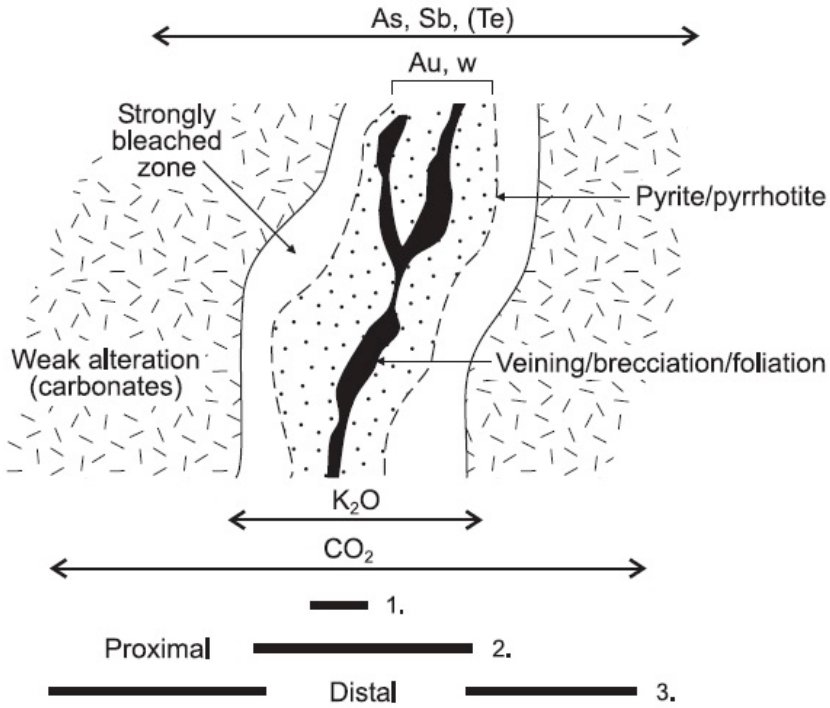

Figure 4: *Element zonation and alteration patterns around orogenic lode Au deposits in mafic rocks. Alteration minerals: 1. K-micas, V-, Cr-bearing micas; 2. Sericite-carbonates (siderite, ankerite, dolomite), biotite-amphibole-plagioclase ± magnetite-epidote; 3. Chlorite-calcite ± magnetite-epidote (McQueen, 2004).*

2.4 GEOCHEMISTRY AND HYDROTHERMAL ALTERATION

Geochemistry is a fundamental field in the study of mineral deposits. As has been discussed in the above sections, mineralisation within a specific deposit type involves a number of different processes, of which chemical processes are the ones that finally result in the precipitation and expression of metals or ore forming minerals (Carranza, 2012). Studying and understanding the geochemical characteristics of the diverse range of mineral deposit types is therefore very important in: (a) mineral deposit classification; (b) understanding ore genesis; (c) mineral exploration; and (d) extractive metallurgy or mineral processing (Brown and Milton, 2005). On a utilitarian level, geochemical datasets that are used in mineral exploration are very important tools for the identification of broad chemical haloes and gradients (or vectors to mineralised zones), and also discriminating between prospective and non-prospective targets (Carranza, 2012). There are a wide range of established and mature analytical techniques that are employed in geochemistry, with each technique specifically developed to target different characteristics of a given sample (Kemp and Gotze, 2008). In mineral deposit systems, the trace elements that occur are considered to represent important indicators of the

physiochemical conditions of mineral genesis and subsequent alteration (Kempe and Gotze, 2008).

2.4.1 Hydrothermal Alteration Haloes

Zones of alteration or replacement are frequently developed around a number of structural features, such as shear zones, faults, plugs, dykes, and unconformities (Bierlein et al., 2000). These areas are either defined as alteration haloes, where the pre-existing properties of the host rock are enhanced or depleted, or replacement zones, where the original properties of the rock are completely replaced without regard for the original values (Brown and Milton, 2005). The mineralogy of many ore systems can largely be attributed to hydrothermal alteration processes where the chemical alteration of the host rock results in metal-rich zones (Au, Cu, Sn, etc.). Tectonics, volcanism, and heated water all combine to form a hydrothermal alteration process, where the initial mineralogy of a given rock is altered due to changes imposed by the chemical composition of the externally derived fluids (Bierlein et al., 2000).

The passing of hydrothermal fluids from a source to nearby igneous and metamorphic rocks is controlled by rock fractures or porous spaces, allowing the focused flow of fluid (Brown and Milton, 2005). These fluids have the ability to carry metals and other elements into and out of the vicinity of a forming ore body, which generates an alteration halo in the wallrock as a chemical reaction occurs (Bierlein et al., 2000; Brown and Milton, 2005). The characterisation of the exact nature of the alteration can be difficult, however systematic descriptions of alteration textures, alteration mineral assemblages, patterns of distribution and overprinting relationships, and preservation of relict minerals and textures, combined with interpretations of alteration indices and compositional changes all provide important information for subsequent alteration indices and meaningful genetic interpretation (Bierlein et al., 2000). A common issue that can arise with alteration identification is misclassification with either metamorphism or diagenesis. The latter two processes are regionally extensive processes that result in weakly altered rocks with delicate volcanic textures that have been preserved from the original rock. In contrast, hydrothermally altered rocks, especially those associated with

mineralisation, have variable intensity, are local in their distribution, and generally destroy primary textures (Polat and Kerrich, 2000).

Eilu et al. (2001) summarised a number of factors that determine the hydrothermal alteration in a given body of rock. They suggested that: (a) temperature is the most significant factor in hydrothermal alteration because most of the chemical reactions require elevated temperatures, and minerals are also thermodynamically stable; (b) the permeability and structure of the rocks controls the access of thermal fluids, which cause hydrothermal alteration of the rocks and precipitation of secondary minerals in open spaces; (c) pressure indirectly affects hydrothermal alteration, as it controls the depth at which boiling occurs; (d) the initial chemical composition of the host rock determines the availability of components to form alteration minerals; and (e) the pH and composition of the fluid greatly determine the rate and types of hydrothermal minerals to be formed in a given geothermal system.

Understanding the alteration zones in a mineral system has a number of useful applications (Brown and Milton, 2005). Alteration minerals that form from the passing of a hydrothermal fluid can be used as geothermometers, as these minerals will only form in a specific temperature range (Eilu et al., 2001). For example, the alteration mineral albite may only form at temperatures between 160°C – 320°C, and prehnite may only form at temperatures between 220°C – and 320°C (Brown and Milton, 2005). In addition, understanding the alteration mineralogy allows researchers to understand the exact nature of the reservoir, such as upflow, outflow, and marginal zones; the structures that control the geothermal fluids; prediction of possible boiling and/or high gas zones; and identifying past fluctuations in the thermal system (Bierlein et al., 2000). Lastly, the analysis of alteration haloes around an ore-zone allows us to acquire geochemical vectors to mineralisation that can be used to pigeonhole new undiscovered mineral systems.

2.4.2 Geochemical Vectors to Ore

Studying the alteration-related variations in wall-rock geochemistry around mineralised systems allows the characterisation of a geochemical signature for a given deposit type (Eilu et al., 2001). Each deposit type has its own unique geochemical signature, whereby the different metal zoning and alteration patterns around these

deposit types provides vectors to ore (Dube et al., 2007). Knowing this geochemical signature allows explorers to 'vector-in' towards as yet undiscovered mineralisation, whereby movement into the ore zones results in a stronger expression of the geochemical signature. For example, as described in section *2.3.4 Classic Orogenic Lode Au*, the ores in this specific deposit type have an association of Au-Ag-As-W-Sb-Te-Ba with variable Cu-Pb-Bi-Mo-Zn. There are a number of elements in this geochemical signature that demonstrate a useful primary dispersion halo, which include As, Sb, Te, Au, and Ba. The orogenic fluids that control the distribution of these elements produce characteristic wall rock alterations, resulting in the formation of Fe sulphides, K ± Na metasomatism, and carbonate alteration. Therefore, knowing the primary ore deposit expressions (i.e. element and mineral distributions) useful tool for uncovering deep or blind ore systems (McQueen, 2004).

3. REGIONAL AND LOCAL GEOLOGY

The Yilgarn Block in Western Australia is one of the world's most ancient cratonic blocks, believed to have formed principally between 3000 and 2600 Ma (Swager and Nelson, 1997). The block is a highly mineralised granite-greenstone terrane with surface geology consisting of more than 80% granitic gneiss and granitoid rocks (Hodkiewicz et al., 2005). The remainder of the block is largely made up of metasedimentary and metavolcanic rocks in arcuate greenstone belts, which on the basis of distinct sedimentary and magmatic associations, geochemistry, and ages of volcanism, has been divided into a number of distinct terranes (Figure 5). These include the older Narryer Terrane in the northwest of the craton, the more deformed South West Terrane (which is largely composed of medium and high-grade metamorphic rocks), the dominantly younger EGS, and the Youanmi Terrane (Cassidy et al., 2006). The Youanmi Terrane is further subdivided into the Southern Cross and the Murchison Domains, which are defined along a major shear zone (Swager and Nelson, 1997).

Phillips (2004) estimated that orogenic Au deposits have accounted for 5,300 t (170 million oz) of Au production from the Yilgarn Craton since the 1890's, with a noticeable amount of this production coming from the greenstone belts of the EGS. Although the EGS is one of the most Au endowed regions in the world, the Murchison Domain within the Youanmi Terrane is also widely enriched in Au mineralisation, with major mining camps including Mount Magnet, Big Bell, and Cue. An underexplored area of the Murchison Domain is the GGB which contains numerous mined-out or partially mined-out open pits and historic underground workings, as well as up to 80 known soil geochemistry, gravity, or aeromagnetic geological anomalies (Godden, 2008). From the most western margin of the Yilgarn, which is defined by the Darling fault, the GGB is the first occurring greenstone belt of any significance within the craton, occurring approximately 70 km East of the Darling Fault. In addition, the GGB also contains the deposit that is the focus of this Honours study, Doray Mineral's Deflector Au-Cu project, which occurs 50 km southwest of Yalgoo and 70 km NNE of Morawa (Hayden and Steemson, 1998). This section of the report will review the regional and local geology of the Deflector project area.

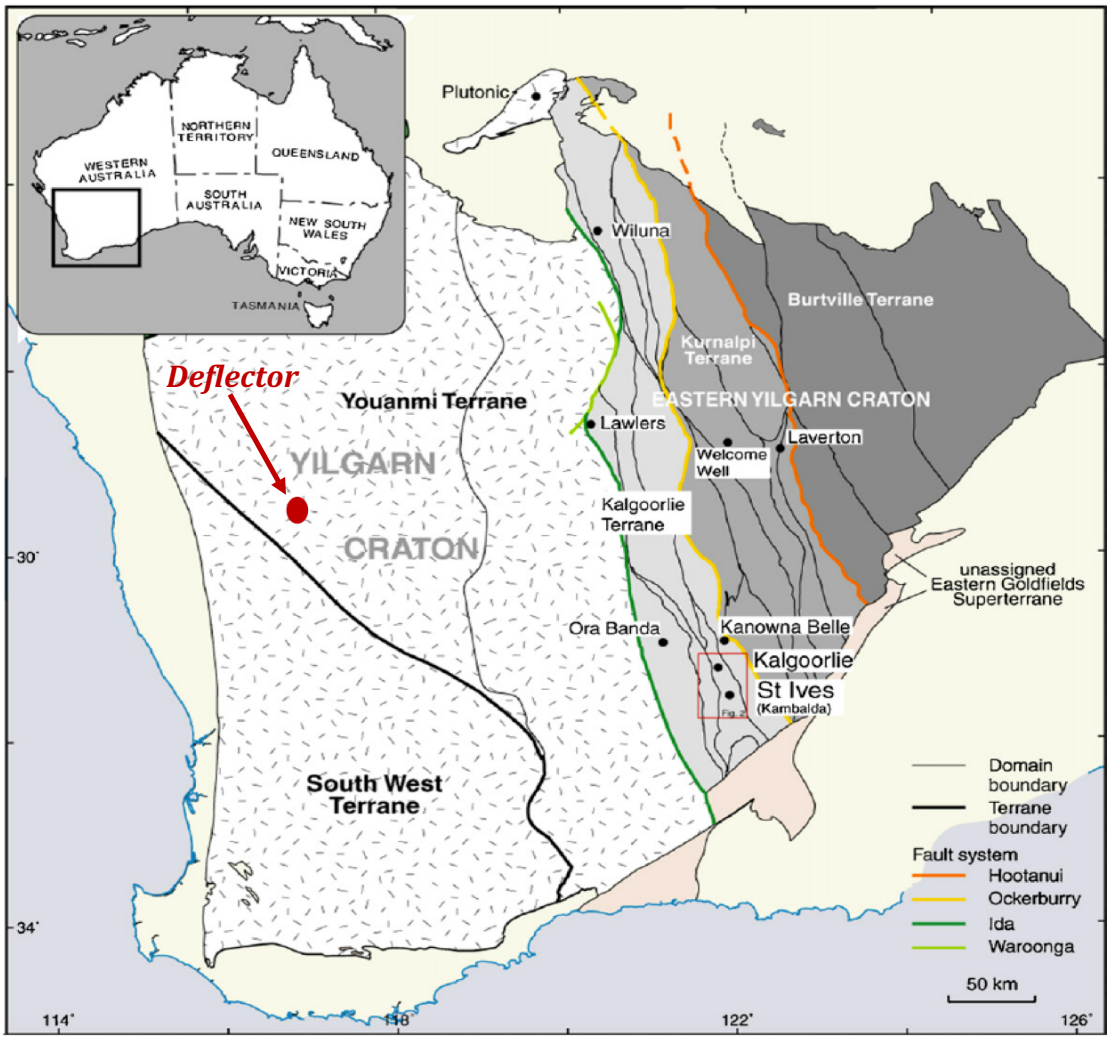

Figure 5: *The Yilgarn craton with subdivisions. The Youanmi terrane is divided by a thin black line into the Murchison in the southwest, and Southern Cross in the southeast. Red dot indicates the location of Deflector, which sits in the southern Murchison domain (Cassidy et al., 2006).*

3.1 REGIONAL GEOLOGY

The Gullewa area is defined by a stratigraphic sequence comprising a lower group of ultramafic and mafic greenstones with minor local BIF, overlain by intermediate and felsic volcanic rocks, with an upper association of clastic sediment including shale, sandstone, conglomerate, and turbidites (Hayden and Steemson, 1998). A regional outcropping mapping exercise completed by Outhwaite (2016) of the Gullewa area proximal to Deflector identified three distinct lithological domains: northern, southern, and eastern. The ensuing discussion will provide details of their characteristics in sequential order.

The Gullewa Goldfield and Deflector occur in the northern domain, which is dominated by high-Mg basalt (Figure 6). The northern Gullewa area contains a distinct package of tholeiitic basalt and banded-iron-formation (BIF), which appears to be the preferred host for much of the known mineralisation. A thin sequence of turbidites and black shales is present in drilling southeast of the Deflector trend, where these rocks appear to young to the southeast towards the Gearless Well trachyandesite. Whilst the Gearless Well trachyandesite has previously been described as a Proterozoic intrusion, the work cited by Outhwaite (2016) suggests that the Gearless Well rocks are an Archean volcanic sequence sitting above the Deflector sedimentary rocks. A typical biotite monzogranite defines the main regional granite, and has a foliation similar in style and orientation to the S1 fabric that affects the greenstones. This suggests that it was intruded prior to, or during, this event. The northern domain of the GGB is cut by quartz-feldspar porphyries, most of which run parallel to S1, but also possess the S1 fabric and associated stretching lineation. These observations suggest that these porphyries cut through folds, and intruded syn-D1. North of Monarch, a distinctive K-feldspar-rich granitoid is exposed. This graitoid appears to have intruded into the S1 foliation, as it does not possess it, however instead has a pervasive, weak S2 fabric. This suggests that it has intruded pre- or syn-D2, meaning it is younger than the regional monzogranite. Northwest of Deflector, there exists another granitic intrusion that is zoned, with a K-feldspar-rich magnetic rim, and a plain monzogranite core (Outhwaite, 2016).

The southern domain is divided into two areas across an interpreted unconformity, whereby the far south is a weathered and poorly exposed mafic. This mafic sequence is observed to contain some additional shale-turbidite-BIF packages, occurring with intermediate-felsic volcanic rocks. The northern half of the southern domain across the unconformity (the centre of the project area) consists of a thick, northward-fining sedimentary sequence, which is interpreted to comprise the youngest rocks in the whole Gullewa project area. The unconformity that separates the two halves of the southern domain appears to truncate the far southern rocks at a low angle. A distinctive polymictic conglomerate that is dominated by jaspilitic BIF and chert clasts lies close to the unconformity, and gradually thickens towards the Salt River fault zone. This infers that it was sourced from the east, where jaspilitic BIF are known to occur. The polymictic conglomerate transitions westward into a pebbly quartz- and lithic-rich grit, which

transitions further westward into mixed quartz grit and black shale. Overlying this is a thick quartzo-feldspathic turbidite sequence, which extends to the northern edge of the margin (Outhwaite, 2016).

The eastern domain, east of the Salt River Fault, is comprised of a mafic- and jaspilitic BIF-dominated sequence. Based upon the observations made above, this domain is likely older than the southern domain conglomerate and turbidite sequence, based on the fact that the conglomerate is dominated by jaspilitic BIF clasts and thickens to the east. The Gullewa project area has been previously interpreted as representing an east-west syncline, whereby mafic rocks exist on the northern and southern limbs, and sedimentary rocks in the core (Hayden & Steemson, 1998). This has been disproved by Outwaite (2016) through the application of various geologic principles to his observations. For example, Outhwaite (2016) states that the bedding-cleavage relationships and minor folds on the southern limb of the belt are S-vergent (indicating the F1 syncline to the northeast), not Z-vergent as would be expected if an ~east-west syncline lay to the north. In addition, the northern domain is stated to have an almost orthogonal major fold trend to the southern domain, and appears to fold back on itself rather than 'wrap around' to the southern limb (Outhwaite, 2016).

There are a number of Au prospects within the GGB that provide scope to this report. Au prospects include Gearless Well, Golden Stream, King Soloman, Monarch, Michelangelo, Gullewa Hill, and Rocksteady, to name a few (Godden, 2008). Comparatively, the occurrence of Au-only mineralisation within the GGB far outweighs base-metal mineralisation occurrences. Isolated intercepts of Cu and Zn have also been recovered at Rocksteady and beneath a gossan at Murdalyou Range at Mugga King, however have been described by other workers as being insignificant (Bromley, 1975). The occurrence of economic grades of Cu mineralisation at Deflector is a significant finding that may have important implications for the prospectively of additional base-metal discoveries within the GGB.

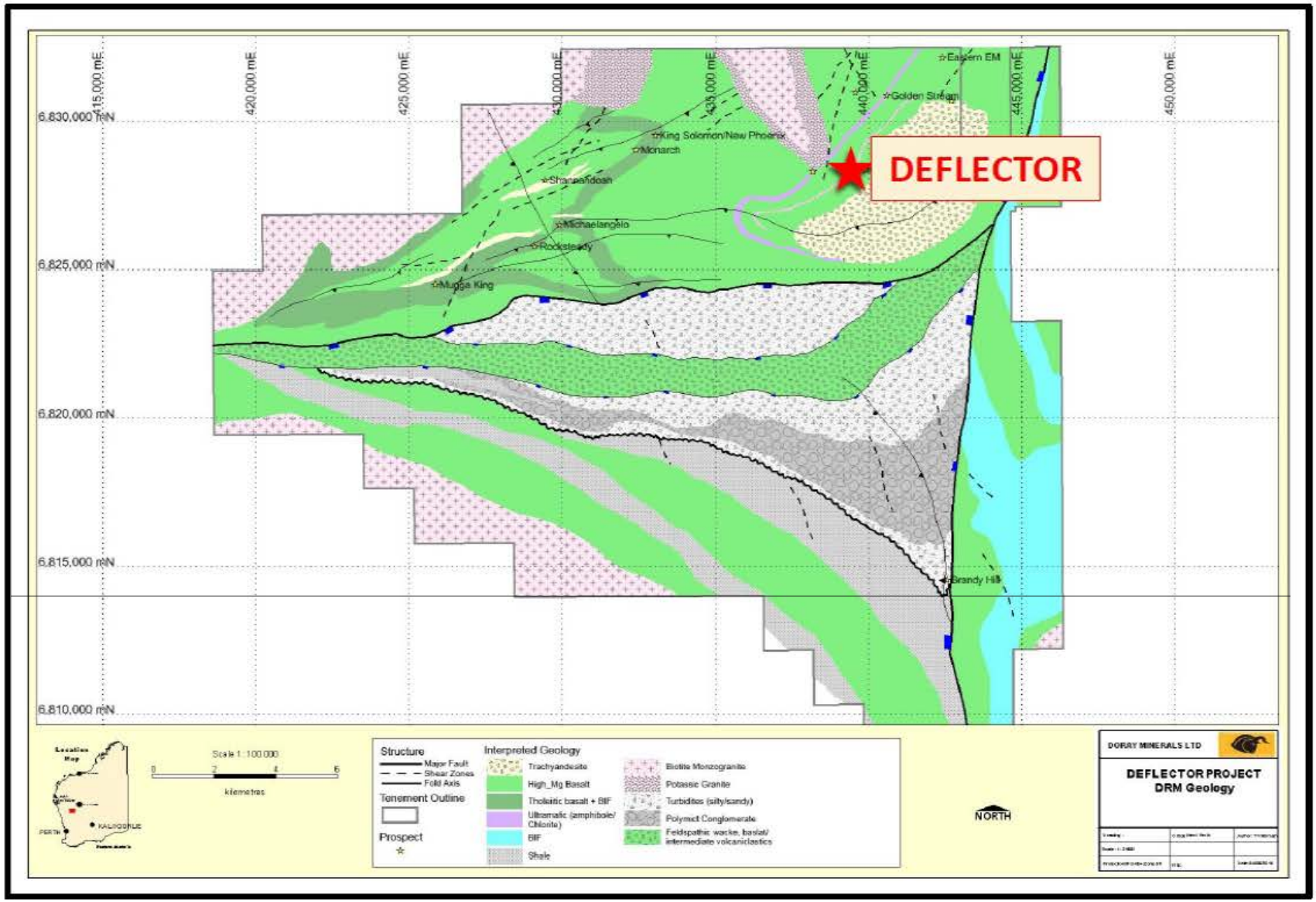
DEFLECTOR
415,000 mE
420,000 mE
425,000 mE
430,000 mE
435,000 mE
440,000 mE
445,000 mE
450,000 mE
6,830,000 mN
6,825,000 mN
6,820,000 mN
6,815,000 mN
6,810,000 mN
Eastern EM
Golden Stream
King Solomon/New Phoenix
Monarch
Shamrock/Doan
Michaelangelo
Rocksteady
Mugga King
Brandy Hill
Scale 1:100,000
kilometres
Structure
Major Fault
Shear Zones
Fold Axis
Tenement Outline
Prospect
Interpreted Geology
Trachyandesite
High_Mg Basalt
Tholeiitic basalt + BIF
Ultramafic (amphibole/ Chlorite)
BIF
Shale
Biotite Monzogranite
Potassic Granite
Turbidites (silty/sandy)
Polymict Conglomerate
Feldspathic wacke, basalt/ intermediate volcaniclastics
NORTH
DORAY MINERALS LTD
DEFLECTOR PROJECT
DRM Geology

3.2 LOCAL GEOLOGY AND PREVIOUS WORK

There is minimal research literature on the Deflector Au-Cu deposit, with the most recent paper dating back to 1998 (Hayden & Steemson, 1998). The Deflector deposit local geology is summarised here from Hayden and Steemson (1998). According to Hayden and Steemson (1998), the Deflector Au-Cu deposit contained an Indicated plus Inferred Mineral Resource of 665 000 t at 4.6 g/t Au and 1.8 % Cu at the time of publication. Au and Cu mineralisation was documented to fall naturally into three steeply dipping, near-vertical veins, herein referred to as West, Central, and Contact lodes.

3.2.1 Cover

The Deflector deposit is hosted within a broad drainage system comprised of sheetwash plus braided channel deposits that transports alluvium from the northwest, through the project area, towards the Salt River (Hayden and Steemson, 1998). The system is documented to be 5 km wide at Deflector, and a total of 12 km long.

3.2.2 Rock Types

The deposit is hosted by a monotonous sequence of pillowed, variolithic, high-magnesium basalts that are intruded by dacitic porphyry, dolerite, and dolerite-lamprophyre dykes (orientated 45 degrees towards 240 degrees) and an exolithic stock (Standing, 2004). Underlying the north-west side of Deflector is a large area of metabasalt that has a stratigraphic thickness of at least 300 metres, strikes 045° magnetic, and dips steeply to the south-east (Hayden and Steemson, 1998). The metabasalt is in contact with a sedimentary unit dominated by siltstone on the south-east side of the deposit.

The high magnesium metabasalt is generally black, fine-grained, extremely hard, and lacks cleavage. A needle-like texture that is similar to spinifex textures in komatiities are observed in approximately half of the basalt units, and the others have poorly developed pillows (Hayden & Steemson, 1998).

The heterogeneous nature of the sedimentary sequence makes rock identification difficult. Siltstone is thought to be the major rock type in the sedimentary zone, which is mostly black and graphitic, however locally pale brown or grey. There is an absence of

cleavage or fissile bedding, and there is evidence to suggest that it has probably been hornfelsed. Quartz-feldspar porphyries and dark grey to black, intermediate biotite lamprophyres are observed to cut the sedimentary sequence. Hayden and Steemson (1998) suggest the lamprophyres are probably offshoots of the Gearless Well trachyandesite, which sits approximately 300 metres south-east of the basalt-sediment contact. Biotite-rich rocks are observed to occur locally within the sedimentary sequence, and are hypothesised to represent the product of potassic metasomatism associated with the biotite porphyries (Hayden and Steemson, 1998). Thin porphyries are observed throughout the entire deflector area, however porphyry dykes are most abundant east of the basalt-sedimentary contact. A dome or pipe-like intrusion of black biotite porphyry has been indicated by drilling data, with its roof approximately 10 metres below the surface. This intrusion appears to be cut by West lode (Hayden & Steemson, 1998).

3.2.3 West, Central and Contact Lodes

All three lodes within Deflector are documented by Hayden and Steemson (1998) to be tabular sheets of mineralisation, all striking northeast with a moderate variation in thickness, and occurring parallel to the enclosing strata. West lode is transgressive and dips vertically to steeply northwest, central lode is near vertical, and contact lode dips east at about 70° and parallel to the basalt-siltstone contact. A unique feature of mineralisation at Deflector compared to other Au deposits of the Yilgarn craton is that the lodes do not appear to occupy shear zones, and the host rocks also lack cleavage. In addition, the quartz-sulphide vein material fills open spaces, and brecciation is common. These features are not characteristic of typical late Archean orogenic Au-only Yilgarn deposits.

Chalcopyrite is documented as being the only significant Cu-bearing mineral in the primary unweathered mineralised areas of the lodes, with the sulphide mineral pyrite also occurring. An oxidized zone exists from the base of the alluvium to a depth of approximately 40 metres, below which there is a transitional zone extending to approximately 70 metres that is dominated by chalcocite and pyrite. The oxidized zone contains the Cu minerals malachite and chrysocolla, with native Cu being common in the lower parts of the zone and closely correlated with cuprite. Hayden and Steemson (1998) document little evidence for pervasive alteration adjacent to the lodes, however state that

rock within the lodes is always chloritised, with biotite alteration occurring locally and carbonate being rare. The hydrothermal fluid and associated mineral assemblage (quartz, orthoclase, chlorite, epidote, biotite, calcite, and pyrite) suggest low temperature, greenschist conditons, and the brittle fracture style of the lode and veinlets suggest mineralisation occurred at a relatively shallow depth (Hayden and Steemson, 1998).

3.2.4 Deflector Geochemistry

Hayden and Steemson (1998) report that the Deflector lodes have a fairly simple geochemical signature. Cu, Ag, and S are strongly anomalous, and also correlate strongly with Au. In addition, Bi, As, Se, Te, W, Mo, and Co are mildly anomalous, and also show a correlation to Au. Sb, Zn, Pb, Sn, and Hg are not present in any anomalous amounts (Hayden and Steemson, 1998).

4. METHODOLOGY

4.1 FIELD WORK AND CORE SAMPLING

Field work and core sampling for this project was completed on-site at Doray Minerals' Ltd. Deflector mine in Yalgoo, Western Australia. Deflector is located 400 km north of Perth, and 160 km east of Geraldton. Samples were taken from ten diamond drill holes, seven of which had intercepts in either West, Central, or Contact lodes. Samples were selected based upon a number of observed characteristics, one of the most important being mineralisation. Particular attention was paid to sections of the core that were barren of any mineralisation, as well as sections of the core that extended into the high grade zones. It was desirable that samples extending into the high-grade zones contained either elevated Au and Cu, elevated Au with low Cu, or elevated Cu with low Au. In addition, the selection of samples with various alteration, textural, and structural features was also of importance.

A total of 80 samples of approximately 7 cm to 38 cm in length were selected from the ten diamond drill holes, which were already either in half or quarter core. From West Lode, four samples were taken from BDRCD042, nine samples were taken from BDRCD073, five samples were taken from 12DD094, and 13 samples from 9DEF037. From Central Lode, nine samples were taken from 12DD059, and five samples were taken from BDRCD031. From the Contact Lode and shales, 11 samples were taken from 12DD081, nine samples were taken from 9DEF021, nine samples were taken from 9DEF013, and six samples from 9DEF031. Sample depths and drill core numbers can be seen in Appendix 1. All samples were photographed and put into sample bags with their associated drill hole number and meterage intervals (Appendix 2). Core trays from which the samples were retrieved from were also photographed.

Samples were transported back to the University of Sydney, where they were prepared for analyses. In the rock-saw facility at the Sydney University School of Geoscience, each sample was cut into a thin section block and a reference block, with the remainder of the sample to be sent for geochemical analysis. Thin section blocks were sent to *Petrographic International, Clontarf, Queensland.* Details of the geochemical analysis can be found in section 5.2, *Geochemical Methods.*

Petrographic thin sections were examined using a Zeiss Primotech transmitted and reflected light microscope. Thin section photos were captured by the Zeiss Primotech's integrated IP 3MP camera.

4.2 GEOCHEMICAL METHODS

All 80 samples were sent to the Australian Laboratory Services (ALS) in Brisbane where they were each submitted for the complete rock characterisation package. This package allows quantification of the major and trace elements in a given sample, as well as base-metals and an additional analysis performed for Au and Ag (Appendix 1). All sample preparation and geochemical analyses were performed by ALS.

Major element oxide concentrations (SiO_2, Al_2O_3, Fe_2O_3, CaO, MgO, Na_2O, K_2O, Cr_2O_3, TiO_2, MnO, P_2O_5, SrO, BaO) in each sample were quantified using Inductively Coupled Plasma – Atomic Emission Spectroscopy (ICP-AES). As the name suggests, the ICP-AES combines a high-temperature inductively coupled plasma (ICP) source with an atomic emission spectrometer, allowing the ICP to convert the atoms of the elements in the sample to ions, at which point the ions are separated and detected by the spectrometer (Caughlin, 2007). This process is fundamentally characterised by the fact that each element emits energy at specific wavelengths that is peculiar to its atomic number. As the electrons fall back to ground state, the energy transfer is unique for each element, allowing for quantification (ALS Global, 2013).

At ALS Brisbane, each prepared sample (0.200 g) is added to 0.90 g of lithium metaborate/lithium tetraborate flux (12:22, $LiBO_2$:$Li_2B_4O_7$). The two components are mixed well and fused in a furnace at 1000 °C. The melt that results from this process is cooled and dissolved in 100 mL of 4% nitric acid/2% hydrochloric acid, where it can then be analysed by ICP-AES, and the results corrected for spectral inter-element interferences. Oxide concentration is calculated from the determined elemental concentration and the result is reported in that format. The total oxide content is determined from the ICP analyte concentrations and loss on ignition (LOI) values. A prepared sample (1.0 g) is placed in an oven at 1000 °C for one hour, cooled, and then

weighed. The percent loss on ignition is calculated from the difference in weight. Carbon and sulfur were also quantified by combustion furnace using a Leco sulfur analyser. Prepared samples (0.01 to 0.1 g) were heated to approximately 1350 °C in an induction furnace whilst passing a stream of oxygen through the sample. The sulfur dioxide that was released from the sample was then measured by an infrared detection system and the Total Sulfur and Total Carbon result provided (ALS Global, 2013).

Inductively Coupled Plasma – Mass Spectrometry (ICP-MS) was used to quantify the trace elements including the full rare earth element suites (Ba, Ce, Cr, Cs, Dy, Er, Eu, Ga, Gd, Hf, Ho, La, Lu, Nb, Nd, Pr, Rb, Sm, Sn, Sr, Ta, Tb, Th, Tm, U, V, W, Y, Yb and Zr). Each sample was prepared (0.200 g) and added to lithium metaborate flux (0.90 g). The two components were mixed well and fused in a furnace at 1000°C. Once the resulting melt had cooled, it was dissolved in 100 mL of 4% HNO_3 / 2% HCl_3 solution, where the resulting solution was then analysed by ICP-MS (ALS Global, 2013).

The lithium metaborate fusion that is used to quantify the trace elements is not the preferred method for the determination of base-metals. Many sulphides and some metal oxides are only partially decomposed by the borate fusion and some elements such as cadmium and zinc can be volatilized. Due to this, Cd, Co, Cu, Li, Mo, Ni, Pb, Sc and Zn concentrations were determined using four acid digestion, and then analysed by ICP-AES (ALS Global, 2013).

As, Bi, Hg, Sb, Se, Te, and Ti concentrations were determined using ICP-MS. Prepared samples (0.50 g) were digested with aqua regia in a graphite heating block. After cooling, the resulting solution was diluted with deionized water, mixed and analysed by ICP-MS (ALS Global, 2013).

Each sample was also submitted for a separate analysis for Au and Ag. Selection of the best fire assay method for the accurate determination of total Au content in a sample is highly dependent on the sample matrix, the grain size and distribution of Au, and the objective of the analytical result. A wide variety of minerals and metals (such as chromite, base-metal sulfides and oxides, selenides, and tellurides) in moderate to high concentrations can interfere with the fire assay process, generally leading to low precious

metal recoveries. With prior knowledge of these minerals and metals, ALS geochemistry can modify flux constituents to improve recoveries. Samples were prepared for fire assay fusion, with a gravimetric finish. For the gravimetric finish, each prepared sample is fused with a mixture of PbO_2, Na_2CO_3, Na_2B_4O, SiO_2, and other reagents in order to produce a Pb button. The Pb button containing the precious metals is cupelled to remove the Pb, where the remaining Au and Ag bead is parted in dilute nitric acid, annealed, and weighed as Au. Ag is then determined by the difference in weights (ALS Global, 2013).

4.2.1 Precision and Accuracy

The upper and lower limits of detection for the geochemical methods described above are presented in Appendix 3.

4.2.2 Data Normalisation

Raw data from the sample analyses performed by ALS were converted to be evaluated without volatile components. Both major and minor element values were multiplied by 100 then divided by the sum of all major element oxides (ALS Global, 2013).

The Magnesium number Mg# was determined using the following formula:

$$\frac{\left[\frac{(0.603\times MgO)}{24.31}\right]}{\left[\left(\frac{(0.9\times Fe2O3)}{55.85}\right)+\left(\frac{(0.603\times MgO)}{24.31}\right)\right]}$$

5. RESULTS

5.1 DEFLECTOR PETROGRAPHY

5.1.1 Rock Type

Thin section analyses of the 80 samples reveal two main rock types for the Deflector lodes. These have been classified as either mafic volcanics, or sedimentary siltstones and shales.

Samples taken from West and Central lodes have a volcanic host, which from prior research and current petrographic analyses can be identified as being a high-magnesium, variolitic basalt. The volcanic samples are observed to have either a needle-like spinifex texture that is similar to that of komatiites (Figure 7A), whilst the others having a texture typical of variably altered basalts (Figure 7B). Multiple thin sections of Deflector samples indicate that the volcanics have been intruded by a series of quartz-feldspar rich porphyries as well as intermediate biotite lamprophyres. The porphyries are characterised by variably altered coarse-grained phenocrysts of quartz and feldspars set in an aphanitic, silicate-rich groundmass (Figure 8A). The lamprophyres are also porphyritic, however with large phenocrysts of biotite and finer amphibole agglomerations, also set in a fine-grained silicate-rich groundmass (Figure 8B).

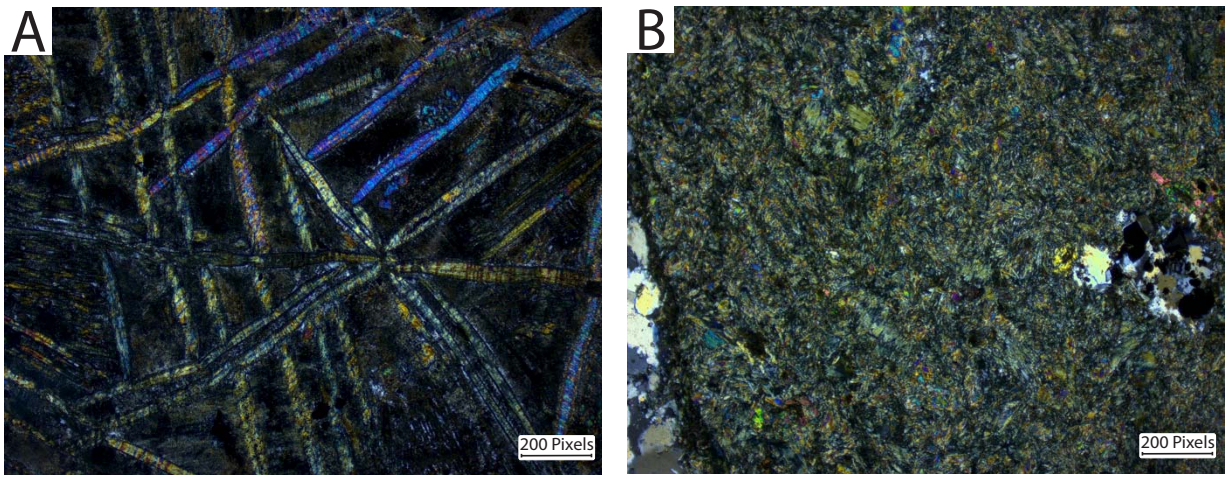

Figure 7: *A) Volcanic sample B732067 with 'komatiite-like' spinifex texture and; B) Sample 12942610 illustrating a weakly altered aphanitic basalt, both in transmitted light XPL.*

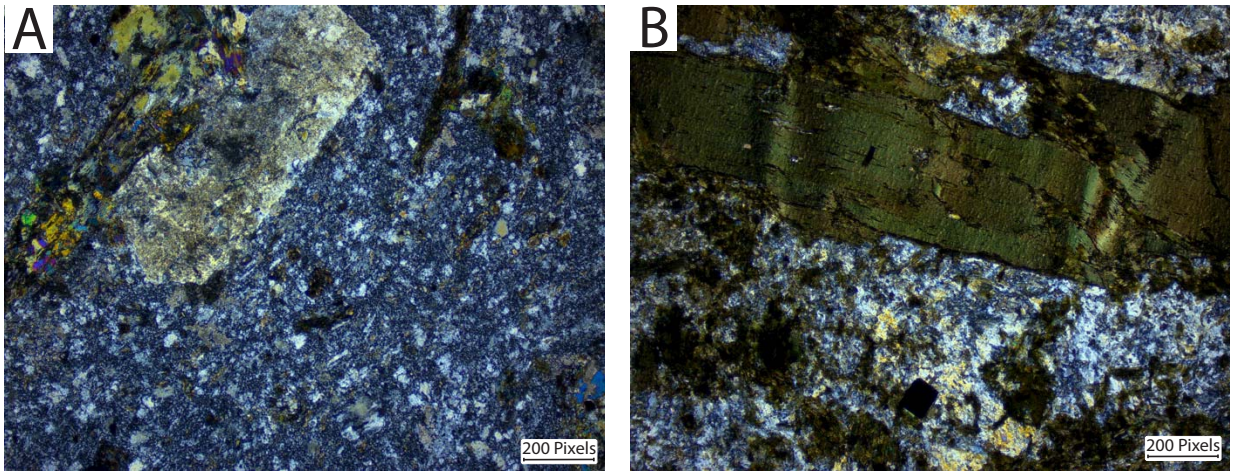

Figure 8: *A) Sample B312218 illustrating a quartz-feldspar rich porphyry and; B) Sample 12952125 illustrating a biotite-rich lamprophyre, both in transmitted light XPL.*

Samples taken from Contact lode have a sedimentary host, with the two major sub-types being siltstones and shales. Hand-sample analyses indicate the siltstones are fine-grained and grey, whilst the shales are pale-brown to black. Referral to the geochemical dataset indicates that that the siltstones are carbon-poor, whilst the shales are carbon-rich. Cleavage and fissile bedding characteristics are lacking, and no evidence for contact metamorphism was encountered in the sedimentary-sample thin sections. Similar to the volcanics, the sedimentary samples have been cut by felsic quartz-feldspar porphyries as well as intermediate biotite lamprophyres, which have the same characteristics as those described above. The carbon-rich shales appear to contain more abundant sulphides, which occur within open-spaced fractures in the host-rock (Figure 9A). By comparison, the carbon-poor siltstones exhibit much less sulphide mineralisation, which when present, occur as fine-grained disseminations within the host-rock groundmass (Figure 9B).

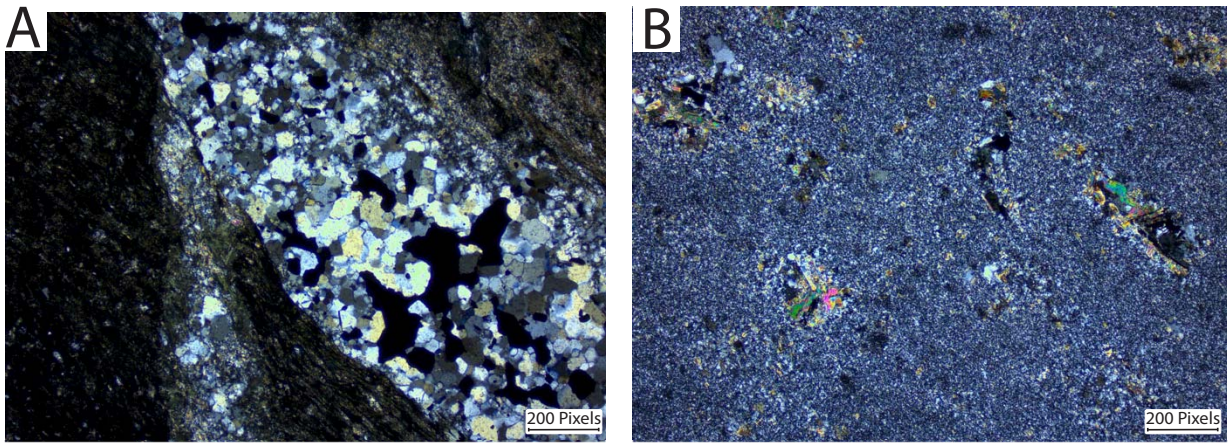

Figure 9: A*) Sedimentary sample 9212045 illustrating brown/black shale with quartz sulphide mineralisation and; B) Sedimentary sample 9131496 illustrating a silicate-rich fine-grained siltstone with 'pods' of micas, epidote and disseminated sulphides, both in transmitted light XPL.*

5.1.2 Alteration Mineralogy

Chlorite is the most abundant alteration mineral within the samples, occurring both within the host-rock groundmass and within fracture-controlled veinlets. When occurring within host-rock, chlorite most commonly occurs as blades (Figure 10A), and is more abundant when proximal to a vein or veinlet. Chlorite takes this same form when found within veins, however when it forms its own veins, takes more of a spiralled form (Figure 10B).

The same observation applies to calcite and epidote, however they not occur as abundantly as chlorite. Epidote forms commonly as prismatic blocks, with its perfect cleavage clearly visible, and is well associated with sulphide disseminations within volcanic-sample groundmass (Figure 11A). Calcite is clearly distinguished in the samples by its rhombohedral cleavage, where its main association is in quartz-carbonate veins. Calcite is also observed to form its own veins.

A number of samples are also slightly altered with sericite dusting of feldspars (Figure 11B). High birefringence amphibole is observed least commonly within the samples (Figure 12B). The alteration minerals described above show no preference for the sedimentary or volcanic-hosted samples, and occur within both.

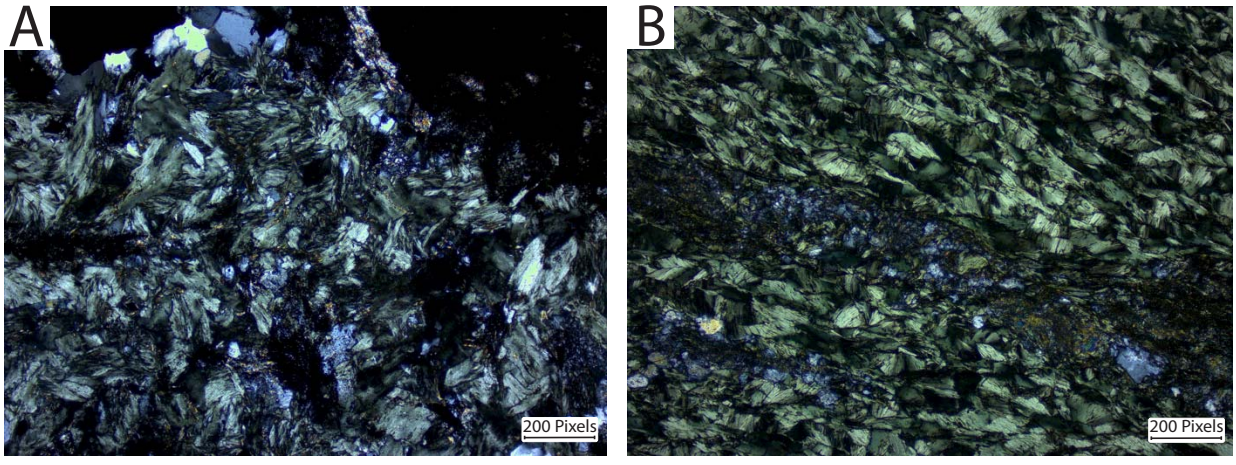

Figure 10: *A) Sedimentary sample 9131246 illustrating bladed chlorite within host-rock and; B) Volcanic sample 9371350 illustrating a chlorite-quartz vein, both in transmitted light XPL.*

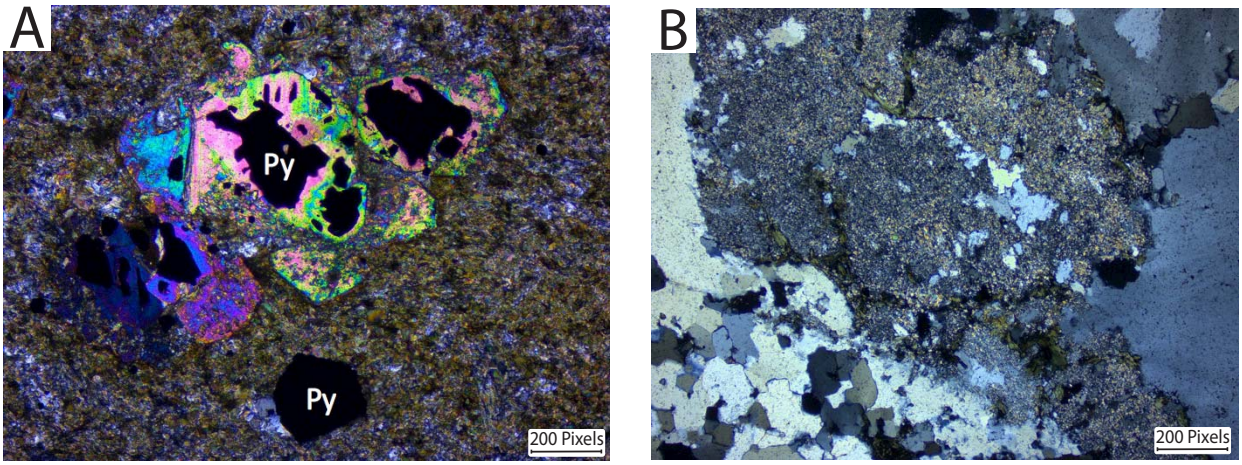

Figure 11: *A) Volcanic sample 12592161 illustrating blocky epidote and carbonate veinlet with euhedral disseminated sulphides and; B) Volcanic Sample 9371006 demonstrating sericite dusting of feldspar, both in transmitted light XPL.*

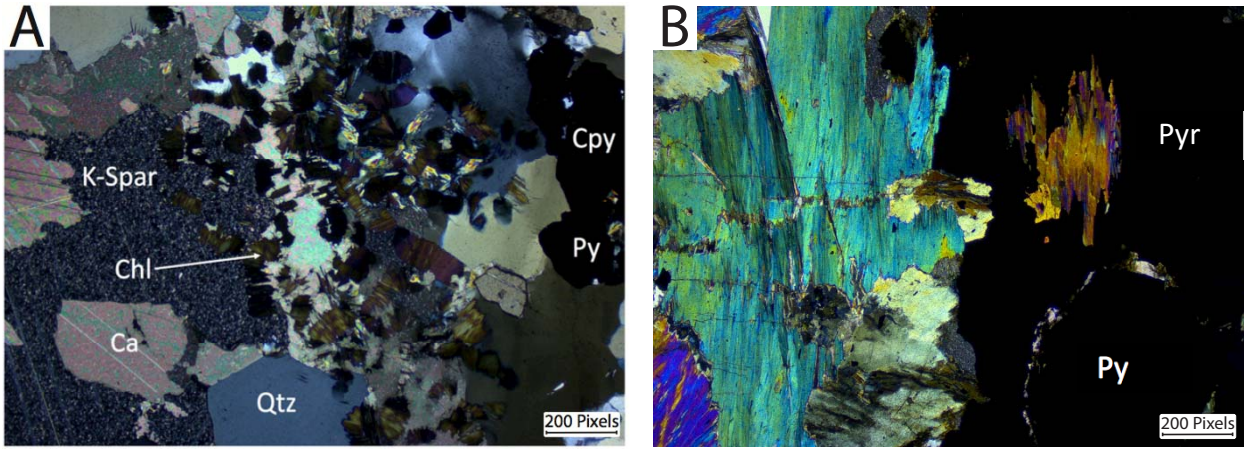

Figure 12: *A) Volcanic sample 12591877 illustrating K-feldspar, calcite, and chlorite and; B) Volcanic Sample 12811777 demonstrating amphibole with massive sulphide mineralisation, both in transmitted light XPL.*

5.2.3 Multiple Vein Generations and Characteristics

Inspection of drill core and petrographic analyses reveal a number of different vein generations that display different characteristics. Distinct vein and veinlet mineral assemblages and their limited cross-cutting relationships only allow a few of these vein generations to be placed in a paragenetic sequence.

Veins and veinlets may consist of variable proportions of quartz, chlorite, carbonate, epidote, feldspar and sulphide phases. They include quartz-only, chlorite-only, carbonate-only, quartz-chlorite, quartz-chlorite-carbonate, carbonate-epidote, and feldspathic. These features are observed to occur within brittle fractures of the host-rock, with the vein and veinlet material filling open-spaces, and are also associated with brecciation (Figure 13).

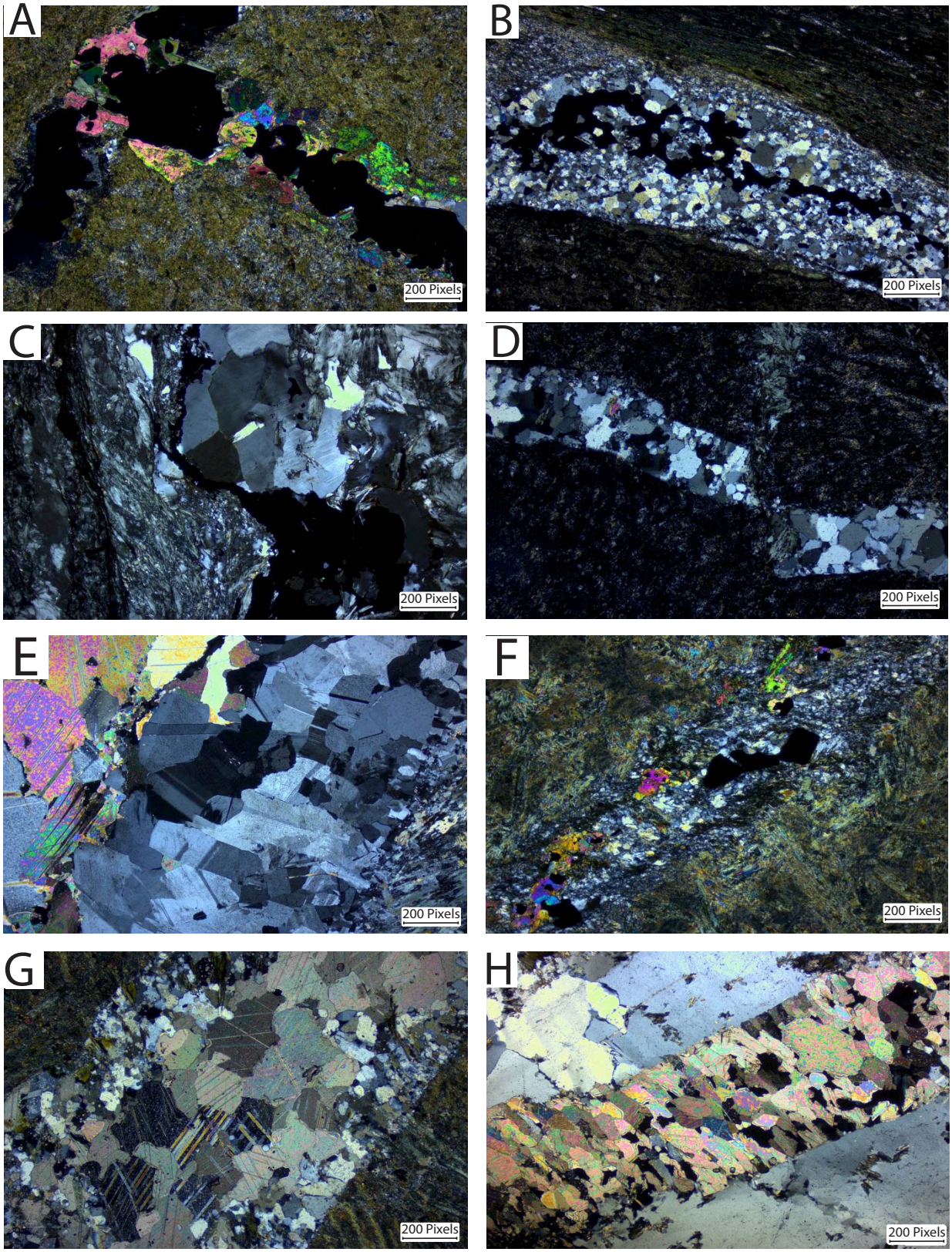

Figure 13: *A) Volcanic sample 12942601 illustrating an epidote-carbonate veinlet with sulphides; B) Sedimentary sample 9212045 illustrating quartz-only veinlet with sulphides; C) Sedimentary sample 9131275 illustrating quartz-chlorite vein with sulphides; D) Sedimentary sample 9131190 illustrating chlorite-only veinlet displacing quartz-epidote veinlet: E) Volcanic sample B422939 illustrating feldspathic-vein proximal to carbonate-only vein; F) Volcanic sample 9371082 illustrating quartz-epidote veinlet with sulphides; G) Spinifex sample B732053 illustrating quartz-carbonate veinlet and; H) Volcanic sample 12811797 illustrating carbonate-only veinlet cross-cutting quartz, all in transmitted light XPL.*

Vein features that are commonly associated with well-developed shear zones in orogenic Au deposits, such as crack-and-seal vein structures, are lacking in the samples and not observed in the drill core.

A number of earlier vein and veinlet assemblages appear to be cross-cut by later generations of vein systems. A photomicrograph image of figure 13D illustrates a later chlorite veinlet cross-cutting and displacing a quartz veinlet. Figure 13H illustrates a carbonate veinlet cross-cutting a quartz vein. Figure 14 shows both a hand sample that demonstrates the cross-cutting and displacement of a sulphide veinlet by a later quartz-carbonate veinlet, and also a thin section micrograph of a chlorite veinlet cross-cutting a quartz-carbonate veinlet.

The mineralisation features of the various vein and veinlet types will be discussed in the sub-section below.

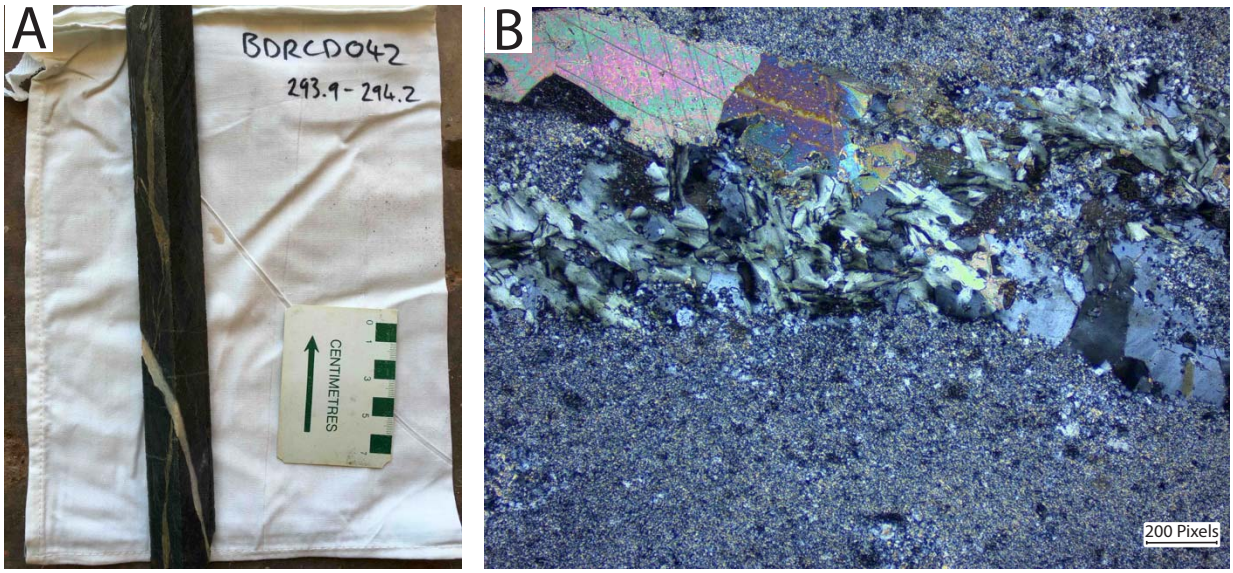

Figure 14: *A) Volcanic B422939 core-sample illustrating quartz veinlet displacing sulphide veinlet and; B) Sedimentary sample 9131496 illustrating a chlorite veinlet cross-cutting a quartz-carbonate veinlet in transmitted light XPL.*

5.2.4 Mineralisation and Au-Occurrences

Samples for this study were only taken from Deflector's primary mineralisation zone (> 70 metres depth), and therefore negligible secondary supergene sulphides are encountered. The most common sulphide minerals within the volcanic-zone are pyrite and chalcopyrite, with trace pyrrhotite, sphalerite, and arsenopyrite. Free Au is also

observed in the high-grade vein samples. Within the sedimentary-zone, sulphide mineralogy consists of pyrrhotite, sphalerite, and trace chalcopyrite.

Chalcopyrite is the main Cu-bearing sulphide mineral in the volcanic-zone, where it predominantly mineralises as an open spaced-filling texture commonly in an anhedral form. At least two textural generations of pyrite are detected in the veins based on textures and associations with chalcopyrite and Au, as illustrated in sample B422937 (Figure 15A). Type I pyrite displays well-defined edges versus chalcopyrite. It consists of individual subhedral to euhedral grains and masses of grains that can be locally distinguished by small amounts of chalcopyrite along boundaries. Type II pyrite is generally anhedral in form, even when adjacent to chalcopyrite. It displays a patchy surface defined by darker areas with a dusty or pitted appearance, generally surrounded by cleaner or smoother areas. In areas where Type II pyrite is best developed, chalcopyrite commonly shows signs of similar zoning that is defined by these pitted and non-pitted areas (Figure 15B). The Type II pyrite has been deformed in some samples where host veins have been fragmented. Au has not also been observed in Type II pyrite, although occurs abundantly in Type I pyrite.

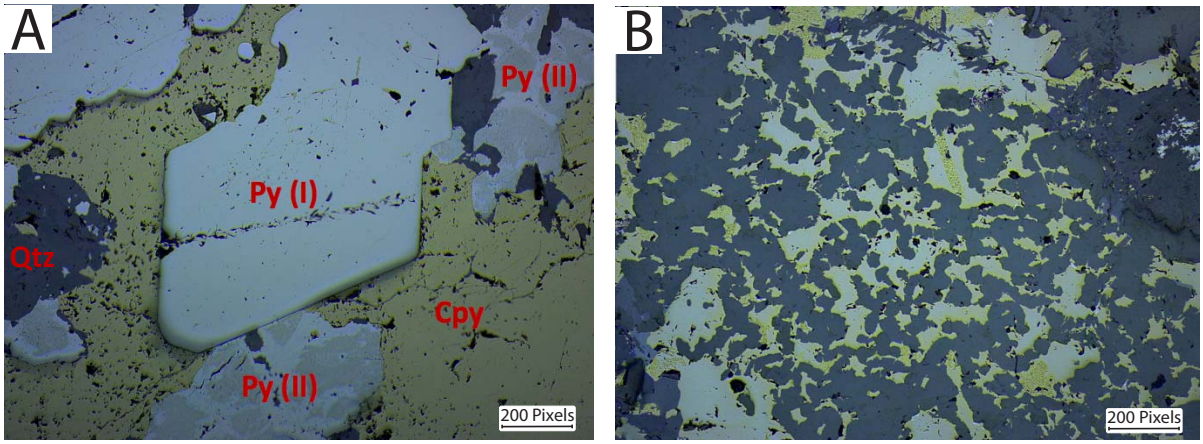

Figure 15: *A) Vein sample B422937 illustrating Type I and Type II pyrite, with Type I pyrite demonstrating euhedral grain boundaries and Type II pyrite demonstrating anhedral grain boundaries with zoning defined by pitted and non-pitted areas and; B) Vein sample 12811797 illustrating disequilibrium texture with areas of pitted chalcopyrite, both in reflected light.*

Heavily mineralised samples were taken from quartz veins, and always demonstrate high-grade Au and Cu that are represented in the sample thin-sections by the chalcopyrite, Type I and Type II pyrite that is described above (Figure 15A). Traces of sphalerite are present in these volcanic-hosted vein samples, occurring on the edges of

Type I pyrite. In some samples, chalcopyrite demonstrates a disequilibrium mineralisation texture that is reminiscent to those seen in retrograde-skarn deposits (Figure 15B). In low-grade samples, pyrite occurs as euhedral disseminations, either within veinlets (Figure 13A), or within the host-rock groundmass (Figure 11A) with or without chalcopyrite.

Pyrrhotite and sphalerite appear to occur preferentially within the sedimentary-zone in the low-Au periphery of the Deflector system, however they are also observed much less commonly in the volcanic-zone. Similar to chalcopyrite in the volcanics, anhedral pyrrhotite and sphalerite fill open-spaces that have been caused by micro-fracturing within the sedimentary host-rocks (Figure 16). Minor veinlets of chalcopyrite also occur locally in the sedimentary zone. In the volcanics, pyrrhotite occurs in samples from diamond hole 12DD081, once again as anhedral masses around subhedral Type I pyrite, and in an association to chalcopyrite (Figure 17).

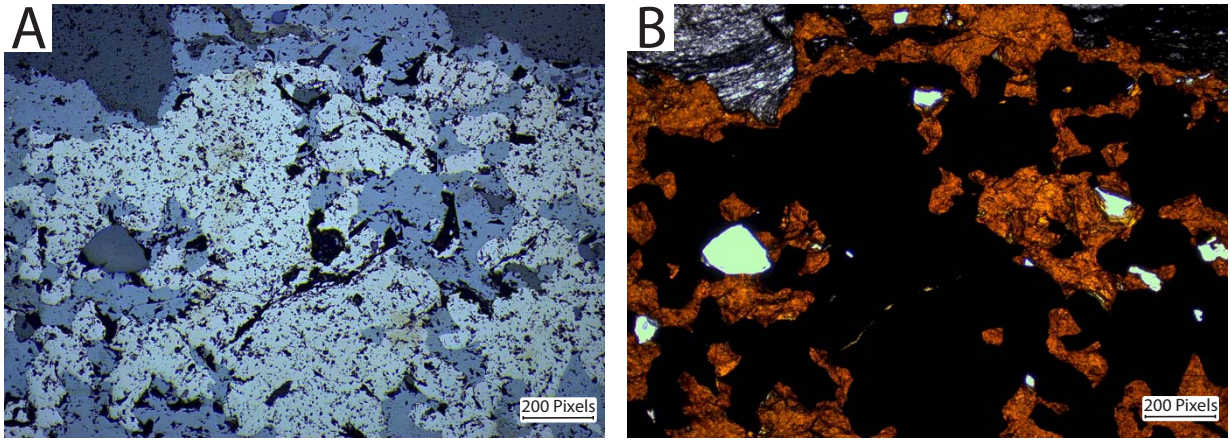

Figure 16: *A) Sedimentary sample 9132432 illustrating open-spaced pyrrhotite and sphalerite mineralisation in reflected light and; B) Same as A, however in transmitted light XPL.*

Visible Au within the Deflector samples is observed to have a number of different mineral associations. In high-sulphide quartz-carbonate vein samples, Au most abundantly occurs either embedded in the Type I pyrite grains (Figure 18A), or within minor cavities or spaces between coalescing pyrite grains. In addition, Au within these veins is also observed to occur along quartz grain boundaries (Figure 18B). Chalcopyrite occurs abundantly in these vein samples.

Visible Au is also observed to occur less commonly in quartz-carbonate veins that lack chalcopyrite (Figure 19A). Three samples from 12DD094 demonstrate small specs of Au occurring on quartz grain-boundaries. At the macroscopic level, all three samples contain stock work quartz-carbonate veining (Figure 20). At the microscopic level, sulphide mineralisation is dominated by coarse-grained pyrite disseminations, where epidote shows an association with the pyrite disseminations (Figure 19B).

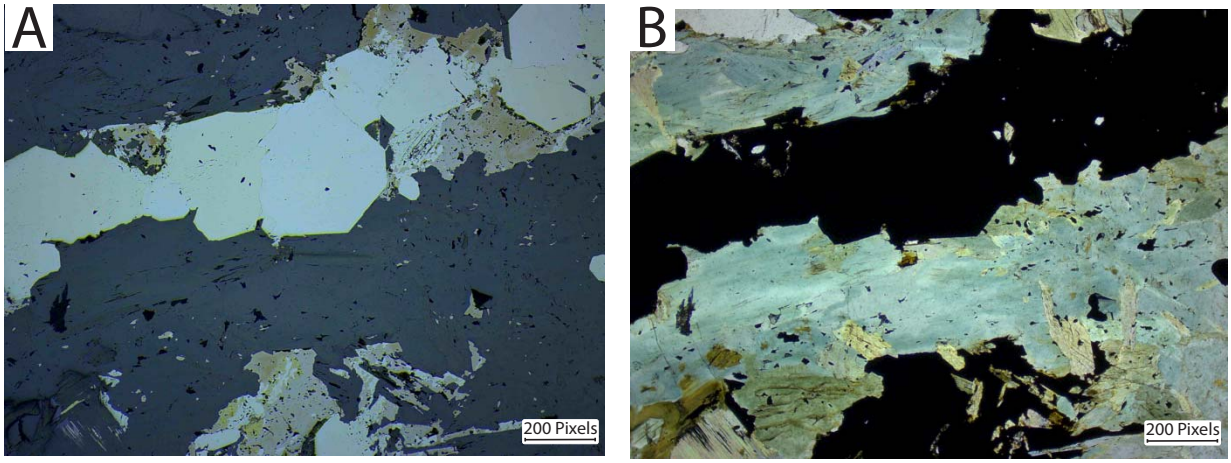

Figure 17: *A) Volcanic Sample 12811777 illustrating pyrrhotite with internal pyrite and chalcopyrite in reflected light and; B) Same as A however in transmitted light PPL.*

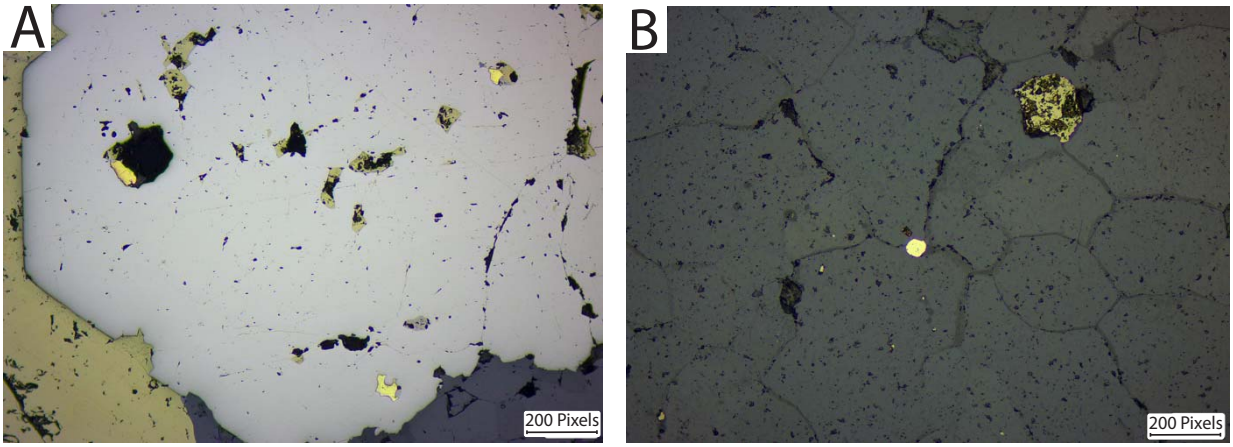

Figure 18: *A) Vein sample 12591872 illustrating Au embedded in Type I euhedral pyrite grains and; B) Vein sample 12591877 embedded in pyrite and on quartz grain boundaries in high Au-Cu samples, both in reflected light.*

Lastly, another type of Au occurrence is encountered in sample 9371037, where it is associated with arsenopyrite and pyrrhotite, and Cu is present in chalcopyrite (Figure 21). However, this is the only sample in which this mineral association occurs, where other As-rich samples are generally sediments that contain insignificant Au.

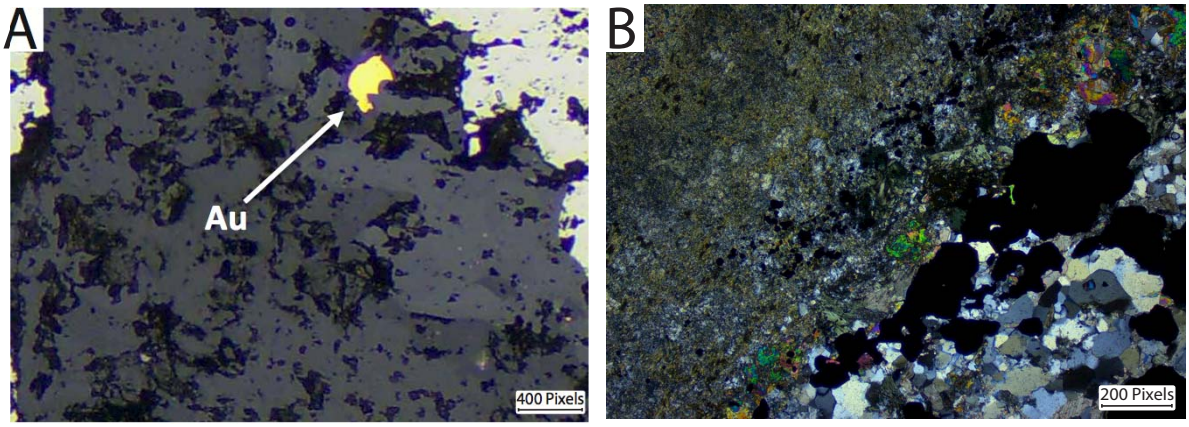

Figure 19: *A) Volcanic sample 12942594 showing free Au occurring in a quartz-carbonate veinlet with pyrite in reflected light and; B) Volcanic sample 12942610 showing quartz-carbonate veinlet carrying disseminated pyrite and epidote, in transmitted light XPL*

Figure 20: *Volcanic core samples of 12942603, 12941610, and 12942594 that show stockwork veining of quartz-carbonate veins.*

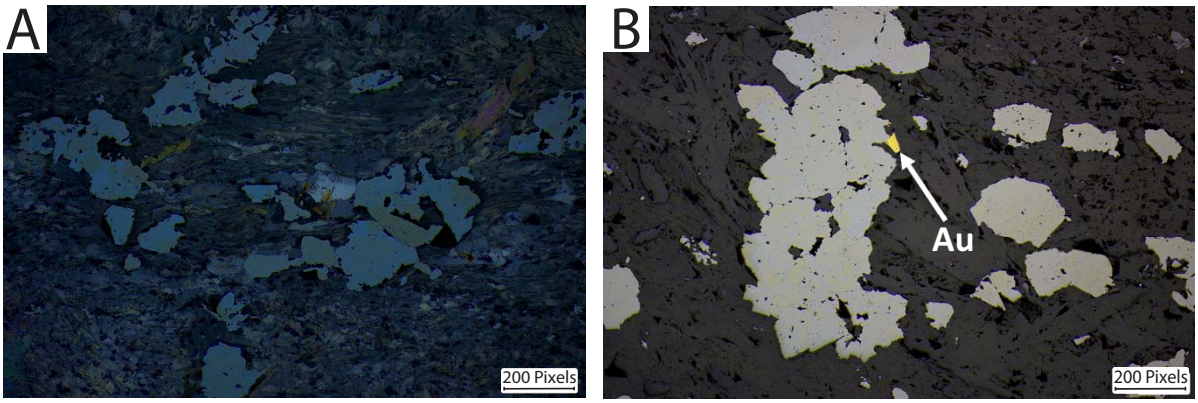

Figure 21: *A) Volcanic sample 9371037 illustrating arsenopyrite in reflected light XPL and; B) Volcanic sample 9371037 as A but with Au spec on arsenopyrite grain-boundary, in reflected light.*

5.2.5 Inclusions

Acicular to fibrous trains of silicates (stilpnomelane) occur in both quartz and neighbouring pyrite and chalcopyrite (12811797, 12811854, 12811775). In sample

12811797, the stilpnomelane is not present where chlorite occurs with quartz (Figure 22).

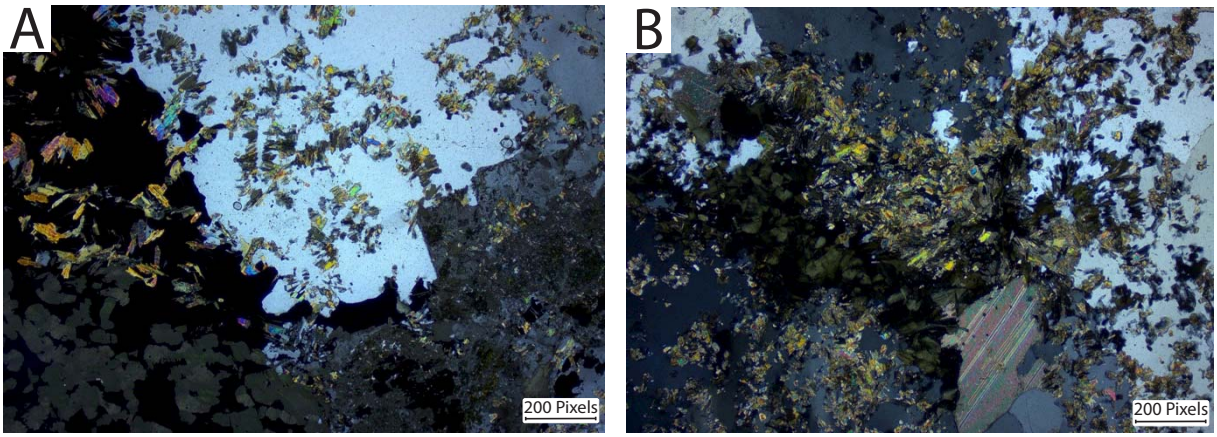

Figure 22: *A) Vein Sample 12811797 illustrating stilpnomelane inclusions in quartz and neighbouring sulphides and; B) Same sample as A, however with chlorite and carbonate. Stilpnomelane does not occur as inclusions in chlorite or the carbonate. Both micrographs in transmitted light XPL.*

5.2.6 Structure

Volcanic host rock samples generally do not display a strong structural fabric. As noted by Hayden and Steemson (1998), the preservation of delicate spinifex textures in the metabasalt suggests that these volcanic rocks have never suffered pervasive deformation, possibly because of their strong competency versus the associated sedimentary rocks.

In contrast to the mafic flows, many sedimentary samples (e.g., 9131489, 9131493, and 9131496) displayed offset and folded veins that indicate that a shearing or deformation event has taken place (Figure 23).

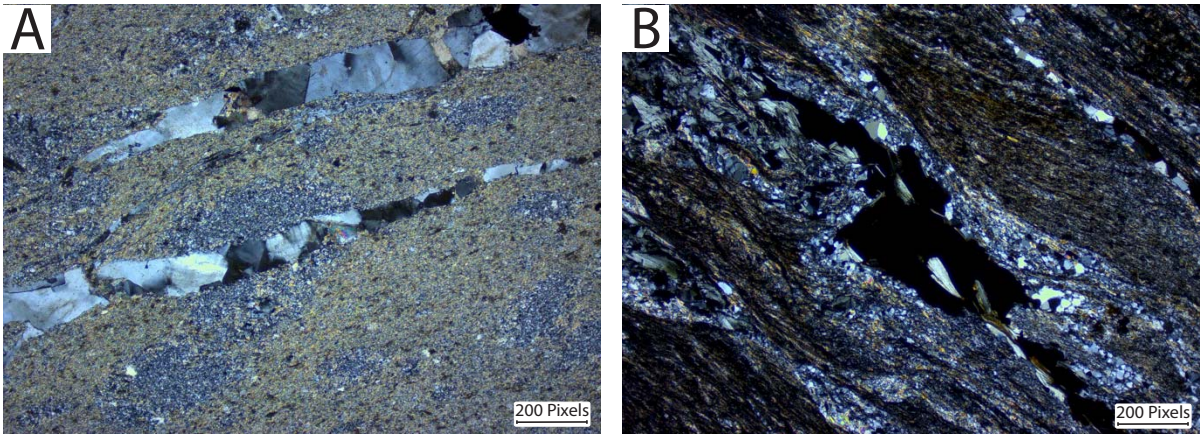

Figure 23: *A) Sedimentary sample 9131489 illustrating offset veinlet and; B) Sedimentary sample 9212173 demonstrating a ductile deformation fabric, both in transmitted light XPL.*

5.2 DEFLECTOR GEOCHEMISTRY

Geochemical analysis of the Deflector samples has illustrated a number of different elemental associations that occur between sample types. A range of immobile and mobile elements were analysed, and a number of specific elements were added to the ALS package in order to provide a more comprehensive analysis between Au and Cu. For example, As, Bi, Te, and In are all elements that are all well associated to Au and Cu in mineral deposits, and consequently show enrichment in the Deflector system. Samples have been grouped in the X-Y plots based on whether they are hosted by volcanics, veins, sedimentary rocks, or porphyries. Volcanic samples are in some cases dominated by veinlets, and vein samples are either veins or vein-dominated.

A normalised multi-element plot for volcanic Deflector samples illustrates varying degrees of alteration that occurs between the samples. Out of 80 samples that were allocated for the present study, 38 of these samples represent a volcanic host that demonstrate both enrichment and depletion in a number of elements, including Rb, Ba, K, and Sr (figure 24).

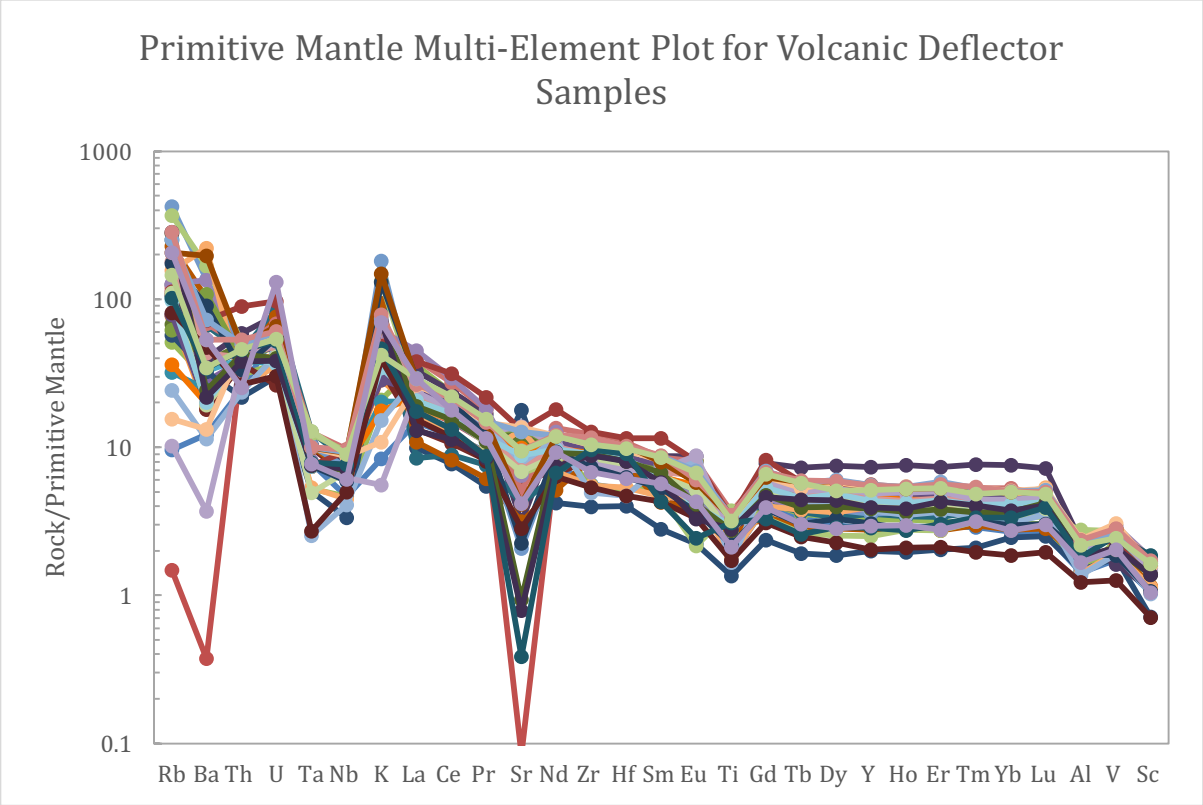

Figure 24: *Multi-element plot for present study volcanic Deflector samples, normalized to the primitive mantle.*

Figure 25 illustrates the full range of Au and Cu values that were obtained through the ALS whole-rock characterisation geochemical assessment. Au in the Deflector samples demonstrates a minimum of 0.001 g/t and a maximum of 194 g/t, whilst Cu a minimum of 3.11 ppm and a maximum of 269,593 ppm. A plot of the full range of Au and Cu concentrations demonstrates some clear trends in the high-grade samples. Figure 25 illustrates that in the majority of high-grade Au and Cu vein samples, significant Au concentrations are coupled with significant Cu concentrations. Volcanic samples can display either elevated Au and Cu, or elevated Au with background Cu concentrations.

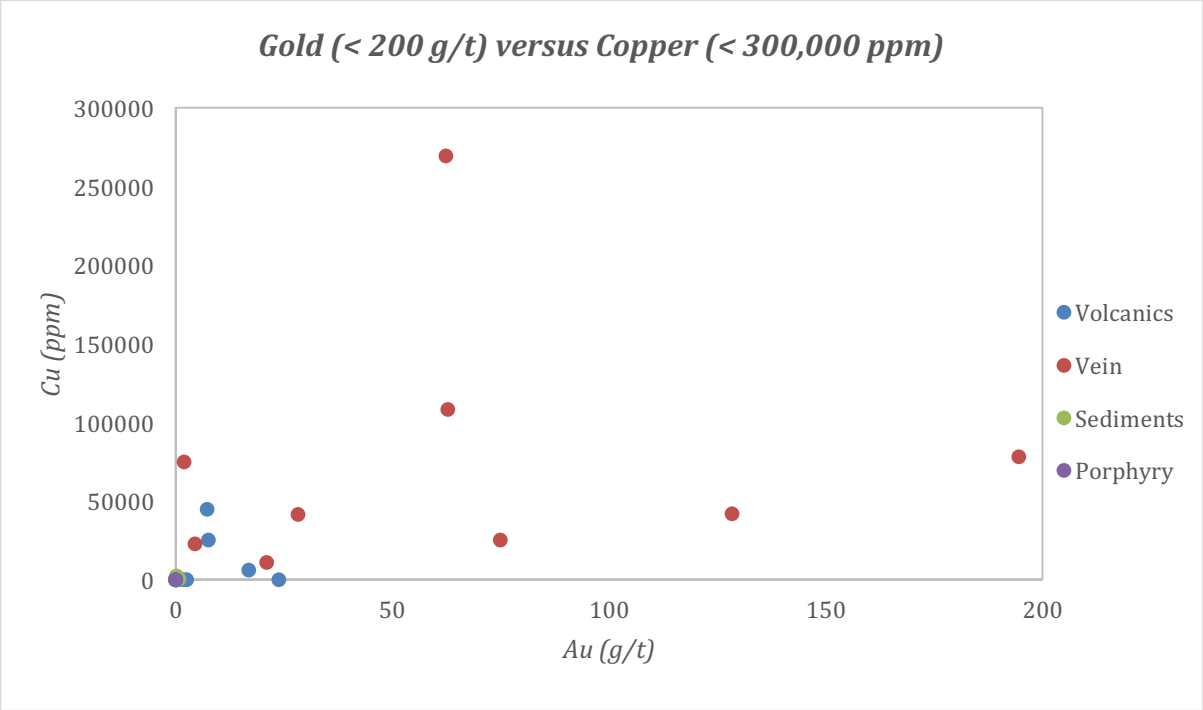

Figure 25: *Au versus Cu of drill core samples at high abundances in the present study.*

Samples with low to moderate Au and Cu contents (< 1g/t Au; < 1000 ppm Cu) are plotted in Figure 26, which illustrates three apparent trends. Most obviously, the plots illustrate a clear trend in the Y direction, whereby Cu concentrations are increasing somewhat independently of Au in vein, volcanic and sedimentary samples. A second trend records co-enrichment of Au and Cu in volcanic samples, while a third possible trend (defined by three volcanic samples) corresponds to Au enrichment independent of background-level Cu contents.

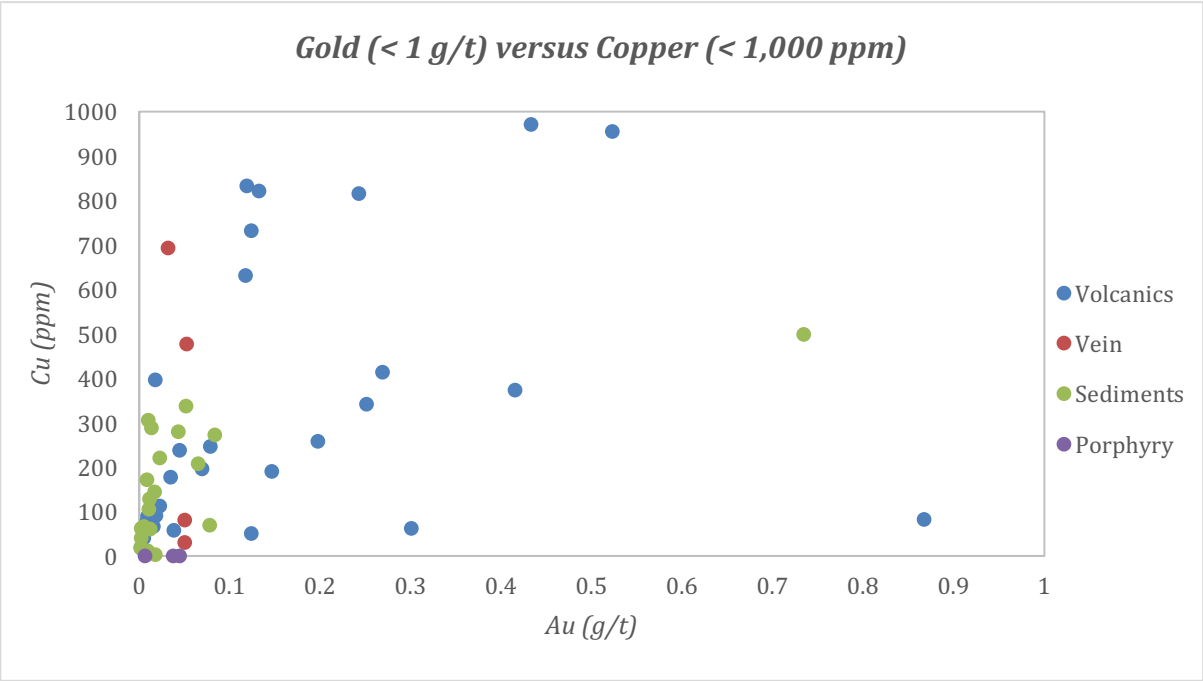

Figure 26: *Au versus Cu of drill core samples at low abundances in the present study.*

A number of samples contain high concentrations of Ag. Figure 27 illustrates Ag plotted against Au, where Ag has a minimum of 0 (LLD 0.5) and a maximum of 135 g/t. Comparison of figure 25 with figure 27 shows that vein samples with high-grade Au and Cu are also high-grade in Ag.

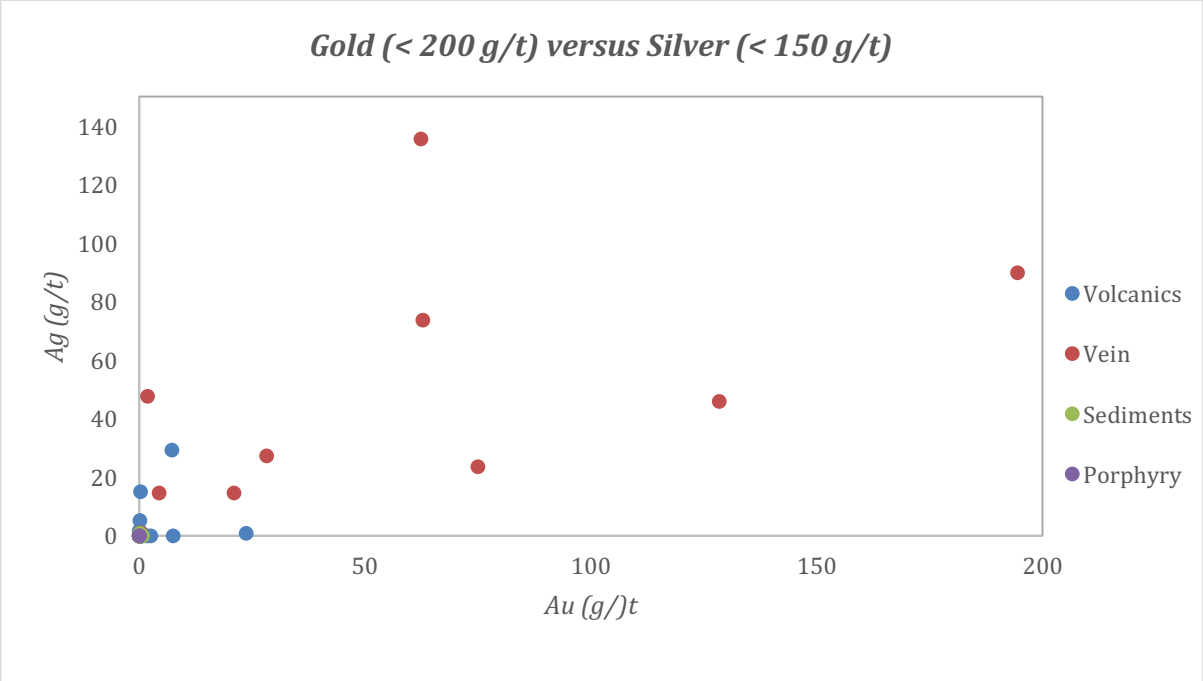

Figure 27: *Au versus Ag drill core samples at high abundances in the present study.*

Geochemical analyses of the Deflector samples also demonstrate anomalous concentrations of the base-metal Zn. Figure 28 illustrates Zn plotted against Au, where Zn records a minimum of 21.15 ppm and a maximum of 6102 ppm. In Figure 29, concentrations were capped at Au = 10 g/t and Zn = 200 ppm. Figure 28 demonstrates no correlation between Zn and Au with a possible exception in vein samples if one sample is excluded. At low abundances, figure 29 illustrates that as Au starts to increase in volcanic samples, Zn content decreases.

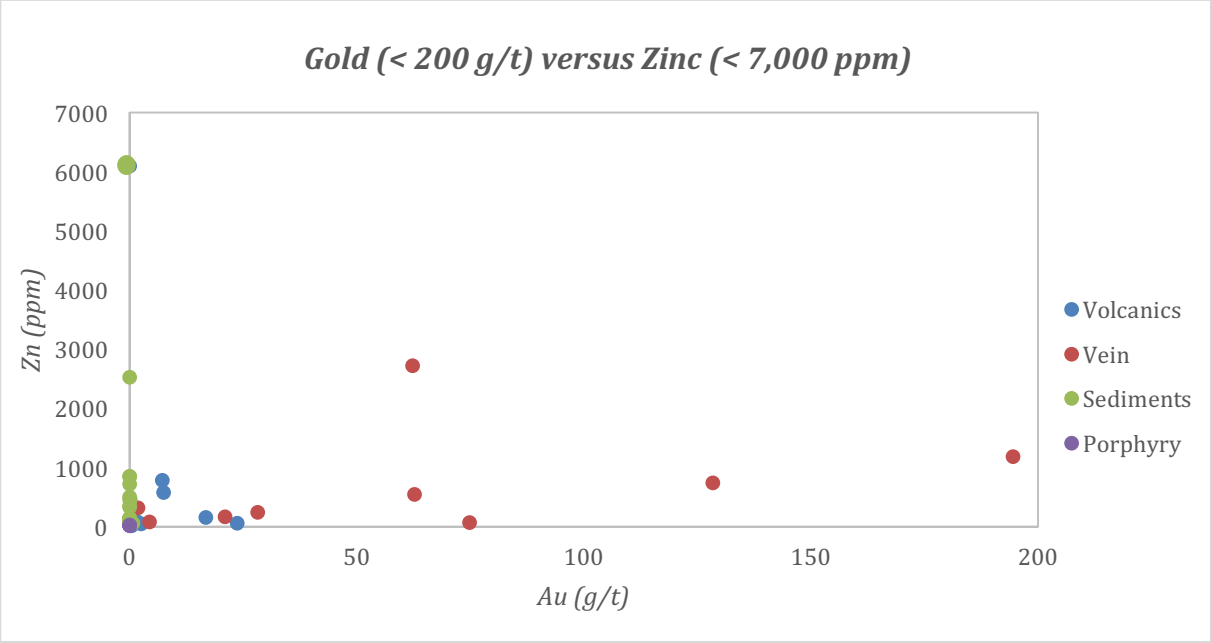

Figure 28: *Au versus Zn of drill core samples at high abundances in the present study.*

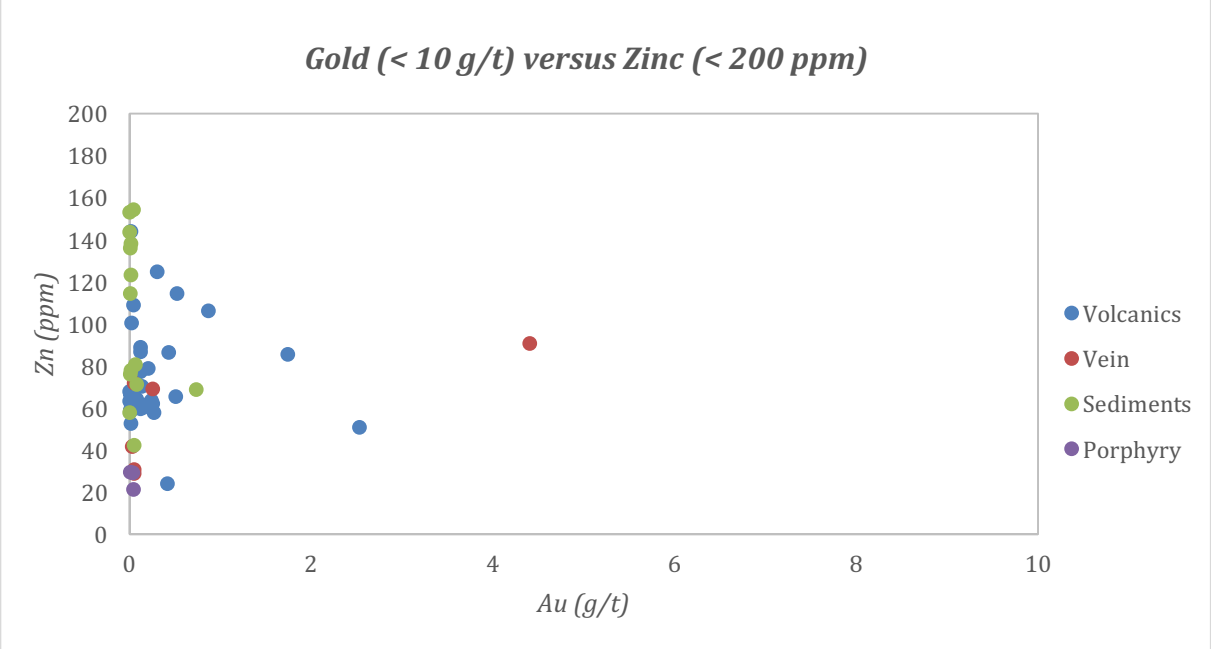

Figure 29: *Au versus Zn of drill core samples at low abundances in the present study.*

Samples in the present study show background levels of the base-metal Pb. Figure 30 illustrates Pb plotted against Au, where Pb records a minimum of 0 (LLD 1.0) and a maximum of 34.9 ppm. All vein samples contain levels of Pb less than 10 ppm, with highest levels occurring in the sedimentary rocks and porphyries. Figure 31 illustrates Au versus Pb at low abundances, whereby volcanic samples appear to show similar trends to the high abundance vein samples in figure 30, and the sedimentary rocks and porphyries showing identical trends to those seen in figure 30.

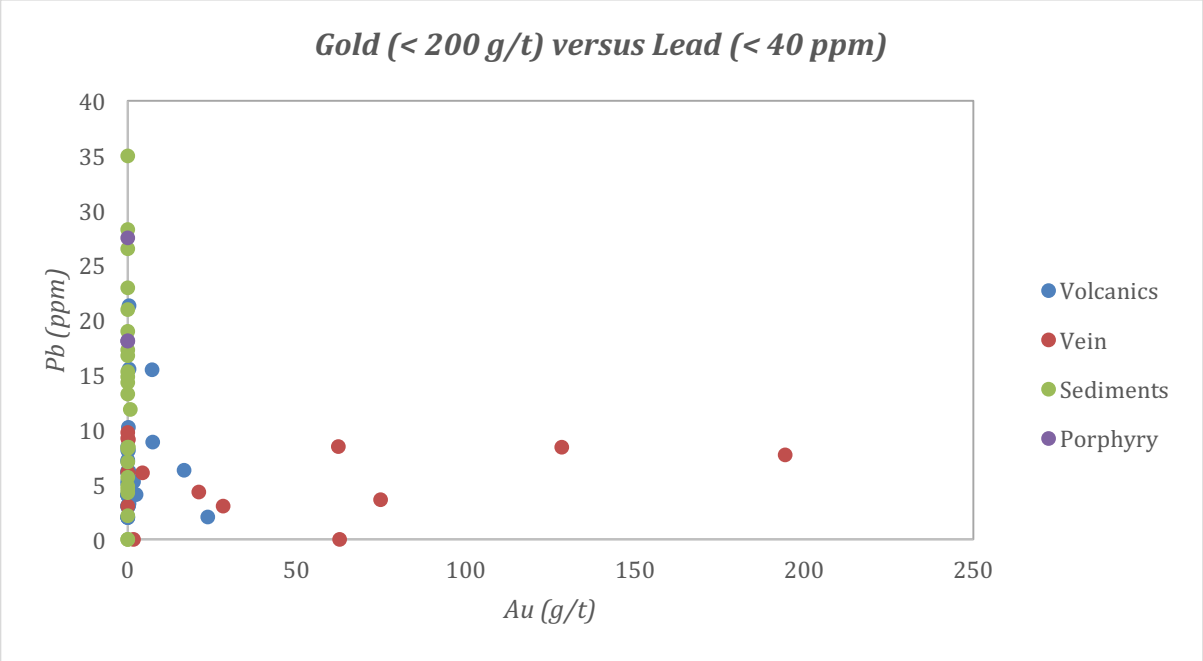

Figure 30: *Au versus Pb of drill core samples at high abundances in the present study*

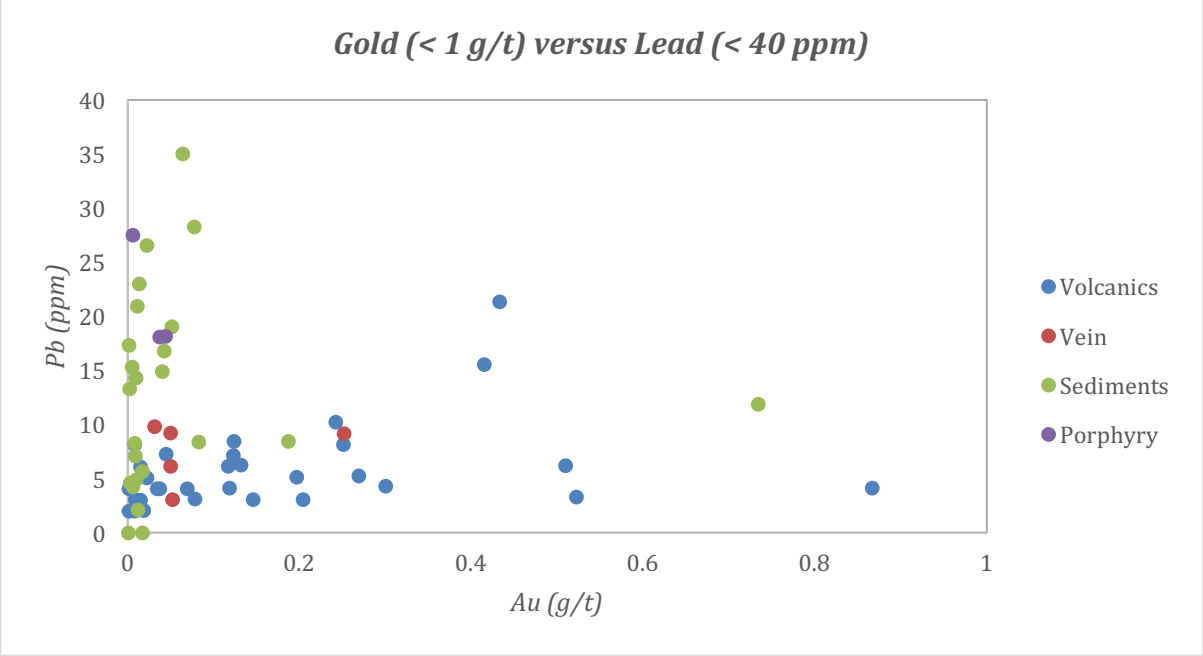

Figure 31: *Au versus Pb of drill core samples at low abundances in the present study.*

Cu versus Zn shows multiple trends. At high abundances, figure 32 indicates that increases in Zn in the sedimentary rocks are completely independent of Cu. In the vein samples and two volcanic samples, increases in Cu are coupled with gentle increases in Zn. When Cu is capped at 2000 ppm, and Zn at 1000 ppm, identical trends are observed within the sedimentary rocks in figure 33, however the volcanics, vein, and porphyries show no Zn enrichment as Cu increases.

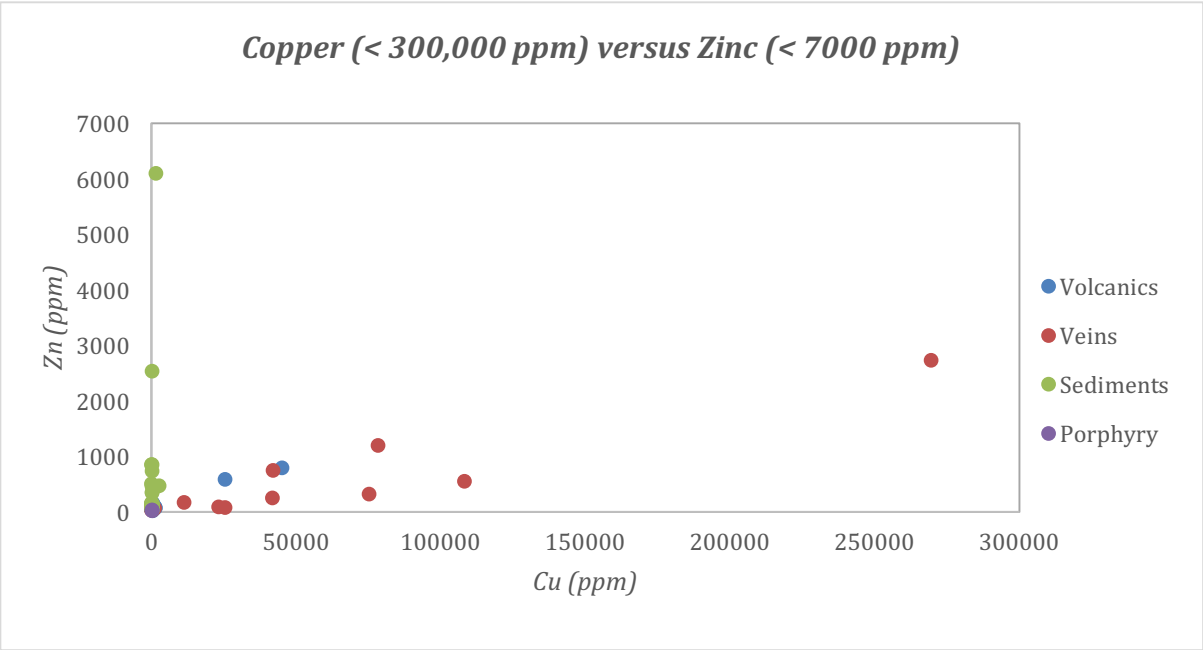

Figure 32: *Cu versus Zn of drill core samples at high abundances in the present study.*

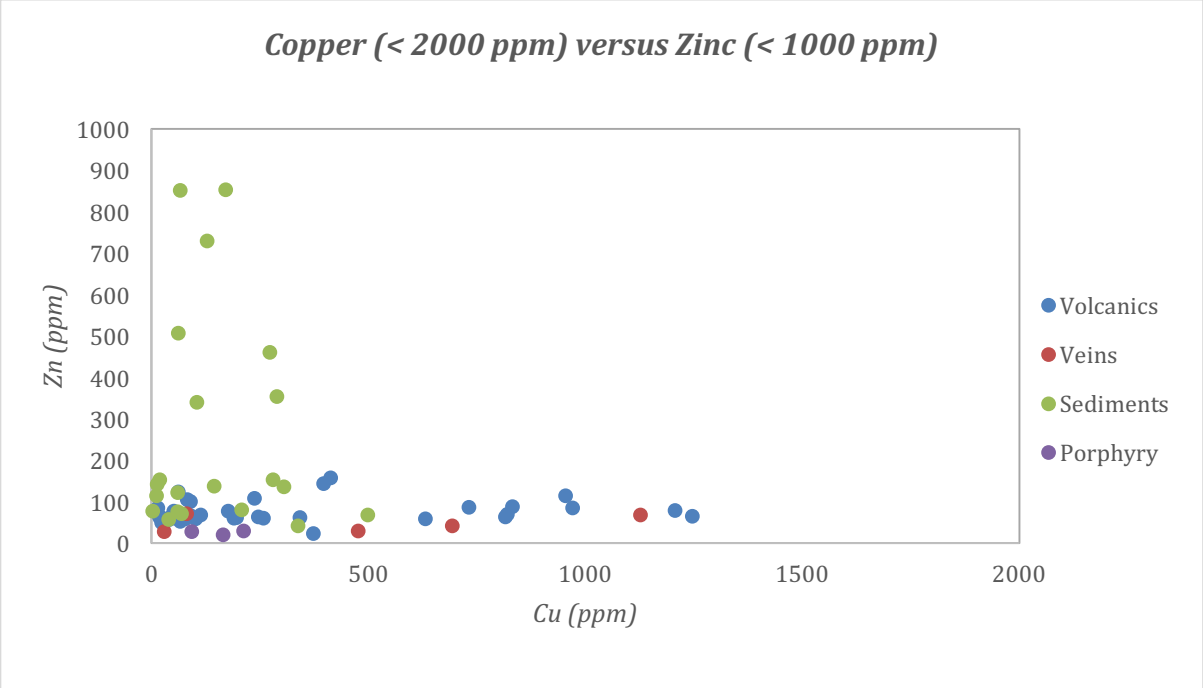

Figure 33: *Cu versus Zn of drill core samples at low abundances in the present study.*

Figure 34 illustrates Zn versus Pb at high abundances, where three sedimentary samples broadly indicating that as Zn increases, Pb decreases. In addition, the same trends are encountered at low abundances in the vein and volcanic samples, as demonstrated in figure 35.

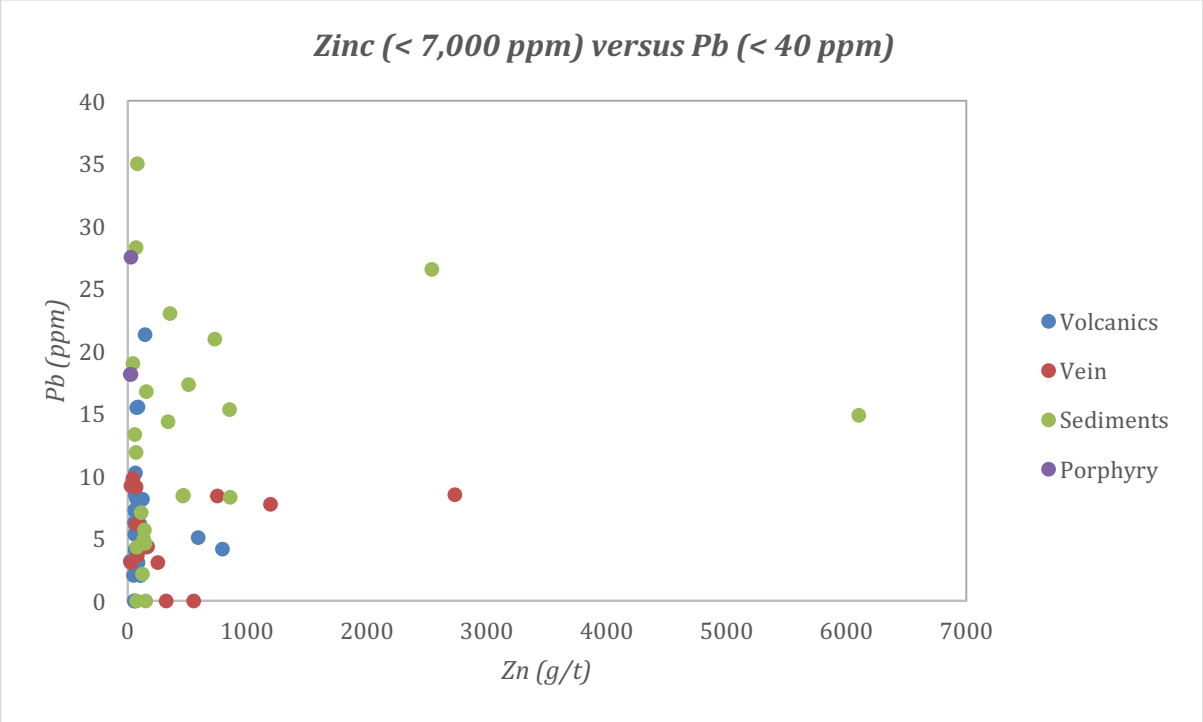

Figure 34: *Zn versus Pb of drill core samples at high abundances in the present study.*

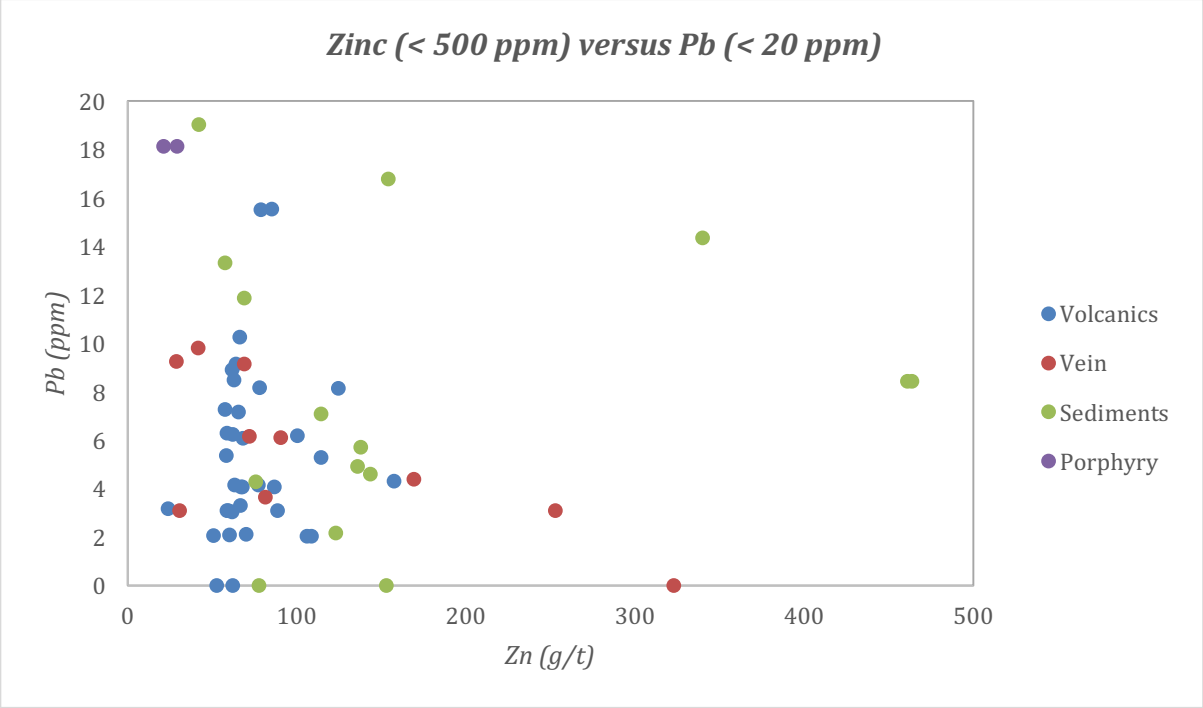

Figure 35: *Zn versus Pb of drill core samples at low abundances in the present study.*

6. DISCUSSION

The Deflector deposit has long been known as an unusual Yilgarn deposit that contains significant reserves of both Au and Cu. The unusual character of this deposit comes both from its anomalous metal inventory, where economic concentrations are encountered in both base-metals and Au, as well as the fact that it lacks the fundamental structural characteristics that are typical of most Yilgarn Au deposits (Hayden and Steemson, 1998). With these characteristics of the deposit in mind, the present study is assessing whether Deflector is a modified orogenic deposit (i.e. a rare hybrid-type), an orogenic Au overprint on an earlier deposit, or a distinct Au-Cu deposit type.

Petrographic and geochemical analyses for 80 samples from the Deflector deposit have provided a number of significant insights into the characteristics of the Deflector lodes. Thin section studies revealed a diverse range of vein and mineralisation characteristics, with these observations providing some important constraints for the interpretation of geochemical data. As previously noted, the base-metal and Au mineralisation at Deflector occurs in three distinct zones: West, Central and Contact (Figure 36). All three lodes strike NE, with West and Central sitting within the metabasalt, and Contact lode occurring on the metabasalt-metasedimentary contact. For simplicity, interpretations will start at the periphery of the system in the sedimentary-zone, and work inwards towards the volcanic-zone.

6.1 GEOLOGICAL CONSIDERATIONS

An analysis of the regional geology has identified a number of geological features that provide a basis for the interpretations presented in this chapter. Deflector's proximity to the Golden Grove VMS deposit suggests that a similar VMS system may have acted as a source for the base-metals located at Deflector. With Golden Grove occurring within the Gossan Hill Group of the Warriedar greenstone belt, approximately 55 km east of Deflector, it is possible that there may be a suite of similar undiscovered VMS systems in close proximity if the Deflector host rocks are underlain by the older sequence. Alternatively, there are numerous base-metal occurrences within the GGB itself, such as Mugga King to Deflector's west (Bromley, 1974), and their presence may have played a role in the development of Deflector's metal inventory. Lastly, the overwhelming

presence of "typical" orogenic deposits in the GGB, combined with the close proximity of the biotite monzogranite stock and other intrusions to the anomalous Deflector deposit, are all potentially important factors to be considered in the interpretation of the present geochemical and petrological data.

6.2 SEDIMENTARY PERIPHERY

6.2.1 Structures in the Sedimentary Zone

Samples taken from the periphery of the Deflector system come from drill holes 9DEF021, 9DEF013, and 9DEF031, and all contain a sedimentary host-rock. Petrographic analyses have allowed some important micro-structural interpretations to be made in relation to Deflector's sedimentary-zone.

Early thin veinlets within the sedimentary-zone (Figure 23B) suggest minor brittle behaviour, probably associated with emplacement of the biotite monzogranite into the Gullewa Goldfields shallow crust (Figure 6). Many of these early veinlets appear to be offset and deformed, which provides evidence that a later episode of shearing took place (Figure 23A). No similar deformation fabric is present in the mafic volcanic rocks, possibly due to their hardness. For example, the mafic volcanics preserve delicate spinifex textures, indicating that these rocks never suffered any pervasive deformation (Hayden and Steemson, 1998). The competency contrast between the sedimentary and the mafic volcanic rocks has resulted in the shearing features being concentrated in the sedimentary-zone and has resulted in slip-displacement along the volcanic-sedimentary boundary, which has been calculated to dip eastward at 70 degrees. Goodwin and Tikoff (2002) explain this phenomenon, where the competency contrast between rock types promotes strain partitioning between compositional bands, which is subsequently accommodated by domain-boundary sliding. Furthermore, a regional outcrop mapping exercise completed by Outhwaite (2016) for Doray Minerals Ltd. also infers that a major structure exists, separating the northern domain mafic rocks at Deflector from the southern sedimentary rocks. Outwaite (2016) further suggests that this structure may be a first-order control on the northern domain Au mineralisation, and potentially also a boundary to it. The structural observations made through thin section analyses of the sedimentary-zone support the interpretations of Hayden and Steemson (1998) and Outhwaite (2016).

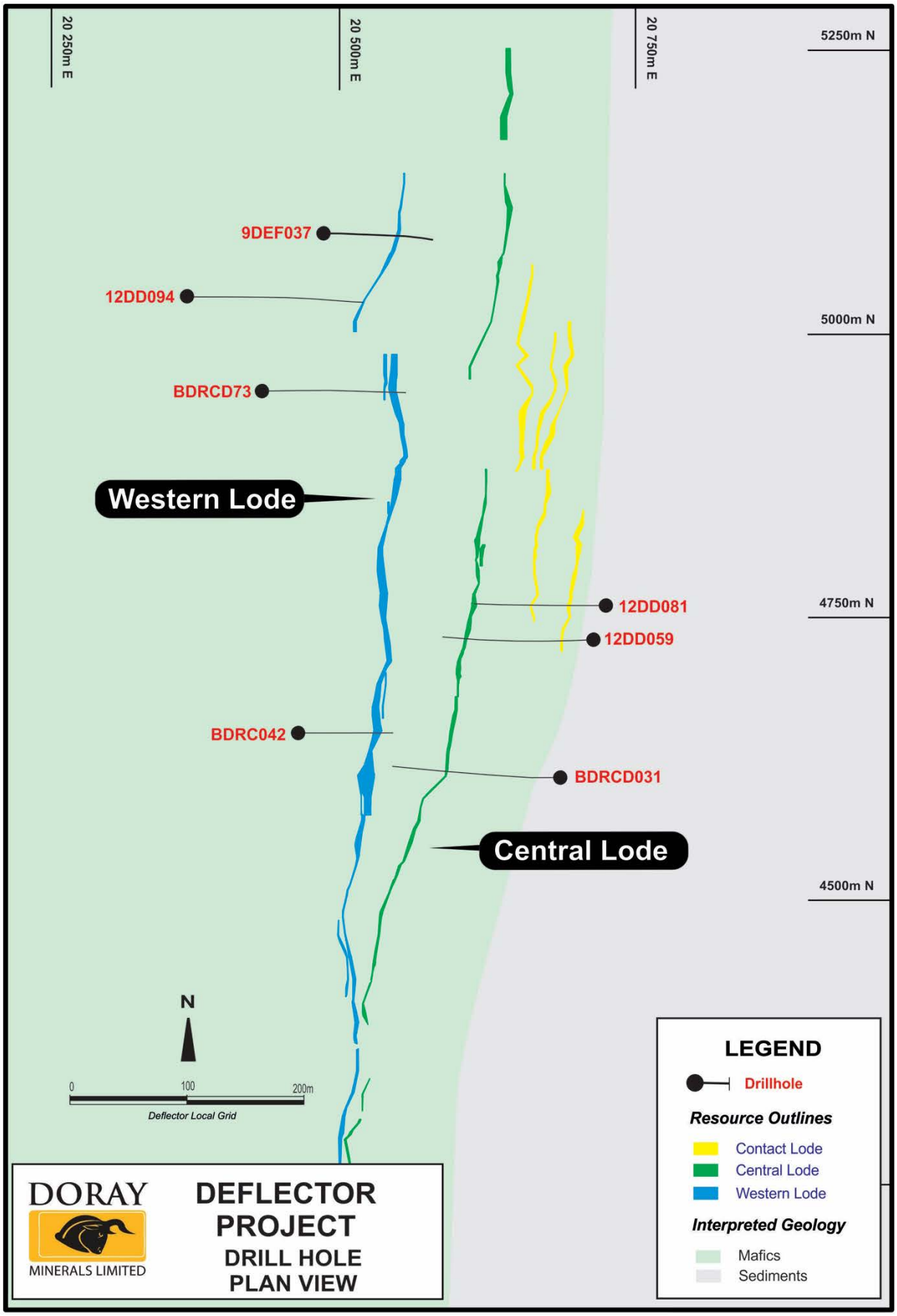

Figure 36: *Drill hole plan view for the present study Deflector samples.*

The significant number of sedimentary samples that exhibit a brittle deformation fabric support the above interpretation, with the monzogranite resulting in brittle fracturing of the sedimentary rock. Hayden and Steemson (1998) suggest that pluton emplacement may have resulted in contact metamorphism of the sedimentary rocks, as well as the volcanics. However, no well-developed contact metamorphic effects were observed in our samples.

6.2.2 Sediment-Hosted Mineralisation

As determined in the results section of this report, sedimentary samples are either high or low in carbon, with sulphide mineralisation more commonly occurring in the high-carbon sedimentary rocks. Petrographic analyses indicate that the main mineralisation signature occurring in these high-carbon sedimentary samples is dominantly pyrrhotite + sphalerite and trace chalcopyrite. This mineralisation signature is representative of a base-metal rich hydrothermal fluid, and suggests that at some point in Deflector's formation history, this base-metal-rich fluid has deposited its contents in the broad area in which the three lodes sit. Pyrrhotite and sphalerite within the sediment-hosted veins predominantly have an anhedral space-filling texture, with pyrrhotite having a preference for the middle of the veins and sphalerite ± chalcopyrite occurring at the edges (Figure 16). Very minor off-shoot veinlets of chalcopyrite also occur. These observations suggest that the base-metal mineralisation was controlled by small-scale fracturing in the sedimentary host-rock (and presumably in the more competent volcanic rocks), which from previous discussion may have been the result of pluton emplacement. The upwardly-mobile base-metal fluid therefore fills the open-space fractures that were created by the pluton.

The only other gangue minerals in these base-metal sulphide veinlets are quartz and chlorite, with quartz almost always accompanying sulphide mineralisation, and chlorite only sporadically so. This suggests the base-metals were transported by a silicate-rich fluid.

6.3 VOLCANIC ZONE

6.3.1 Volcanic-Hosted Mineralisation

Petrographic analyses of the volcanic samples identified a mineralisation signature that is in many ways different to those observed in the sedimentary rocks. For example, mineralisation in both the veins and veinlets of the volcanic rocks is dominated by chalcopyrite + pyrite, and accessory pyrrhotite + sphalerite. The comparison of the volcanic-hosted mineralisation signature with the sediment-hosted mineralisation signature (pyrrhotite + sphalerite, with trace chalcopyrite) indicates that hydrothermal zonation is present in the distribution of base-metals at Deflector. If this zonation is thought of as a single hydrothermal "system", then it is characterised by a copper-iron rich core (chalcopyrite + pyrite) that zones out to an iron-zinc rich periphery (pyrrhotite + sphalerite). Using base-metal sulphide theory as a guide, this zonation sequence is analogous to that seen in a Kuroko-type mineral system, whereby black ore minerals such as sphalerite and pyrite have been reported to form at a temperature of T = ~ 200° to 330° C, and yellow ore minerals such as chalcopyrite having a formation temperature at T = ~ 330 ° ± 50 °C (Pisutha-Arnold and Ohmoto, 1983). In the case of Deflector, this base-metal zonation was likely established by the heat associated with the granitic intrusion emplacement.

Thin section studies of Deflector samples identified two textural generations of pyrite (Figure 15A), which is a key piece of evidence that suggests multiple independent hydrothermal events have interacted to produce the Deflector mineralisation. Type II pyrite has been interpreted as belonging to an earlier base-metal mineralisation event. The Fe and S in Type II pyrite was initially derived from unidentified massive sulphides that were remobilised and transported from deeper crustal levels and then re-precipitated at shallower levels within the crust. Type I pyrite is interpreted as belonging to a second hydrothermal mineralising event, which most likely introduced Au into the system. The pitted texture of the Type II pyrite was a result of the second mineralising fluid overprinting and mixing with the earlier base-metal sulphides, which can also be attributed to the pitted texture of chalcopyrite observed in multiple samples. It is unlikely that two distinct textural generations of pyrite would have co-existed in an independent hydrothermal fluid. In addition, the presence of the two textures in pyrite and

chalcopyrite indicates that whilst a strong reaction between two hydrothermal fluids has taken place, evidence of the older base-metal system is preserved.

In further support of the premise that multiple hydrothermal fluids have interacted, some samples display textures suggestive of disequilibrium states (abundant inclusions in sulphides and quartz and mutually cross-cutting relationships between mineral phases), and resemble mineralisation textures similar to those seen in retrograde skarn deposits (sample 12811797, Figure 15B).

6.3.2 Evidence for Orogenic Fluids

If a "fossil" base-metal system predated the introduction of Au at Deflector, then it is possible that some of the later Au-bearing fluids did not interact extensively with the pre-existing system. Thin section analyses identified three samples that may represent potential end-member orogenic mineralising events. At the macroscopic level, the three consecutive samples from drill hole 12DD094 (12942594; 12942601; 12942603) have a volcanic host that appears to have been cut by a stockwork of quartz veinlets carrying coarse-grained disseminated sulphides. Petrographic analyses reveal that the veinlets cutting these samples are quartz-carbonate veinlets, where pyrite is the main sulphide mineral present, and chalcopyrite is absent. In addition to pyrite occurring within the quartz-carbonate veinlets, the sulphide also occurs as finer grained disseminated cubes within the groundmass of the volcanics, often having an additional association with epidote. As mentioned in the results section of this report, all three of these samples contain free Au that occur along the grain-boundaries of quartz or in Type I pyrite.

6.4 DEFLECTOR LAMPROPHYRES

The fact that Archean lamprophyres are present in and near the Deflector ore zones provides further evidence in support of an orogenic input for Deflector's formation. The results of the present study identified intermediate biotite-rich lamprophyres in multiple samples (12592061; 12592125). This is significant because these rocks commonly occur in orogenic Au deposits and reflect the presence of deep structures that allow ascent of magmas from the base of the crust (Kerrich and Wyman, 1994). Whilst controversies about the exact sources of the Au are still being resolved, it is widely accepted that at the very least the Au-lamprophyre association is structural, with both using the same

transporting medium for migration through the crust (Craw et al., 2006). Figure 37 plots two intermediate biotite-rich lamprophyres (12592061; 12592125) against two quartz-feldspar porphyries (B312216; B312218), with the lamprophyres showing a strong enrichment of the light REE and other hydrous fluid-mobilised elements, combined with prominent depletions of Nb-Ta as found in subduction related rock types. The presence of these lamprophyres provides direct evidence of a suitable "plumbing system" for the ascent of Au-bearing fluids, as well as circumstantial evidence to support the existence of orogenic fluids at Deflector.

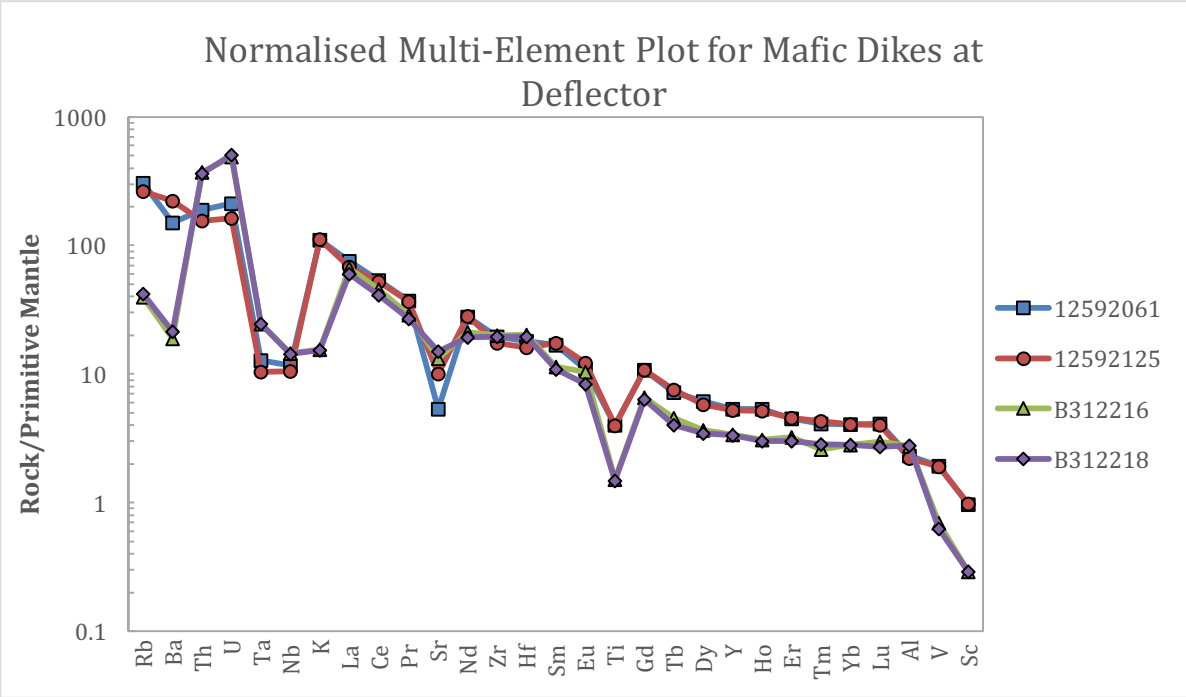

Figure 37: *Normalised multi-element plot for mafic dikes at Deflector, whereby 12592061 and 12592125 represent shosonitic (orogenic) lamprophyres, and B312216 and B312218 represent quartz-feldspar porphyries.*

6.5 STRUCTURAL AND CHEMICAL TRAPS AT DEFLECTOR

The identification of lamprophyres in the Deflector ore zones and the surrounding area prompts a further consideration of the structural characteristics exhibited at the Deflector deposit. As noted previously, the setting of the Deflector deposit exhibits many of the structural elements that are commonly associated with orogenic deposits, such as an association with a splay off of a regional structure (Salt River Lineament), and a local high-angle strike-slip displacement of a contact between host rocks by faulting (Hayden and Steemson, 1998; Outwaite, 2016). In addition, analysis of drill core on-site at

Deflector revealed stockwork networks, fracture arrays, and breccia zones in the competent volcanic rocks, as well as small displacements of mineralised structures, which are all well-documented characteristics of orogenic Au deposits. However, as identified by Hayden and Steemson (1998), Deflector does not sit in shear zones that are typical of many Archean Au deposits. From an "Ore systems" perspective, Wyman et al. (2016) argue that different examples of orogenic Au systems may be very similar in all respects except for the nature of the "trap" that localises ore at a specific site. In the case of Deflector, it appears that the system was lacking a key structural feature that exists in many Yilgarn Au deposits: a shear zone and the classic crack-and-seal veins that are associated with them. Relating this back to the mineral system concept, whereby a multitude of parameters operate coevally to favour the formation of significant mineralising systems, preservation of a primary depositional zone requires a trap that prohibits mineralising fluids from escaping at the surface. Therefore, it is proposed that due to Deflector's lack of a structural trap, the presence of a pre-existing base-metal sulphide-rich zone must have provided a chemical trap for auriferous fluids that would otherwise not have formed an economic concentration of Au. At Deflector, the existing base-metal sulphides not only provided the chemical trap required for Au accumulation, they also account for the unusual Au-Cu association at the deposit.

6.6 DEFLECTOR SAMPLE GEOCHEMISTRY

Attempts to define simple geochemical correlations between Au and other elements from the Deflector samples encountered a number of complexities. These are likely the result of the interaction between the Au-rich fluids and a zoned but irregular base-metal fossil hydrothermal system developed in multiple rock types under a different structural regime. Despite these complexities, a number of fundamental geochemical observations support those made during petrographic analyses, and point towards a final genetic model for the Deflector Au-Cu deposit.

6.6.1 High Au/High Cu Vein Samples

Geochemical analyses of the Deflector samples reveal that vein samples with highest Au contents also have high Cu contents, even though a simple mathematical correlation is not possible (figure 25). This further argues against the possibility that only one hydrothermal system was responsible for Deflector's metal inventory, otherwise a well

correlated trend with Au and Cu would likely be apparent on the X-Y plot.

6.6.2 Cu versus Zn and Au versus Zn

Figure 32 and 33 shows that Cu and Zn are poorly correlated in the sedimentary samples. As inferred on the basis of petrographic observations, this can be explained through the hydrothermal zoning that occurred after re-precipitation of the base-metals within the Deflector trap. The zoning results in a differentiation between the two sulphides.

Au was not observed in the sedimentary rock samples and sphalerite was not commonly found in the volcanic rocks, although it did occur sporadically in volcanic-hosted veins. These two observations are consistent with the poor correlation between Au and Zn that is observed overall in Deflector samples and displayed in Figure 28 and Figure 29. At high abundances, both figures indicate that Zn has a preference to either vary independently of Au within sedimentary-zone samples, or to be present at low abundances within volcanic samples. This observation makes sense in relation to petrographic observations. The Cu-Zn-Au relationships are entirely consistent with the proposal of a late Au overprint on a pre-existing, and zoned, base-metal distribution.

6.6.3 Orogenic Fluid Geochemistry

Linking these observations back to the geochemistry of the samples provides further evidence in support of them representing an orogenic end-member. Geochemical assessment indicates that samples 12942594, 12942601, and 12942603 have elevated Au concentrations with Cu concentrations < 50 ppm (Au = 23.7, 2.5, 1.7 g/t; Cu = 42, 24, 15 ppm, respectively). In addition, the samples also show background levels of Ag, Zn, Pb, and In, as well as enrichments in As, Bi, and Te. Groves et al., (2003) establish that orogenic Au deposits have a distinctive metal enrichment association of Au-Ag ± As ± Bi ± Sb ± Te ± W. In addition, the ores in this deposit type are commonly observed to have background values to slight enrichments in Cu, Pb, Zn, Mo, Sn and In. The identification of these orogenic end-member samples is a very significant finding as it provides evidence that an orogenic-sourced fluid has been involved in the formation of the Deflector Lodes. Figure 39 illustrates the trace element characteristics of these three samples, which all show background levels of Cu, Ag, Zn, Pb and In, with slight

enrichments in As, Bi, and Te with increasing Au.

6.6.4 Background Pb Levels

The Pb concentrations in Deflector samples reveal a maximum value of 34.98 ppm, and the small relative enrichments do not correspond to the Au ore-zones or even correlate with other base-metal contents, suggesting that the base-metal hydrothermal fluid was lacking any significant amount of Pb at all. As previously noted, it was suggested that a system analogous to the Golden Grove VMS system may account for the base-metal sulphides encountered at Deflector. Golden Grove consists of two major VMS projects, namely Scuddles and Gossan Hill, both of which are polymetallic Cu/Zn/Pb/Au/Ag. USGS (2012) reported that Golden Grove had a resource of 26.1 Mt @ 1.2 % Cu, 6.9 % Zn, 0.5 % Pb, 0.9 g/t Au, and 59 g/t Ag. However, based upon Deflectors background Pb levels, a Golden Grove-like input to the Deflector system is now considered unlikely.

The discovery of the Golden Grove deposit in 1979 triggered base-metal exploration in the GGB, and resulted in the discovery a number of prospects (Bromley, 1975). These numerous prospects are Pb-poor, and include Mugga King, Murdalyou Range, Yallabyne Well, Bunnawarra, and Edamurta. Due to the similarity of the GGB base-metal mineralisation signatures to that of Deflector, it is likely that an example of these types of base-metals occurrences was the ultimate base-metals source at Deflector.

6.6.5 Multiple Trends of As at High Abundances

Figure 38 illustrates As plotted against Au at high abundances, where As records a minimum of 0 (LLD 0.1) and a maximum of 546 ppm. There are three main trends that can be identified in this figure and high abundance vein samples can have either high As with low Au, high Au with low As, or high Au with moderate As.

Analysis of the high As trend with low Au reveals that all these samples have been taken from Deflectors sedimentary zone. Whilst As and Au are known to be well correlated in a variety of Au systems (Dube et al., 2001), geochemical data of the sedimentary samples at Deflector show a maximum reading of Au at 0.08 g/t (sample 9121275). The high As with low Au concentrations in these samples can therefore be attributed to the original compositions of the sedimentary host-rocks, given that clay-rich sedimentary rocks naturally contain elevated As concentrations (Plant et al., 2003).

Analysis of the high Au trend with low As (< 3 ppm) reveals three vein samples (9371026, 9371088, 12811797) that are high in Cu (> 40,000 ppm), but also low in Bi (< 10 ppm), Se (< 20 ppm), and Te (< 10 ppm). Comparison of these samples with other high-grade vein samples from different areas within the ore-zones reveals a distinctly different geochemical abundance of the trace elements. For example, sample 12591872 records a Cu value of 269,594 ppm and Au value of 62.36 g/t, with Bi having a value of 64.04 ppm, As value of 232.62 ppm, Se value of 36.06 ppm, and a Te value of 54.72. This means that the high Au/low As samples appear to have lost As, as well as Bi, Se, and Te from that area of the system. Referral of these samples back to thin section analysis demonstrates that these are the samples that exhibit disequilibrium textures (Figure 15B), meaning the event that caused these textures may have also resulted in the loss of various trace elements from this part of the system. Whilst the exact nature of this process cannot be determined for this report, the evidence suggests that the disequilibrium textures correspond to an "open system" where the interactions between two hydrothermal inputs are associated with the introduction and loss of various trace elements.

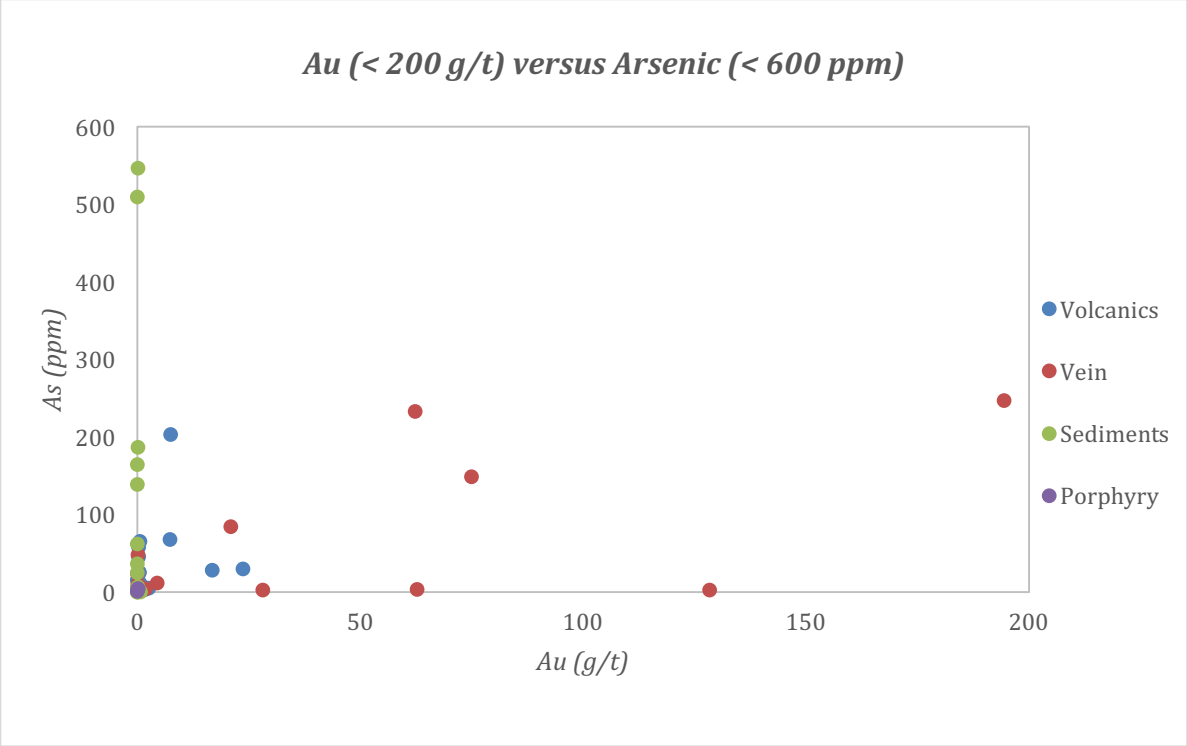

Figure 38: *Au versus As of the present study Deflector samples at high abundances.*

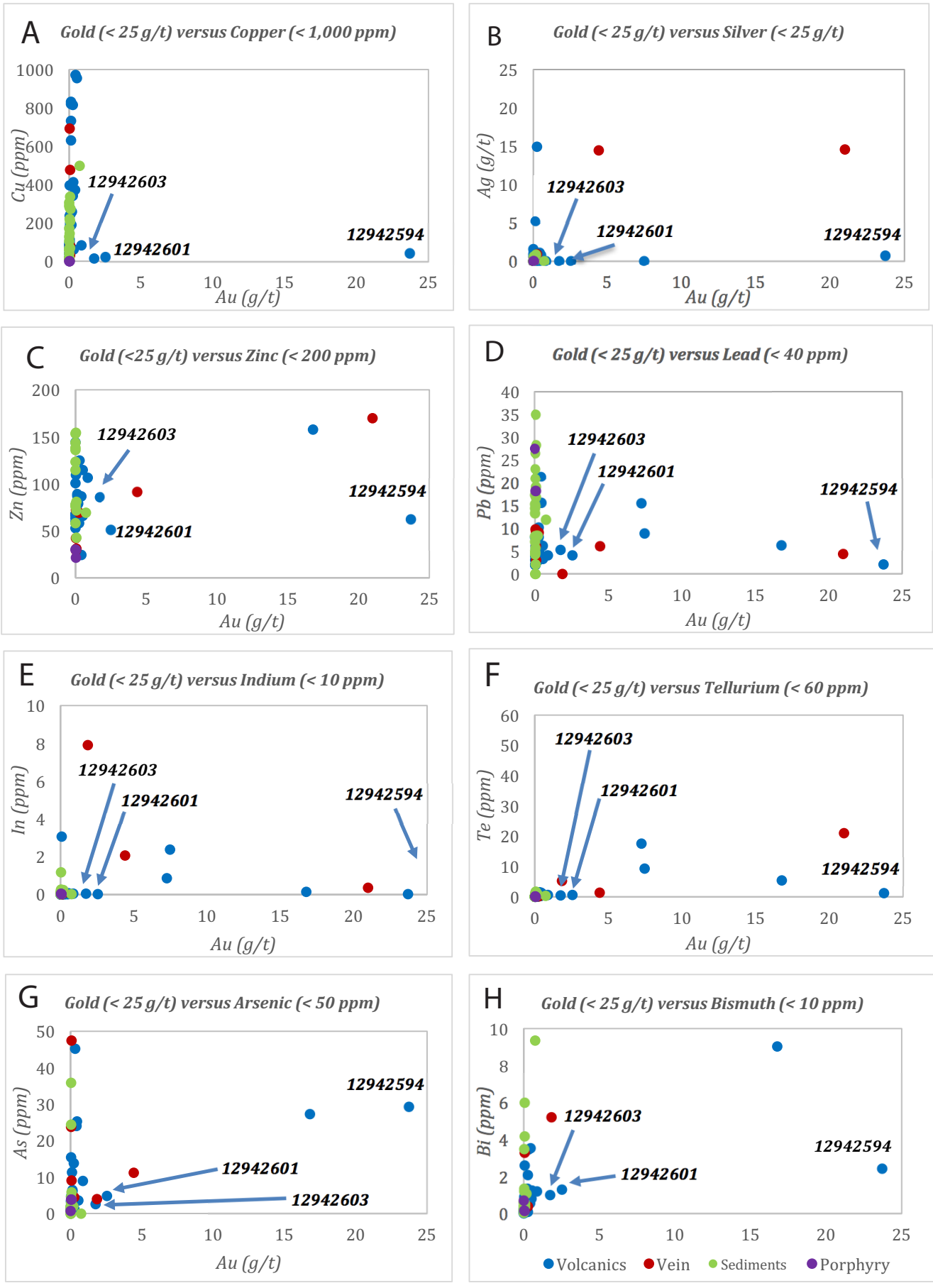

Figure 39: *Geochemical modelling of veinlet-dominated volcanic samples 12942594, 12942601, and 12942603. Petrographic and geochemical analyses have determined these samples as representing orogenic end-members.*

It is expected that the introduction of an orogenic fluid would subsequently introduce As into the Deflector system (Dube et al., 2001). This accounts for the high Au with moderate As vein samples.

6.6.6 Geochemical Vectors to Mineralisation

As previously noted, the input of a hydrothermal fluid into an existing mineral system acts to mobilise trace elements in a number of different ways. For example, a Au rich hydrothermal fluid will introduce a suite of elements to a system, whilst at the same time dispersing another suite of elements further away. Understanding the behaviour of trace element abundances at Deflector is useful as it allows a geochemical signature to be characterised, which will further assist in the discovery of any remaining Deflector-like deposits in the surrounding GGB. Access to PHD student Roman Teslyuk's geochemical dataset of Deflector volcanic rocks, taken away from ore zones, allow a comparison to be made between the trace element background levels of these rocks with the present study Deflector samples collected in or near ore zones. Due to the limited number of samples taken for this study, however, it should be noted that the potential geochemical vectors are only suggestive, and not to be taken as definitive without a more comprehensive data set.

Geochemical analyses of trace elements at low abundances encountered multiple 'wedge-like' trends in the dataset (Figure 40). This trend suggests that in plots of W, As, Zn, and Ba, increases in Au are coupled with decreases in these 4 elements. In theory, this would indicate that the introduction of a hydrothermal fluid acts to precipitate Au in the system, whilst also flushing out various elements in the process. This results in samples with elevated Au having depletions of W, As, Zn and Ba (relative to background samples), where the flushed out elements are subsequently re-precipitated at the margins of the Deflector system. The "wedge" at very low Au abundances therefore indicates a local re-deposition of the mobilized elements at the edge of a hydrothermal alteration feature, further supporting the interpretation of Deflector as an open system.

Analysing the background values of these elements in samples taken away from ore allows us to further characterise the behaviour of the elements at the margins of the ore. For example, comparisons show that there are regions with below background

concentrations for some elements. This observation supports the possibility that these elements have been removed from some rock rather than just added in variable amounts. The comparisons indicate that W, As, Zn, and Ba can be determined as being geochemical vectors to mineralisation. Given that the ore-zones themselves are characterised by an Au-Cu-Ag ± Zn-As-W-Bi-Se-Te geochemical signature, it is important for exploration programs to be aware of the complex behaviour of these elements at varying distances from the core of the hydrothermal system.

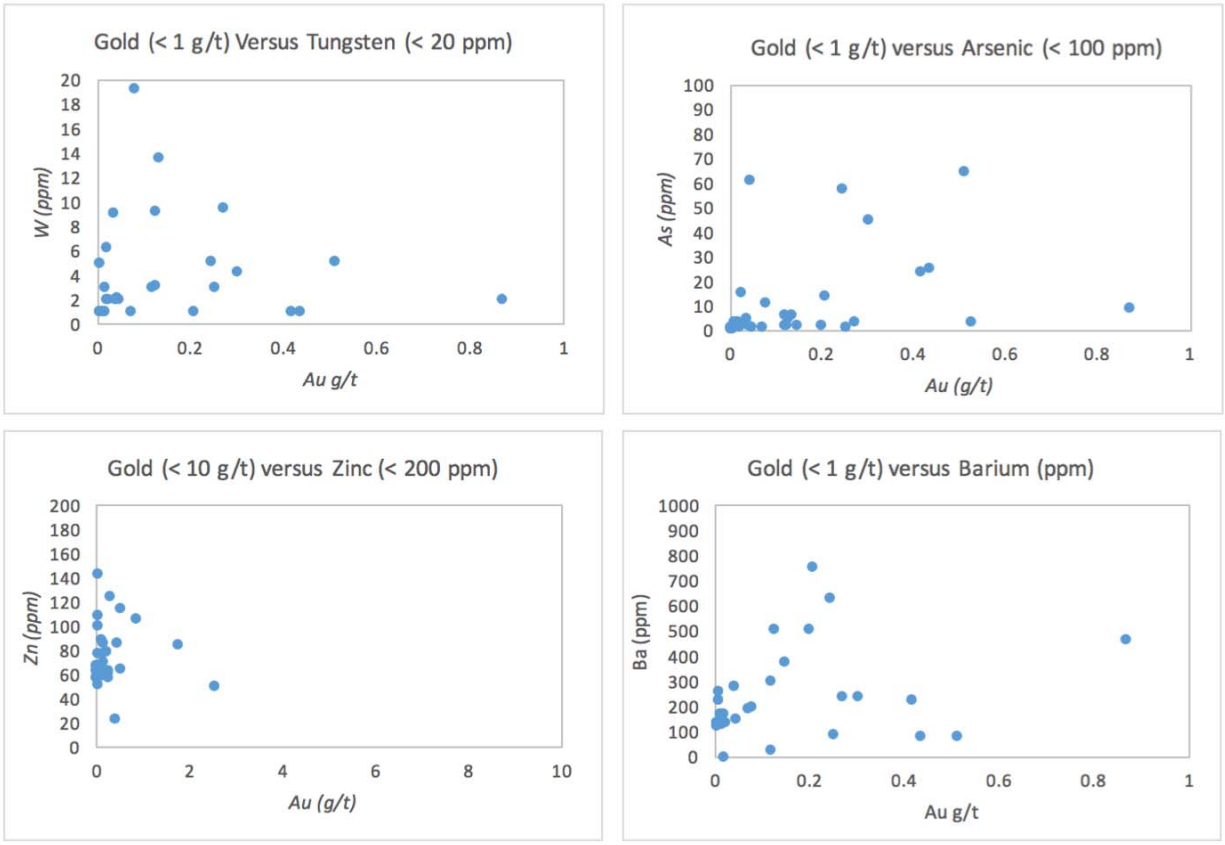

Figure 40: *Wedge-like trends of W, As, Zn, and Ba in volcanic samples. The average background values for these elements has being calculated as 1.22, 4.48, 71, and 193 ppm, respectively. The Au/Zn trend includes three successive samples that indicate micro-fracturing and 'flushing-out' of Zn by disseminated pyrite-rich fluids.*

7. METALLOGENIC IMPLICATIONS

7.1 Alternate Models

The present study hypothesised several models in order to account for Deflectors formation. These models will be synthesised in order to analyse whether or not they can account for the petrographic and geochemical observations that have been made.

7.1.1 Rare Hybrid Au-Cu Type

One possible model for Deflector is that it represents a rare hybrid style of mineralisation where an upwardly mobile orogenic fluid passed through an existing base-metal sulphide anomaly at depth and continued upwards, with modified fluids, to form an "anomalous" Deflector at shallower crustal levels.

In order for this model to be correct, the hybrid fluids must be transported from depth into the structural site at Deflector, and cool in a way that permits a hydrothermal zoning sequence. As previously noted, massive sulphide "black ore" minerals such as sphalerite and pyrite have been reported as having a formation temperature at T = ~ 200° to 330° C, with yellow ore minerals such as chalcopyrite having a formation temperature at T = ~ 330 ° ± 50 °C (Pisutha-Arnold and Ohmoto, 1983). If these temperatures were applicable to Deflector, then the orogenic Au fluids would have to be at least 330 ° ± 50 °C in order to remobilise the chalcopyrite in the base-metal sulphide body, and create a hybrid Au-Cu mineralising fluid. This temperature is at the high-T end of the range typically found in orogenic deposits at sub- to mid-greenschist facies (McCuaig and Kerrich, 1998). Consequently, it is difficult to account for the base-metal zoning at Deflector with this model. Seafloor massive sulphides have a local heat source and larger temperature gradients but deeply sourced Au fluids are not known to display highly variable temperatures within individual deposits. In order for these fluids to create the zoning sequence of minerals that are observed at Deflector, they would have to have undergone two separate cooling events, whereby a first cooling event results in the chalcopyrite + pyrite rich inner core, and a second cooling event resulting in the pyrrhotite + sphalerite rich periphery. In addition, the zoning needs to occur in a way that allows Zn ± Cu to accumulate in the sedimentary zone, but Au only within the volcanic-zone.

Similarly, a hybrid Au-Cu model does not support the presence of Type I and Type II pyrite that are observed in the Deflector system. The mixing of two fluids at depth, followed by this hybrid fluid being transported to shallower crustal levels, only supports the presence of one textural type of pyrite. For additional textural types to be present, an additional independent fluid would be required to overprint, or be superimposed upon, the already existing hybrid fluid.

Lastly, the fact that Deflector samples cannot be modelled chemically as a simple mixing problem indicates that a mixing event has not taken place. Geochemistry of the samples demonstrates that even though samples with the highest Au contents also have high Cu contents, a simple mathematical correlation is not possible. If a single hybrid fluid was produced at depth, then it is probable that geochemical modelling would indicate a good correlation between Au and Cu. This correlation does not exist in the Deflector samples. Finally, the presence of orogenic end-member samples suggests that the orogenic fluids entered Deflector system as an independent system, and in this case, were superimposed on an existing base-metal sulphide system.

7.1.2 Distinct Au-Cu Type

A second possible model put forward in this report hypothesised that Deflector is representative of a distinct Au-Cu mineralisation type. If a skarn, porphyry, epithermal, or VMS model can be applied to the Deflector system, it should exhibit characteristics that allow it to be categorised into one of these distinct types.

Samples from Deflector exhibited a number of features that may be indicative of a skarn-type deposit. The presence of carbonates in the Deflector system as well as the comparatively small number of samples with mineralisation textures resembling those seen in retrograde skarn deposits can be used as evidence to support this. However, these textures are minor features at Deflector. Instead, the evidence that suggests that interaction between two independent hydrothermal systems occasionally replicated retrograde-skarn similarities, which can broadly be characterised as the product of one hydrothermal fluid reworking the existing products of an earlier hydrothermal system.

The mineralogy of the Deflector system can be used as evidence against a skarn model for the deposit. Skarns are known to be mined for a variety of elements, including Fe, W, Cu, Pb, Zn, Mo, Ag, Au, U, REE, F, B, and Sn (Mueller, 2007). In addition, whilst most skarns are found to occur in lithologies that contain at least some limestone, they have been discovered to form in almost any rock type, including shale, sandstone, granite, basalt, and komatiite. However, mineralogy is what predominantly determines a skarn classification, with high-grade Au skarns having a mineral assemblage dominated by iron-rich pyroxene, with proximal zones potentially containing abundant intermediate garnet. Cu-rich skarns have a relatively oxidized skarn mineralogy dominated by andraditic garnet, as well as diopsidic pyroxene, vesuvianite, wollasonite, actinolite, and epidote (Mueller, 2007). Deflector does not have these mineral characteristics.

Similarly, the presence of classic quartz-carbonate-sulphide veins at Deflector and the absence of massive sulphides or a feeder system rules out a VMS model for the deposits formation. In addition, the alteration styles and metal distributions that are present are not characteristic of porphyry or epithermal systems.

7.2 Deflector Superimposed Au-Cu - Final Synthesis

The observations made through petrographic and geochemical analyses reflect the superposition of a late Au hydrothermal event on an earlier Cu-rich event at the site of the Deflector ore bodies (Figure 41).

The evidence points to a hybrid origin for Deflector, where the base-metal sulphide mineralisation that has been sporadically identified in the GGB was likely remobilised as a granite intrusion moved upwards through the crust from deeper crustal levels, where it was eventually emplaced into a favourable structural setting. The heat associated with this intrusion acted to remobilise the base-metals, which previously existed at deeper levels within the crust. The original constituents of this base-metal sulphide mineralisation has been interpreted as consisting of chalcopyrite, pyrite and sphalerite. Sulphur would have been mobilised along with Cu and Zn as the metals were transported to shallower crustal levels but was probably more mobile and likely to escape the system. The effect would be most obvious at the periphery of the system, meaning that pyrrhotite

(FeS) was precipitated at the margins of the Deflector system even though pyrite (FeS_2) may have been present in the original massive sulphide at depth. In the core of the system, enough sulphur existed for the remobilised Fe to be re-precipitated as pyrite, where it was accompanied by chalcopyrite.

As the granite intrusion moved through the upper crust and remobilised the base-metal sulphides, it created additional brittle fractures in the rock that provided a pathway for the hydrothermal base-metals to travel. The structures caused at Deflector by the emplacement of this intrusion into the shallow crust provided a favourable setting for the Cu-Zn mineralisation to be re-precipitated. This overall process resulted in elevated Cu contents over a wide area and high Cu abundances in preferred structural sites. Volcanic samples collected in this study consistently have Cu > 50 ppm, which appears to be above the background content of the mafic unit in Deflector samples collected away from ore. In addition, samples taken from drill holes 9DEF021 and 9DEF013 demonstrate abundances in iron-zinc, indicating that the base-metal mineralisation penetrated beyond volcanic-sedimentary contact and was re-precipitated within the sedimentary zone. This model proposes that this occurred prior to the development of the major structure that exists on the mafic-sedimentary contact.

The identification of three end-member orogenic samples, coupled with the dominant presence of quartz-carbonate veining and veinlets throughout the Deflector system, provides strong support on the plausibility that a late orogenic-sourced fluid has been superimposed on the earlier Cu-Zn mineralisation. The major structure inferred by Hayden and Steemson (1998) and Outhwaite (2016) at the mafic-sedimentary contact allowed for orogenic Au-rich fluids to be pumped into the Deflector system from very deep in the crust. However, as described by Czarnota et al. (2009) and Bleeker (2015), a structure of this size has clear tectonic implications, with its development tapping a Au-source from deep in the crust, therefore providing Au-rich fluids with a pathway to travel to shallower levels within the crust. This implies that the structure prior to Au-mineralisation, which is why Au exists in the volcanic-zone and not the sedimentary-zone. The development of this structure has prohibited Au from being able to permeate into the sedimentary-zone.

The introduction of Au-rich fluids into the Deflector system resulted in a "mixing" of the two hydrothermal systems taking place (i.e., one active and one fossil system). The overprinting of this Au-rich system resulted in the existence of the two textural types of pyrite at Deflector. As Type I pyrite was introduced by the orogenic fluids, the existing pyrite (Type II pyrite) was affected in a way that resulted in its pitted texture. This same process resulted in the pitted appearance of some chalcopyrite. As demonstrated in a small number of samples, the mixing that occurred between these two independent hydrothermal systems also occasionally represented mineralisation textures that characterise retrograde-skarn deposits. This can be broadly characterised as the product of one hydrothermal fluid reworking the existing products of an earlier hydrothermal system. The absence of Type II pyrite or pitted chalcopyrite in many ore samples indicates that the sulphides they contain formed during the time of Au deposition and include a mixture of sulphur from the two events. The introduction of later orogenic fluids subsequently accounts for the free Au that exists within the quartz-carbonate veins and veinlets, both on quartz grain-boundaries and embedded in the Type I pyrite.

Based on this model, the presence of an existing base-metal sulphide anomaly provided a chemical trap upon which allowed the superposition of the orogenic Au fluids on top of it. If these base-metals did not exist, it is possible that the orogenic fluids may have been lost to the surface, in which the base-metal mineralisation compensated for the lack of a more typical fault valve trap for Au that is common for orogenic lode systems.

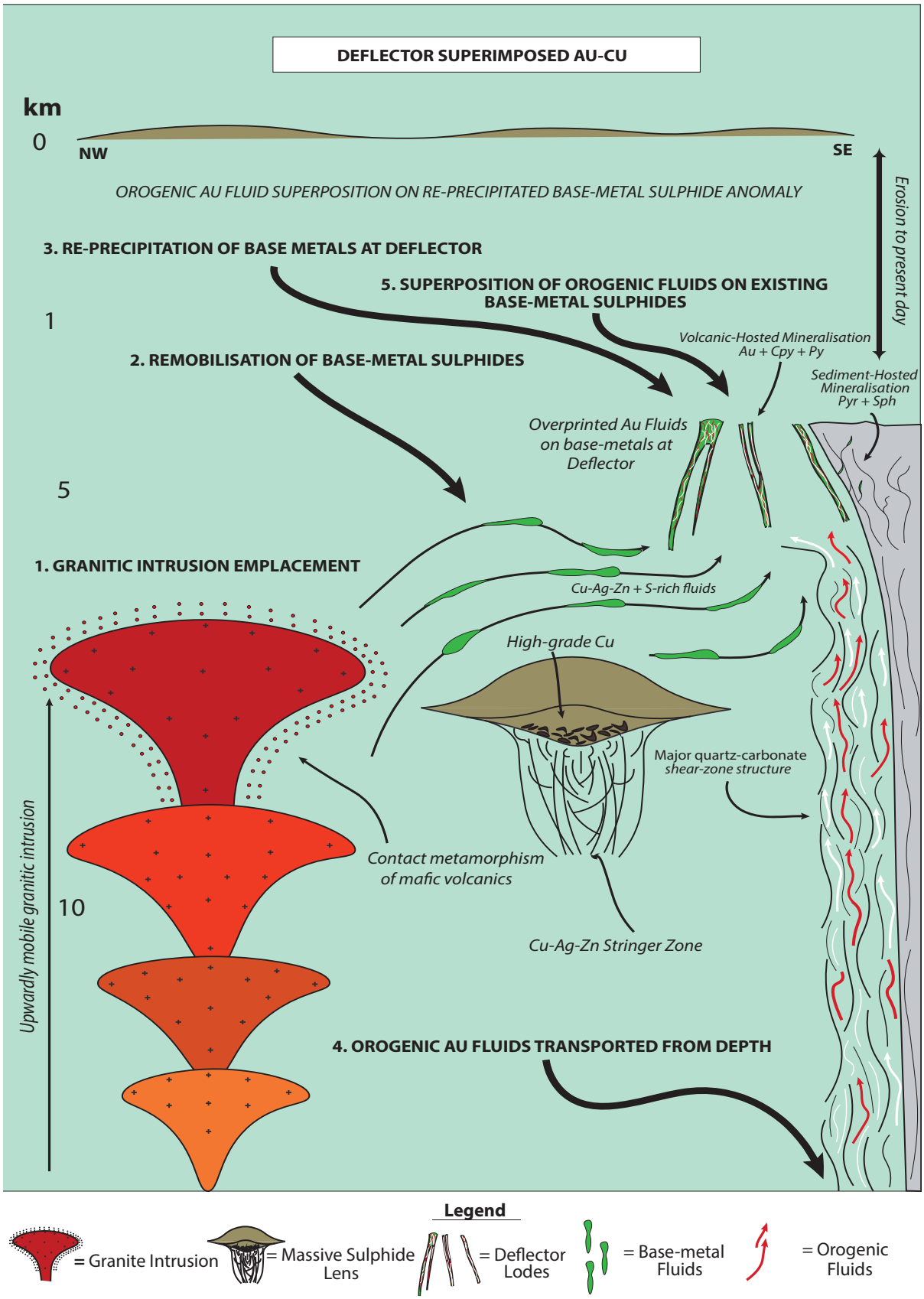

Figure 41: *Final model for the Deflector superimposed Au-Cu deposit. Granitic intrusion emplacement results in a remobilisation of a base-metal sulphide anomaly at depth, which is re-precipitated within structural traps at Deflector. The development of a later, major shear zone taps an orogenic-sourced fluid from depth, which is superimposed on the existing base-metal sulphides at Deflector. The development of this shear-zone does not permit Au to accumulate within the sedimentary-zone. Note: Geologic structures not to scale.*

8. CONCLUSIONS

Petrographic and geochemical analyses of the 80 samples collected for this study provide strong evidence that an orogenic Au event was superimposed on an existing "fossil" base-metal system. For example, the presence of two textural types of pyrite, as well as the disequilibrium textures within these samples, indicate that two independent hydrothermal fluids have interacted within the deposit itself. In addition, the identification of orogenic end-member samples provides evidence that one of these fluids was an orogenic fluid sourced from depth. This is further supported by the presence of shoshonitic lamprophyres in and around the Deflector area, indicating that a major structure exists by which these fluids were able to travel from deep in the crust. Geochemical studies further support this model, given that high Au samples also have high Cu, even though a simple mathematical correlation is not possible. In addition, Au and Zn also show a negative correlation, which is expected given that these two metals were introduced by independent hydrothermal systems. In the case of Deflector, the known occurrences of base-metal showings in the GGB suggests that these played a role in the development of Deflector's unusual metal inventory.

By comparison, the evidence collected provides strong constraints against the plausibility of the two additional models considered at the start of this study. For example, petrographic and geochemical evidence rules out the possibility that an orogenic fluid system passed through an existing base-metal sulphide anomaly at depth, and continued upwards with modified fluids to form an anomalous Deflector at shallower crustal levels. In addition, the presence of abundant quartz-carbonate veins as well as the lack of features that would allow characterisation into a distinct Au-Cu type disprove a distinct skarn, porphyry, epithermal or VMS model for Deflectors formation.

The assessment of trace element contents at low Au abundances has provided important insights into the possible use of chemical vectors to ore in the Deflector area. The trace elements W, As, Zn and Ba occur at concentrations above background levels taken away from ore. However, the wedge-like trend that occurs in these trace elements at low abundances indicates a bleaching out of these elements as the ore-zones are vectored in towards, followed by a peak in concentrations when the ore-zones are

entered. Given that the ore-zones themselves are characterised by an Au-Cu-Ag ± Zn-As-W-Bi-Se-Te geochemical signature, it is important for exploration programs to be aware of the complex behaviour of these elements at varying distances from the core of the hydrothermal system. Geochemical modelling of the samples at low Au abundances suggests that the introduction of a Au-rich orogenic fluid has resulted in the flushing out of a number of other trace elements, which may complicate exploration for an undiscovered resource.

Future research at Deflector may endeavour to collect a more comprehensive geochemical dataset for this superimposed system, whereby a definitive geochemical signature can be obtained. This will significantly aid in the exploration strategy for similar Deflector-like deposits in the surrounding Gullewa Goldfield.

9. REFERENCES

Allibone, A. H., Windh, J., Etheridge, M. A., Burton, D., Anderson, G., Edwards, P. W., Miller, A., Graves, C., Fanning, C. M. and Wysoczanski, R. (1998). Timing Relationships and Structural Controls on the Location of Au-Cu Mineralisation at the Boddington Au Mine, Western Australia. *Economic Geology 93,* 245 – 270.

ALS Global (2013). Schedule of Services and Fees. *Retrieved from: http://www.alsglobal.com/Our-Services/Minerals*

Anhaeusser, C. R. (2014). Archean Greenstone Belts and Associated Granitic Rocks – A Review, *Journal of African Earth Sciences 100,* 684 – 732.

Barley, M. E and Groves, D. I. (1992). Supercontinent Cycles and Distribution of Metal Deposits through Time. *Geology 20,* 291 – 294.

Brown, R. J. C. and Milton, M. J. T. (2005). Analytical Technical for Trace Element Analysis: An Overview. *TrAC Trends in Analytical Chemistry 24:3,* 266 – 274.

Bierlein, F. P., Arne, D. C., McKnight, S. Lu, J., Reeves, S., Besanko, J., Marek, J. and Cooke, D. (2000). Wall-Rock Petrology and Geochemistry in Alteration Halos Associated with Mesothermal Au Mineralisation, Central Victoria, Australia. *Economic Geology 95,* 283 – 312.

Bierlein, F. P., Groves, D. I. and Cawood, P. A. (2009). Metallogeny of Accretionary Orogens – The Connection between Lithospheric Processes and Metal Endowment. *Ore Geology Reviews 36:4,* 282 – 292.

Bierlein, F. P., Whitam, R., McKnight, S. and Dodd, R. (2003). Intrusive-Related Au Systems in the Western Lachlan Orogen, SE Australia. *In:* Eliopoulos et al. (eds.), *Mineral Exploration and Sustainable Development*. Millpress, Rotterdam, 239 – 242.

Bleeker, W. (2015) Synorogenic Au Mineralisation in Granite-Greenstone Terranes: The Deep Connection between Extension, Major Faults, Synorogenic Clastic Basins, Magmatism, Thrust Inversion, and Long-Term Preservation, *In:* Targeted Geoscience Initiative 4: Contributions to the Understanding of Precambrian Lode Au Deposits and Implications for Exploration (ed.), Dube, B. and Mercier-Langevin, P., *Geological Survey of Canada, Open File 7852,* 24 – 47.

Cassidy, K. F., Champion, D. C., Krapez, B. B., Brown, S. J. A., Blewett, R. S. Groenewald, P. B., and Tyler, I. M. (2006). A Revised Geological Framework for the Yilgarn Craton,

Western Australia. *Geological Survey of Western Australia, Record 2006/8,* 8.

Caughlin, B. (2007). Developments in Analytical Technology. *Proceeds of Exploration 7, 14 – 24.*

Cooke, D. R., Hollings, P. and Walshe, J. L. (2005). Giant Porphyry Deposits: Characteristics, Distribution, and Tectonic Controls. *Economic Geology 100:5,* 801 – 818.

Corbett, G. J. (2002). Epithermal Au for Explorationists. *AIG Presidents Lecture.*

Corbett, G. J. (2009). Anatomy of Porphyry-Related Au-Cu-Ag-Mo Mineralised Systems: Some Exploration Implications. *AIG Bulletin 49,* 33 – 46.

Corbett, G. J. and Leach, T. M. (1998). Southwest Pacific Au-Cupper Systems: Structure, Alteration and Mineralisation. *Special Publication 6, Society of Economic Geologists,* 238.

Craw, D., Begbie, M. and Mackenzie, D. (2006). Structural Controls on Tertiary Orogenic Au Mineralisation during Initiation of a Mountain Belt, New Zealand. *Mineralium Deposita 41,* 645 - 659.

Czarnota, K. Blewett, R. S., and Goscombe, B. (2009). Structural and Metamorphic Controls on Au through Time and Space in the Central Eastern Goldfields Superterrane – A Field Guide, *Geological Survey of Western Australia, 66.*

Davis, G. F. (1992). On the Emergence of Plate Tectonics. *Geology 20,* 963 – 966.

Dube, B. and Gosselin, P. (2007). Greenstone-Hosted Quartz-Carbonate Vein Deposits. In: Goodfellow, W. D. (Ed.) Mineral Deposits of Canada: A Synthesis of Major Deposit-Types, District Metallogeny, the Evolution of Geological Provinces, and Exploration Methods: *Geological Association of Canada, Mineral Deposits Division, Special Publication 5*, 49 – 73.

Dube, B., Gosseline, P., Langevin, P., Hannington, M. and Galley, A. (2005). Au-Rich Volcanogenic Massive Sulphide Deposits, *In:* Goodfellow, W. D., (ed.), Mineral Deposits of Canada: A Synthesis of Major Deposit-Types, District Metallogeny, the Evolution of Geologic Provinces, and Exploration Methods. *Geological Associations of Canada, Mineral Deposits Division, Special publication 5,* 75 – 94.

Eilu, P. and Groves, D. I. (2001). Primary Alteration and Geochemical Dispersion Haloes of Archean Orogenic Au Deposits in the Yilgarn Craton: The Pre-Weathering Scenario. *Geochemistry: Exploration, Environment, Analysis 1,* 183 – 200.

Gaboury, D. and Pearson, V. (2008). Rhyolite Geochemical Signatures and Association with Volcanogenic Massive Sulphide Deposits: Examples from the Abitibi Belt, Canada. *Economic Geology 103,* 1531 – 1562.

Gibson, H. L., Allen, R. L., Riverin, G., and Lane, T. E. (2007). The VMS Model: Advances and Application to Exploration Targeting. *Ore Deposits and Exploration Technology 49,* 713 – 730.

Gifkins, C. (2005). Altered Volcanic Rocks: A Guide to Description and Interpretation. *Centre for Ore Deposit Research,* 275.

Godden, S. (2008). Gullewa Au-Copper Project. *ATW Venture Corp., Unpublished Consultancy Report.*

Goldcorp, (2013). Red Lake: Mining and Processing. *Retrieved from: http://www.goldcorp.com/English/Unrivalled-Assets/Mines-and-Projects/Canada-and-US/Operations/Red-Lake/Mining-and-Processing/default.aspx.*

Goldfarb, R. J., Groves, D. I. and Gardoll, S. (2001). Orogenic Au and Geologic Time: A Global Synthesis. *Ore Geology Reviews 18,* 1 – 75.

Goodwin, L. B. and Tikoff, B. (2002). Competency Contract, Kinematics, and the Development of Foliations and Lineations in the Crust. *Journal of Structural Geology 24: 7,* 1065 – 1085.

Groves, D. I. and Foster, R. P. (1991). Archean Lode Au Deposits. *Au Metallogeny and Exploration,* 63 – 103.

Groves, D. I., Goldfarb, R. J., Gebre-Mariam, M., Hagemann, S. G. and Robert, F. (1998). Orogenic Au Deposits: A Proposed Classification in the Context of their Crustal Distribution and Relationship to other Au Deposit Types. *Ore Geology Reviews 13,* 7 – 27.

Groves, D. I., Goldfarb, R. J., Robert, F., and Hart, C. J. R. (2003). Au Deposits in Metamorphic Belts: Overview of Current Understanding, Outstanding Problems, Future Research, and Exploration Significance. *Economic Geology 98,* 1 – 29.

Hart, C. J. R. (2005). Classifying, Distinguishing, and Exploring for Intrusion-Related Au Systems. *Canadian Institute of Mining – Geological Society "The Gangue",* Issue 87.

Hart, C. J. R. and Goldfarb, R. J. (2005). Distinguishing Intrusion-Related from Orogenic Au Systems. *In:* New Zealand Minerals Conference: Realising New Zealands Minerals Potential Proceedings, *Australasian Institute of Mining and Metallurgy*,

125 – 133.

Hayden, P. and Steemson, G. (1998). Deflector Au-Cu Deposit. *Geology of Australian and Papua New Guinea Mineral Deposits,* 167 – 172.

Hodkiewicz, P. F., Weinberg, R. F., Gardoll, S. J. and Groves, D. I. (2005). Complexity Gradients in the Yilgarn Craton: Fundamental Controls on Crustal-Scale Fluid Flow and the Formation of World-Class Orogenic-Au Deposits. *Australian Journal of Earth Sciences 52,* 831 – 841.

Jaireth, G. L. and Huston, D. (2010). Metal Endowment of Cratons, Terrances, and Districts: Insights from a Quantitative Analysis of Regions with Giant and Super-giant Deposits'. *Ore Geology Reviews 38,* 288 – 303.

Kerrich, R. and Polat, A. (2006). Archean Greenstone-Tonalite Duality: Thermochemical Mantle Convection Models or Plate Tectonics in the Early Earth Global Geodynamics? *Tectonophysics 415,* 141 – 164.

Kerrich, R. and Wyman, D. A. (1994). The Mesothermal Au-Lampropyre Association: Significance for an Accretionary Geodynamic Setting, Supercontinent cycles, and Metallogenic Processes. *Mineral Petrology 51,* 147 – 172.

Knight, J. A., Burger, K. and Bieg, G. (2000). The Pyroclastic Tonsteins of the Saberco Coalfield, North Western Spain, and their Relationship to the Stratigraphy and Structural Geology. *International Journal of Coal Geology 44,* 187 – 226.

Korenaga, J. (2006). Archean Geodynamics and the Thermal Evolution of the Earth. *Geophysical Monograph Series on Archean Geodynamics and Environments 164,* 7 – 32.

Laurent, O., Martin, H., Moyen, J. F., and Doucelance, R. (2014). The Diversity and Evolution of Late-Archean Granitoids: Evidence for the Onset of "Modern-Style" Plate Tectonics between 3.0 and 2.5 Ga, *Lithos 205,* 208 – 235.

Mason, T. F. D., Weiss, D. J., Chapman, J. B., Wilkinson, J. J., Tessalina, S. G., Spiro, B., Horstwood, M. S. A., Spratt, J. and Coles, B. J. (2005). Zn and Cu Isotopic Variability in the Alexandrinka Volcanic-Hosted Massive Sulphide (VHMS) Ore Deposits, Urals, Russia. *Chemical geology 221,* 170 – 187.

McCulloch, M. T. and Bennett, V. C. (1994). Progressive Growth of the Earth's Continental Crust and Depleted Mantle: Geochemical Constraints. *Geochimica et Cosmochimica Acta 58,* 4717 – 4718.

Outhwaite, M. (2016). Deflector Regional Mapping Summary. *Model Earth: Global*

Geological Services, Unpublished Consultancy Report.

Penczak, R. S. and Mason, R. (1997). Metamorphosed Archean Epithermal Au-As-Sb-Zn-(Hg) Vein Mineralisation at the Campbell Mine, Northwestern Ontario. *Economic Geology 92,* 696 – 719.

Phillips, G. N. (2004). Au in the Yilgarn Craton, Australia: A Quarter Century of Successful Exploration and 100 Million Ounce Production. *In:* Muhling, J., Goldfarb, R., Vielreicher, N., Bierlein, F., Stumpfl, E., Groves, D. I. and Kenworthy, S. eds. *SEF 2004: Predictive Mineral Discovery Under Cover; Extended abstracts 33,* 22 – 28.

Pisutha-Arnold, V. and Ohmoto, H. (1983). Thermal History, and Chemical and Isotopic Compositions of the Ore-Forming Fluids Responsible for the Kuroko Massive Sulphide Deposits in the Hokuroku District of Japan. *Economic Geology 5,* 523 – 558.

Plant, J. A., Kinniburgh, D. G., Smedley, P. L., Fordyce, F. M. and Klinck, B. A. (2003). Arsenic and Selenium. *Treatise on Geochemistry 9,* 17 – 66.

Polat, A. and Kerrich, R. (2000). Archean Greenstone Belt Magmatism and the Continental Growth-Mantle Evolution Connection: Constraints from Th – U – Nb – LREE Systematics of the 2.7 Ga Wawa Subprovince, Superior Province, Canada. *Earth and Planetary Science Letters 175,* 41 – 54.

Rey, P. F. and Coltice, N. (2008). Neoarchean Strengthening of the Lithosphere and the Coupling of the Earth's Geochemical Reservoirs. *Geology 36,* 635 – 638.

Richards, J. P. (2003). Tectono-Magmatic Precursors for Porphyry Cu-(Mo-Au) Deposit Formation. *Economic Geology 98,* 1515 – 1533.

Ridley, I. W. (2010). Volcanogenic Massive Sulphide Occurrence Model: Geochemical Characteristics. *U. S. Geological Survey Scientific Investigations Report,* 345.

Robb, L. J. (2008). Introduction to Ore-Forming Processes. *Wiley-Blackwell.*

Robert, F., Brommecker, R., Bourne, B. T., Dobak, P. J., McEwan, C. J., Rowe, R. R., and Zhou, X. (2007). Models and Exploration Methods for Major Au Deposit Types. *Ore Deposits and Exploration Technology 48,* 691 – 711.

Rollinson, H. R. (2002). The Metamorphic History of the Isua Greenstone Belt, West Greenland. *Geological Society of London Special Publications 199,* 620 – 635.

Roth, E., Groves, D., Anderson, G., Daley, L., and Staley, R. (1991). Primary Mineralisation at the Boddington Au Mine, Western Australia: An Archean Porphyry Cu-Au-Mo Deposit. *In:* Brazil Au 91': The Economics, Geology, Geochemistry and Genesis

of Au Deposits, *Balkema, Rotterdam, Netherlands,* 481 – 488.

Sillitoe R. H. (2010). Porphyry Copper Systems. *Economic Geology 105,* 3 – 41

Soloman, M. and Groves, D. I. (2000). The Geology and Origin of Australia's Mineral Deposits. *Centre for Ore Deposit Research and Centre for Global Metallogeny 32,* 1002 – 1018.

Stein, H. J., Markey, R. J., Morgan, J. W., Selby, D., Creaser, T. C. (2001) Re-Os Dating of Boddington Molybdenite, SW Yilgarn: Two Au Mineralisation Events. *Geoscience Australia 37,* 469 – 471.

Swager, C. P. (1997). Tectono-Stratigraphy of Late Archean Greenstone Terranes in the Southern Eastern Goldfields, Western Australia. *Precambrian Research 83,* 11 – 42.

Swager, C. P., and Nelson, D. R. (1997). Extensional Emplacement of a High-Grade Granite Gneiss Complex into Low-Grade Greenstones, Eastern Goldfields, Yilgarn Craton, Western Australia. *Precambrian Research 83,* 203 – 219.

Tomkins, A. G. (2013). On the Source of Orogenic Au. *Geology 41:12*, 1255 – 1256.

White, N. C. and Hedenquist, J. W. (1995). Epithermal Au Deposits: Styles, Characteristics, and Exploration. *Society of Economic Geologists Newsletters 23,* 1 – 13.

Wilkinson, J. J. (2013). Triggers for the Formation of Porphyry Ore Deposits in Magmatic Arcs, *Nature Geoscience 6,* 917 – 925.

Witt, W. K. and Hammond, D. P. (2008). Archean Au Mineralisation in an Intrusion-Related, Geochemically Zones District-Scale Alteration System in the Carosue Basin, Western Australia. *Economic Geology 103:2,* 48 – 62.

Wyman, D. A., Cassidy, K. F., and Hollings, P. (2016). Orogenic Au and the Mineral Systems Approach: Resolving Fact, Fiction, and Fantasy. *Ore Geology Reviews 78,* 322 – 335.

10. APPENDICIES

APPENDIX 1: Sample Drill Hole ID, Depth, and Number

APPENDIX 2: Sample Photos and Core Trays

APPENDIX 3: Upper and Lower Limit of Detection Values for Geochemical Analyses

APPENDIX 4: Drill Hole Sections

APPENDIX 5: Deflector Geochemical Data

RECORD 2020/4

THE DEFLECTOR AU–CU DEPOSIT: DEFINING AN ANOMALOUS YILGARN CRATON MINERALISATION STYLE USING TRACE ELEMENT GEOCHEMISTRY

This Record is published in digital format (PDF) and is available as a free download from the DMIRS website at <www.dmirs.wa.gov.au/GSWApublications>.

Further details of geolscience products are available from:

Information Centre
Department of Mines, Industry Regulation and Safety
100 Plain Street
EAST PERTH WESTERN AUSTRALIA 6004
Phone: +61 8 9222 3459 Fax: +61 8 9222 3444
www.dmirs.wa.gov.au/GSWApublications

Egan